Dissertation Title

The Impact of Polymeric Nanoencapsulation on the Bioavailability of Lutein

Doctoral Student

Alison Kamil, MS, RD, LDN

Thesis Committee

Oliver Chen, PhD

Jeffrey Blumberg, PhD, FASN, FACN, CNS

Eric Decker, PhD

Donald Smith, PhD, CMAR, CPIA

Date

8/8/2014

Acknowledgements

Over the past 5 years I have received substantial support and encouragement from a number of individuals. Foremost, I would like to express my sincere gratitude to my advisor Dr. Oliver Chen for his continuous and incredible support of my PhD study and research. I am especially appreciative for his patience and his immense knowledge. In addition to my advisor, I would like to thank the rest of my thesis committee, Dr. Jeffrey Blumberg, Dr. Eric Decker and Dr. Donald Smith, for their encouragement, insightful comments, and hard questions. I would like to thank Dr. Cristina Sabliov for financially supporting this research and for her stimulating discussions that played a key role in designing this study. I would like to thank my fellow labmates in the Antioxidants Research Laboratory for their invaluable help completing my animal study. My sincere thanks also go to Drs. Lynne Ausman and Edward Saltzman for accepting me into the PhD program and for their much appreciated continued support. Finally, I would like to thank my family and friends for supporting me throughout this experience.

Abstract

Lutein, a fat-soluble xanthophyll, contributes partially to the health benefits from consuming plant foods. Like all dietary carotenoids, lutein has a low bioavailability. In addition to increasing the intake of lutein-rich foods to enhance lutein status, delivery of lutein in polymeric nanoparticles (NP) presents a novel approach to enhancing lutein bioavailability. The overall research objective of this project was to investigate, in rats, the impact of nanoencapsulation using poly(lactic-co-glycolic acid) (PLGA) on the pharmacokinetics of lutein. We also used an *in vitro* cell culture approach utilizing human epithelial colorectal adenocarcinoma (Caco-2) cells grown in both conventional (CONV) and permeable support (PS) systems to investigate the impact of PLGA-NP on the absorption of lutein in intestinal cells.

In chapter one, we compared the efficacy of lutein absorption *in vitro* using Caco-2 cells grown in both CONV and PS systems. We further examined the role of the micelle, the physiological vehicle for lutein within the small intestine, on its intestinal absorption *in vitro* compared to an organic solvent, ethanol, which is safe and consumed by humans. The finding from this study demonstrated that the CONV system displayed a larger efficacy of lutein uptake by Caco-2 cells. Further, in the PS system, micelle components appeared to facilitate more effective intestinal secretion of lutein. These findings suggest that lutein uptake by Caco-2 cells is subject to the influence of culturing system (CONV vs. PS) and delivery vehicle (ethanol vs. micelle).

Chapter two examined the impact of PLGA-NP in rats on lutein pharmacokinetics in plasma and distribution in selected tissues as compared to free lutein. We also investigated the effect of nanoencapsulation on the absorption of lutein in intestinal cells compared to a more physiological vehicle, the micelle, using the PS method. In addition, we explored the need of additional micelles for the ultimate absorption of lutein loaded in a water soluble NP. The findings of the rat study indicated that, compared to free lutein, PLGA-NP improved the pharmacokinetics (C_{max} and AUC) of lutein in the plasma of rats and in general promoted lutein accumulation in mesenteric adipose tissue and spleen but not liver. Yet, compared to micellized lutein, although NP improved the maximal concentration of lutein in the plasma of rats as well as in selected tissues it decreased the cell uptake and secretion of lutein in Caco-2 cells. The negative effect of the NP on cell uptake and secretion was partially remedied by the addition of micelle components. These findings suggest that the delivery of lutein within polymeric NP appears to be a promising approach to improving the bioavailability of lutein in rats. The inconsistent results between the rat and cell culture models warrant further investigations to determine which approach better predicts responses in humans. Further, bile salts and phospholipids, which are necessary to stimulate synthesis and secretion of chylomicrons, appear to facilitate more effective intestinal secretion of PLGA-NP lutein.

In summary, with Caco-2 cells cultured in the PS system reliably grown to display phenotypes and functions of enterocytes in the small intestine, this *in vitro* platform enables the generation of information that is closer to the physiology of the absorptive enterocytes. However, although the CONV system has the physiological attributes of colonic tissue, it appeared to display a greater efficacy of lutein uptake by Caco-2 cells which can provide a rapid preliminary tool for methodology development for nutrient absorption studies. Further, the delivery of lutein in polymeric NP appears to be a promising approach to improve the bioavailability of lutein *in vivo* but raises issues with regard to the comparability and the predictive value of *in vitro* models to *in vivo* responses.

Table of Contents

List of Tables and Figures

Review of the Literature

Chapter 1: Development of a Cell Culture Model to Examine Fat-Soluble Nutrient Absorption In Vitro

Chapter 2: The Divergent Impact of Polymeric Nanoparticles on the Bioavailability of Lutein In Vivo and In Vitro

I. Thesis Objectives

Introduction

A growing body of evidence shows an inverse association between the intake of certain phytochemicals and a reduced risk of chronic diseases such as cancer and cardiovascular disease. However, achieving potential health benefits via foods and beverages is limited by their general low intakes and bioavailability. Since educational strategies to encourage greater intake of colorful plant foods have not been successful for attaining the maximal health benefits, novel strategies are required to help enhance their bioavailability and reach target tissues. Nanotechnology, a technology involving the formation of bioactive carriers with diameters ranging from 1-1000 nm has shown potential for improving the efficiency of the delivery and controlled release of various drugs and has recently offered opportunities for food applications.

To better understand the application of nanotechnology and to address issues of bioavailability and delivery of a bioactive compound, confirmation that encapsulation in nanocarriers enhances absorption and deposition in target tissues compared to the corresponding unmodified form is necessary. This current study addressed this knowledge gap by investigating the central hypothesis that nanoencapsulation using a polymer matrix will improve the bioavailability of a bioactive compared to its unmodified form.

Phytochemicals are generally classified as carotenoids, polyphenols, alkaloids, nitrogen-containing compounds, and organosulfur compounds. The most studied of the phytochemicals are the polyphenols and carotenoids. We selected EGCG (a water soluble flavanol found in green tea) and lutein (a fat soluble xanthophyll found in green

leafy vegetables) to test the hypothesis that nanoencapsulation will improve the bioavailability of a hydrophilic and hydrophobic phytochemical. A series of pilot studies were performed by our collaborator, Dr. Cristina Sabliov at the Louisiana State University to establish the feasibility of entrapping the bioactives in polymeric nanoparticles (NP). Given the low entrapment efficiency for EGCG of 0.4%, we estimated that the lowest dose of poly(lactic-co-glycolic acid) (PLGA)-NP EGCG that could be reliably detected in plasma would likely be unfeasible. Thus, we focused our investigation on lutein which has an NP entrapment efficiency of ~75%. It should be noted that Dr. Sabliov has conducted *in vitro* gastrointestinal stability and toxicity studies in rats on the PLGA-NP lutein (results not shown).

Project Objective

The overall research objective of this project was to investigate the impact of nanoencapsulation using PLGA on the pharmacokinetics of lutein in rats. We also used an *in vitro* cell culture approach to investigate the impact of PLGA-NP on the absorption of lutein in intestinal cells. Our central hypothesis was that polymeric nanoencapsulation would increase the bioavailability of lutein compared to its unmodified form and was tested by pursuing the following specific aims:

Specific Aim 1: To investigate the extent to which polymeric nanoencapsulation will increase the bioavailability of lutein in rats. Our working hypothesis was that nanoencapsulation using PLGA would enhance the bioavailability and modulate the pharmacokinetics of lutein when compared to its unmodified form.

Bioavailability was determined by evaluating the pharmacokinetics (C_{max}, T_{max}, and AUC) in plasma and its distribution in selected tissues.

Specific Aim 2: To investigate the extent to which polymeric nanoencapsulation will increase the absorption of lutein in modeled intestinal cells without the assistance of micelle components. Our working hypothesis was that nanoencapsulation using PLGA would increase lutein uptake into and secretion from the cell compared to a more physiological vehicle, the micelle. We further hypothesized that additional micelle components would not be needed for the ultimate absorption of PLGA-NP lutein. We tested our hypothesis utilizing human epithelial colorectal adenocarcinoma (Caco-2) cells grown in both conventional and permeable support systems.

Significance

A better understanding of the pharmacokinetic properties of bioactive compounds in NP has the potential to promote human health. The major challenge of bioactive compounds includes their poor oral bioavailability (which may be due in part to poor water solubility), gastrointestinal stability, and/or intestinal absorption. Thus, novel delivery systems are needed to resolve these problems. With an enhanced *in vivo* absorption and circulation of bioactive food components resulting from the use of nanoencapsulation methodologies, the desired concentration and biological activity of these compounds could be achieved *in vivo*. While enhanced bioavailability may be beneficial, there is a risk for overconsumption and potential toxicity. Additionally, nutrient-nutrient and drug-nutrient interactions could become more prevalent. Thus, a greater understanding of the

metabolic consequences of nutrients in novel food systems is required as nanotechnology applications expand in the food science industry. With an enhanced bioavailability and efficacy of lutein in polymeric NP (as compared to unmodified lutein) in animal models and longer-term in humans, the current studies could fuel the development of other water-soluble nanoencapsulated fat-soluble compounds.

II. Review of the Literature

Introduction

Findings from numerous epidemiological studies and recent clinical trials provide consistent evidence that diets rich in plant-based foods and beverages can reduce the risk of chronic disease (Dauchet et al. 2006; Hung et al. 2004; Bazzano et al. 2003; He et al. 2004; Smith-Warner et al. 2003). In addition to fiber, vitamins, and minerals, thousands of phytochemicals appear to contribute to this benefit. Research conducted during the last 30 years has revealed that phytochemicals contribute to the promotion of health and reduction in the risk of common chronic diseases (Liu 2003). It is estimated that over 25,000 phytochemicals have been identified, but the potential benefits of a large percentage of these compounds remains unknown. Phytochemicals can be classified as carotenoids, polyphenolics, alkaloids, nitrogen-containing compounds, and organosulfur compounds. The most studied of the phytochemicals are the polyphenolics and carotenoids (Liu 2004).

Polyphenols are moderately water-soluble, secondary metabolites which aid in growth, reproduction and resistance to pathogens, predators, and diseases (Beckman 2000). They also contribute to the color and organoleptic properties of plants. In addition to their role in plants, polyphenols are known for their putative beneficial effects on human health via multiple mechanisms including antioxidation, anti-inflammation, up-

regulation of detoxification pathways, and modulation of cell signal transduction (Nijveldt et al. 2001). Prospective cohort studies have shown an inverse correlation between the consumption of polyphenol-rich fruits and vegetables and the risk of major non-communicable diseases such as cancer, cardiovascular disease, type 2 diabetes mellitus, neurodegenerative diseases, and osteoporosis (McCullough et al. 2012; Gao et al. 2012; Wedick et al. 2012; Geybels et al. 2013). Dietary polyphenolics are classified into different groups as a function of the number of phenol rings that they contain and on the basis of structural elements that connect these rings to one another (Scalbert and Williamson 2000). These compounds are typically categorized into four classes: flavonoids (including the subclasses: anthocyanidins, catechins, flavones, flavonols, flavanones, and isoflavones), coumarins, stilbenes, and tannins, although other dietary constituents (i.e., chalcones and lignans) also have polyphenolic structures. Structures of the 4 polyphenols relevant to the studies in the current work are shown in Fig. 1. The main sources of polyphenols in the human diet are fruits, plant-based beverages (especially tea, coffee, wine and fruit juices), chocolate and, to a lesser extent, vegetables, cereals, legumes, and nuts (Bravo 1998; Scalbert et al. 2005).

Carotenoids are a family of fat-soluble pigmented compounds that are synthesized by plants and contribute to their photosynthetic machinery and protection against photo-damage. Aside from their antioxidation and anti-inflammation properties, carotenoids have received substantial attention because of their provitamin A activity and light-filtering functions (Stahl and Sies 2003; Biesalski et al. 2007; Chatterjee et al. 2012; Stahl and Sies 2012). Carotenoid intake has been inversely associated with an array of chronic diseases, such as cardiovascular disease, some forms of cancer, cataracts, cognitive dysfunction, and age-related macular degeneration (AMD) (Fiedor and Burda 2014; Jomova and Valko 2013; Meyers et al. 2014). Dietary carotenoids are

classified into different groups as a function of the modifications in the parent 40-carbon polyisoprenoid structure (Britton 1995). They are typically categorized into two classes: carotenes (α-carotene, β-carotene, and lycopene) and xanthophylls (β-crypotoxanthin, lutein, and zeaxanthin). More specifically, α-carotene, β-carotene, and β-crypoxanthin are provitamin A carotenoids and can be cleaved, after consumption, to retinol by the intestinal and hepatic enzyme, β-carotene 15,15'-oxygenase (BCO1) (Lindqvist and Andersson 2002). Lutein, lycopene, and zeaxanthin cannot be converted to retinol, so they have no vitamin A activity. The structures for lutein and β-carotene are shown in Fig 2. The main sources of carotenoids in the human diet are deeply pigmented fruits, juices and vegetables (Mangels et al. 1993; Campbell et al. 1994).

Phytochemical intake is low in the U.S. because fewer than 10% of people report eating the number of servings of fruits or vegetables recommended by the Dietary Guidelines for Americans (Kimmons et al. 2009). Using data from the U.S. National Health and Examination Survey, Chun et al. (2007) estimated that the mean daily total flavonoid intake (the most common polyphenol class obtained from typical American diets) was 189.7 mg/d. This level of consumption is considered below the intermediate range of intake (250-750 mg/d) shown to be associated with lower risk of death related to cardiovascular disease (McCullough et al. 2012). The median daily intake for carotenoids in the United States is 1.5 mg/d for lutein and zeaxanthin and 1.7 mg/d for β-carotene (Monsen 2000). These intakes are considered to be low when compared with levels (~6-10 mg/d) necessary to decrease the risk of AMD (Richer et al. 2004; Mares-Perlman et al. 2001).

While increased consumption of phytochemical-rich fruits, vegetables, and whole grains (as well as beverages derived from these foods) would serve to enhance their concentrations in blood and tissues, additional strategies for enhancing their

bioavailability are being considered to maximize their health benefits. For example, co-consumption of polyphenols with selected fats, proteins, or inhibitors of phase II metabolism (such as piperine) (Scheepens et al. 2010; D'Archivio et al. 2010) may act to increase their absorption in the small intestine. Further, , chopping and sautéing carotenoid-rich vegetables will help to release carotenoids from the chloroplasts and plant tissue and co-consumption with lipids improves the efficiency of micellarization to enable uptake by enterocytes (Yeum and Russell 2002). Besides the aforementioned food synergies and manipulations, encapsulation of phytochemicals with nanomaterials presents a novel alternate approach with several advantages such as gastrointestinal protection, controlled release, and targeted delivery to selected tissues (Nair et al. 2010; Acosta 1995; Bonifácio et al. 2014; Ma et al. 2012; Bennet et al. 2014).

Bioavailability of Phytochemicals

In pharmacology, bioavailability is a subcategory of absorption and is defined as the fraction of an administered dose of unchanged drug that reaches the systemic circulation (Chen et al. 2001). In nutrition science, which covers the intake of essential nutrients and other dietary constituents, the concept of bioavailability lacks the well-defined standards commonly used for drugs. In contrast to most drugs, the absorption, distribution, and utilization of nutrients (including phytochemicals) are subject to the influence of the steady-state status of the nutrient and physiological state of the subject (Heaney 2001). Therefore, bioavailability for nutrients can be defined as the proportion of the consumed substance being absorbed and available for use or storage (Srinivasan 2001). Nevertheless, nutrikinetic parameters overlap substantially with pharmacokinetic parameters such as area under the plasma time curve (AUC), peak plasma concentration (C_{max}), time to reach C_{max} (T_{max}), and time required for the concentration to

reach half its original value or elimination half-life ($T_{1/2}$) (Raghuram et al. 1992), so the latter pharmacokinetic parameters will be used throughout this review. The relative oral bioavailability between two formulations of the same compound can be measured by comparing the bioavailability (estimated as AUC) per dose of each formulation. The pharmacokinetics of a compound is the collective function of four processes: absorption, distribution, metabolism, and excretion (ADME) (Thomas et al. 2006). Intrinsic and extrinsic factors affecting the ADME and, thereby, the consequent bioavailability of a nutrient include the nutrient and its dietary source, its physicochemical properties alone and within the food matrix, gastric emptying rate, permeability across intestinal membranes, and extent of metabolism and distribution throughout the body. In addition to pharmacokinetic parameters, measures of bioactivity, including intermediary biomarkers of physiological function or disease pathogenesis, can be employed for making inferences about bioavailability (Verhagen et al. 2004).

The bioavailability of dietary flavonoids are relatively low, ranging from ≈1% to ≈20% for anthocyanins (Milbury et al. 2010) and isoflavones (Hendrich 2002), respectively. The low bioavailability of most polyphenols has been attributed primarily to the low absorption in the GI tract following consumption, extensive biotransformation within the gut and liver, and rapid clearance from the body (see Fig. 3 for a schematic of the ADME of flavonoids). Many dietary flavonoids are found as glycosylated compounds, and this form may diminish diffusion across barriers in the GI tract (Scalbert and Williamson 2000). Many flavonoids are labile under the acidic condition of the stomach and alkaline condition of the small intestine, resulting in dramatically less flavonoid reaching the enterocytes for absorption after consumption (Bermúdez-Soto et al. 2007). For example, the flavanol epigallocatechin-3-gallate (EGCG) is stable in acidic pH but easily oxidized in neutral or basic pH conditions; in a pH 7.4 solution, half of an EGCG

concentration is lost within 2 h (Krook and Hagerman 2012). During absorption, polyphenols are extensively transformed via phase II pathways, predominately methylation, glucuronidation, and sulfation, in enterocytes of the small intestine and then further metabolized in the liver (Scalbert and Williamson 2000). For example, absorption of quercetin glucosides is quite high (≈50%), whereas its excretion in urine is low (<1%), indicating extensive transformation of quercetin via phase II metabolism (Manach et al. 1998). Such biotransformation facilitates quick polyphenol excretion from the enterocytes via the phase III transporters, the liver via the bile, and the body through urine. Generally, polyphenols, including most flavonoids, have a $T_{1/2}$ of ≈1-3 h (Manach et al. 2005).

The bioavailability of dietary xanthophylls is also relatively low. Their peak plasma concentration assessed using a stable isotope tracer approach has been shown to account for ~2.0-9.4% of the dose (Novontny et al. 2005; Kurlich et al. 2003; de Moura et al. 2005; Lienau et al. 2003). The low bioavailability has been attributed to many factors including co-consumed foods and their fat content, binding to elements of the food matrix, efficiency of micellarization in the small intestine, and transport to the lymph system (see Fig. 4 for a schematic of the ADME of xanthophylls). Many dietary carotenoids are found noncovalently bound to protein or fiber within plant foods. It has been suggested that these proteins have an inhibitory effect upon digestion and absorption (Sila et al. 2012). Castenmiller et al. (1999) reported that the relative bioavailability from whole-leaf and minced spinach is 45-55% compared with that of a supplement. Released xanthophylls must then be assimilated into mixed micelles in the lumen of the small intestine which act as a polar carrier through the hydrophilic chyme in the intestine to the mucosal cell surface. The micellarization of lutein utilizing the *in vitro* digestion model is 25-40%, with the efficiency of the reaction modulated by micelle

components, i.e., bile acids and dietary lipids (Garrett et al. 1999; Sy et al. 2012; Brown et al. 2004; van Het Hof et al. 2000). The suggested optimum dietary fat content to promote carotenoid absorption is 3-5 g (Roodenburg et al. 2000). Further, the type of fat present in the diet can affect carotenoid bioavailability. Studies suggest that monounsaturated olive oil, which is rich in oleic acid, improves the absorption of lutein in rats (Lakshminarayana et al. 2007 and 2009). Lutein has also been shown to be more bioavailable in eggs compared to supplements or spinach since the lutein is located in a digestible lipid matrix similar to a micelle composed of cholesterol, triglycerides, and phospholipids (Chung et al. 2004). Other dietary components, such as dietary fiber and other carotenoids, can suppress lutein absorption, possibly by entrapping carotenoids or by interacting with bile acids, which results in increased fecal excretion (Yeum and Russell 2002; Mamatha and Baskaran 2011). Once solubilized into a micelle, uptake into the intestinal mucosa involves passive diffusion or facilitated transport through cholesterol transporters (Reboul et al. 2011; Narushima et al. 2008; Reboul 2013). A fraction of lutein within enterocytes may efflux back into the intestinal lumen possibly via ATP-binding cassette transporter ABCG5 or multi-drug resistance 1 (Herron et al. 2006; Gyémánt et al. 2006). The final step in lutein absorption is assimilation into chylomicrons and secretion into the lymph for systemic distribution. Given the impact of the aforementioned steps, *in vitro* studies have shown that although 7-35% of micellized lutein can be accumulated in intestinal cells, only $\leq$6% is secreted to the basolateral side (Sy et al. 2012; Chitchumroonchokchai et al. 2004).

Although β-carotene is known to be metabolized to vitamin A by symmetric cleavage through action of BCO1 (Lindqvist and Andersson 2002), little is known about the metabolic transformation of nonprovitamin A xanthophylls in the intestine or in other organs such as the liver. The enzymatic oxidation of the secondary hydroxyl group

leading to hydroxyl or keto-carotenoids has been shown to be a common pathway of metabolism predominately in the liver of mice (Yonekura et al. 2010). Other common pathways proposed have included double bond migration leading to meso-carotenoids (predominately in the retina), dehydration products thought to be formed non-enzymatically under acidic conditions in the stomach, or eccentric cleavage by β-carotene 9',10'-oxygenase (BCO2) leading to apo-carotenoids (Khachik 2012; Kotake-Nara and Nagao 2011).

Since nutrient bioavailability must precede bioactivity at tissue sites in the body, a number of strategies have been employed to increase the chemical stability or permeability of nutrients. These approaches for flavonoids usually rely upon the addition of chemical additives such as reducing agents to stabilize chemical structure, dissolving agents to increase solubility (Dube et al. 2010a; Ader et al. 2000), inhibitors of phase I and/or II enzymes to escape biotransformation (Lambert et al. 2004; Brand et al. 2010), modulation of the food matrix or addition of complementary ingredients such as lipids or protein (Lesser et al. 2004), and/or manipulation through conjugation with promoiety groups (Lam et al. 2004). In terms of xanthophylls, chopping and sautéing vegetables will help to release it from chloroplasts and plant tissue, while co-consumption with dietary monounsaturated fats will improve the efficiency of micellarization (Yeum and Russell 2002; Goltz et al. 2012). More recently, encapsulation with food grade or related Generally Recognized as Safe (GRAS) materials that exhibit controlled-release behavior have been used to increase the bioavailability and bioactivity of polyphenols. Encapsulation and controlled-release of active food ingredients can be attained through novel formulations such as microemulsions, matrix systems, solid dispersions, and liposomes (Tan et al. 2013; Cui et al. 2009; Pralhad and Rajendrakumar 2004; Yuan et al. 2006; Musthaba et al. 2009). However, because of the concerns and/or limitations

associated with the safety and stability of these approaches (Windrum et al. 2005; Frijlink et al. 1991; Mu and Zhong 2006), nanoencapsulation of phytochemicals has emerged as a novel strategy to improve compound delivery, distribution, and/or bioactivity.

Nanoencapsulation: Characteristics and Formulations

Nanoencapsulation is defined as a technology involving the formation of actively loaded particles with diameters ranging from 1-1000 nm that result in end-products that exhibit properties or phenomena attributable to its dimensions (FDA, http://www.fda.gov). The term nanoparticle (NP) is a collective name for colloidal systems including nanospheres and nanocapsules (Gurley 2011). A nanosphere is a matrix structure in which the active ingredient is dispersed throughout the particles, whereas nanocapsules have a membrane and an active ingredient in the core. Some examples of natural food-derived or GRAS materials that can fulfill these requirements include polysaccharides of plant (i.e., carrageenan) or microbial (i.e., dextran) origin, food proteins (i.e., whey proteins), and emulsifiers (i.e., lecithin). Polymeric NP have been adopted as a preferred method for improving phytochemical bioavailability and distribution because of its higher compound loading capacity and better stability (He et al. 2013). They have proven more stable in the GI tract than other colloidal carriers, such as liposomes and emulsions, so that they protect encapsulated compounds from the conditions of the GI environment (Brannon-Peppas 1995). The use of various polymeric materials enables the modulation of physiochemical characteristics (i.e., hydrophobicity, zeta potential), compound release properties (i.e., delayed, prolonged, triggered), and biological behavior (targeting, bioadhesion, cellular uptake) of NP (Soppimath et al. 2001). Moreover, the submicron

size of NP and their large surface area favor their absorption compared to larger carriers (Jani et al. 1990; Desai et al. 1996).

Polymeric materials used for the formulation of NP include synthetic poly(lactic acids) (PLA), poly(lactic-co-glycolytic acid) (PLGA), poly(ε-caprolactone) (PCL), poly(methyl methacrylates), and poly(alkyl cyanoacrylates) or natural polymers (albumin, gelatin, alginate, collagen, or chitosan). Synthetic polymers with precise chemical composition display highly predictable physical properties such as solubility, permeability, degradation, and erosion, as well as targeting behavior. Natural polymers, besides being less predictable, are also often mildly immunogenic (des Rieux et al. 2006). Among the different synthetic polymers developed to formulate polymeric NP, PLGA has attracted considerable attention due to its high biodegradability (Kumari et al. 2010). PLGA decomposition yields lactic acid ("milk acid") and glycolic acid ("fruit acid") monomers. Because these two compounds are present in the diet and are easily metabolized via the Krebs cycle, systemic toxicity is presumed to be unlikely with the use of PLGA for nutrient encapsulation. In addition, the polymers are commercially available with different molecular weights and copolymer compositions allowing the degradation to vary from several months to several years. PLA has also been employed for nutrient-based NP, but to a lesser extent than PLGA due to its lower degradation rate.

Transport of Polymeric NP across Intestinal Mucosa

Besides protection from the environment in the GI lumen, strategies have been developed to improve the bioavailability of compounds encapsulated in polymeric NP, focusing principally on approaches to facilitating transport across the intestinal mucosa and enhancing uptake into intestinal cells. For food-related applications, two types of

intestinal cells are most involved in bioavailability: 1) enterocytes, the absorptive cells representing the majority of the GI tract lining, and 2) microfold ("M") cells, mainly located in the follicle-associated epithelium of the Peyer's patch. In contrast to normal enterocytes, M cells lack microvilli on their apical surface but possess broader microfolds with the ability to transport antigens from the lumen via endocytosis or phagocytosis to the basolateral side for processing by immune cells. M cells do not secrete mucus or digestive enzymes and have a small or absent glycocalyx, an extracellular polysaccharide layer found on enterocytes. M cells represent ≈1% of the intestinal surface area.

The mechanisms by which polymeric NP are taken up into intestinal epithelial cells are not entirely clear. There is evidence from *ex vivo* studies in rats and rabbits and from *in vitro* studies in human epithelial colorectal adenocarcinoma cells (Caco-2) that translocation of NP occurs in the villi (Behrens et al. 2002; Reix et al. 2012; McClean et al. 1998; Zhang et al. 2006). However, because of the low endocytic activity of enterocytes, the amount of NP translocated via this route in Caco-2 cells appears minimal (Cartiera et al. 2009; Pietzonka et al. 2002). Thus, the bulk of NP translocation may occur across M cells in the Follicle Associated Epithelium (des Rieux et al. 2005; des Rieux et al. 2007). Hillery et al. (1994) studied the uptake of 60 nm polystyrene particles by gut epithelial cells in female Sprague Dawley rats after 5 d of oral dosing via gavage and found only 10% of the administered dose to be recovered from the entire GI tract. They estimated that 60% of this uptake occurred through the lymphoid aggregates of the Peyer's patches.

Two major obstacles affecting the transport of compounds across the intestinal mucosa are GI transit time and mucus layer barriers. Thus, the absorption of a phytochemical could be improved if its residence time in the gut were to be increased

and its permeability through mucus layers was enhanced. Research efforts are underway to develop mucoadhesive and muco-penetrating NP. Electrostatic interaction is one of the more exploited forms of mucoadhesion, as exemplified by use of chitosan, a cationic natural polymer obtained from deacetylation of chitin, for a variety of oral delivery applications (Chae et al. 2005; Thanou et al. 2001). However, chitosan is only soluble in acidic environments, so its effectiveness is diminished in the slight alkaline environment in the rat small intestine and in Caco-2 cells (Sonaje et al. 2009; Sonaje et al. 2012). A potential solution to the limitation with chitosan is N-trimethyl chitosan chloride (TMC), a derivative that is soluble in neutral and basic environments (van der Merwe et al. 2004). Alternatively, mucoadhesion can also be achieved via conjugation with ligands that recognize particular mucin glycoproteins. For example, wheat germ agglutinin (WGA) from *Tricticum vulgare* specifically binds to N-acetyl-D-glucosamine and sialic acid on the cell surface. WGA conjugated PLGA-NP has been found to bind *in vitro* to the surface of Caco-2 cells as well as *ex vivo* and *in vivo* to the intestinal villous epithelium and Peyer's patches of rats; these NP may also be taken up into cells via receptor-mediated endocytosis involving the epidermal growth factor receptor that is expressed at a considerable density on enterocytes (Weissenboeck et al. 2004; Yin et al. 2007).

Although mucoadhesion originally appear as a promising approach for increasing absorption, these NP adsorb to mucin fibers and so are not efficient in reaching the surface of the enterocyte. As GI mucus has a turnover time of 4-5 h, those NP bound to mucus are excreted rapidly (Galindo-Rodriguez et al. 2005; Bernkop-Schnürch et al. 2005). Hence, this approach will be unsuccessful unless the encapsulated compound is readily released from the NP at the site of absorption and can directly reach the enterocyte. To achieve a longer residence time of NP at mucosal surfaces, especially for

particle systems that require intact intracellular delivery, attempts have been made to develop mucus penetrating particles. One approach has been to synthesize particles with a strong hydrophilicity and neutral charge that mimics the essential surface properties of viruses which allow them to avoid mucoadhesion. Densely coating biodegradable particles with poly(ethylene glyocol) [PEG], an uncharged hydrophilic polymer, has been demonstrated to minimize adhesive interactions between NP and mucins (Vila et al. 2002; Lai et al. 2009). This approach appears to allow NP to rapidly penetrate human mucus by moving through openings between mucin mesh fibers (Huang et al. 2000; Tobío et al. 2000; Yoncheva et al. 2007).

A macromolecule or NP can theoretically cross the intestinal epithelium by paracellular (between adjacent cells) and/or transcellular routes. However, under normal physiological conditions, the overall efficiency of the paracellular route is limited because of the small surface area of the intercellular spaces and the tightness of the junctions between the cells (Anderson 2001). So, the transcellular route has been the most explored for NP translocation. Transport of NP by the transcellular pathway is especially dependent on factors associated with the physiochemical properties of particles, such as size, zeta potential, and surface hydrophobicity. For example, NP transcytosis increases as the particle diameter decreases (Jani et al. 1990; Desai et al. 1996). However, while the available data from Caco-2 cells and rat models on the effect of charge and hydrophobicity using a variety of NP are not consistent, there is agreement that NP surface properties are a critical aspect of developing NP that will enhance oral delivery (Vila et al. 2002; Behrens et al. 2002; Shakweh et al. 2004; Jung et al. 2000). In addition to their mucoadhesive properties, the use of water soluble polymers (such as chitosan and TMC) in Caco-2 cells and in rats do appear to be useful strategies to enhance paracellular transport of compounds alone (Sonaje et al. 2009; van der Merwe et al.

2004). The mechanism for paracellular transport appears to be the formation of entanglements and chemical bonds between the negatively charged cell membrane and the positively charged polymer or by complexing the Ca^{2+} involved in the structure of tight junctions (Smith et al. 2004; Sonaje et al. 2012). The results of previous studies, also conducted in Caco-2 cells and in rats, suggest that the transport is inversely related to molecular weight and is reversible (Chae et al. 2005).

With the challenge of overcoming obstacles to the intestinal uptake and transport of NP delivery systems, strategies are also being pursued that will prolong the $T_{1/2}$ to allow for a greater uptake into target tissues. Hydrophobic particles are generally perceived by the body as foreign. The reticulo-endothelial system (RES) eliminates these particles from the circulation and moves them to the liver or spleen. This RES process presents one of the most important biological barriers to NP systemic delivery (Kumari et al. 2010). To address this issue, NP can be coated with molecules that hide the hydrophobicity by providing a hydrophilic layer on the particle surface. The most common moiety for surface modification is the hydrophilic and non-ionic polymer PEG. In animal models, the attachment of PEG, mostly to injectable polymeric NP, can increase $T_{1/2}$ by several orders of magnitude (Owens and Peppas 2006). Surface modification can also be used to target NP toward specific organs and increase selective cellular binding and internalization through receptor-mediated endocytosis. As noted, surface charges of NP have an important influence on their interaction with and uptake into cells, such as the human dendritic cell line (Foged et al. 2005; Vasir and Labhasetwar 2008). Positively charged NP's seem to be able to escape the lysosomes after being internalized and exhibit perinuclear localization in a variety epithelial, fibroblastic, endothelial, and blood cell lines (Yue et al. 2011). Further, targeted ligands can be grafted at the NP surface (Alexis et al. 2008).

Polymeric NP as Potential Delivery Systems of Phytochemicals

A growing body of literature reveals a careful characterization of the *in vitro* stability and absorption profile of polymeric NP encapsulated phytochemicals. A much more limited number of animal model studies have examined the *in vivo* pharmacokinetic profiles of free versus NP bioactives (Table 1). ADME data from human studies of phytochemicals in NP formulations is not available. A discussion of experimental studies conducted to date using mostly polymeric NP as a potential delivery system for selected bioactives follows. In order to provide a comprehensive discussion of studies to date, the selected bioactives include but are not limited to flavonoids and xanthophylls. It is noteworthy that a more limited number of the selected phytochemicals studied to date include lipid soluble compounds.

i**. Epigallocatechin-3-gallate**

EGCG, a water-soluble flavanol, is found predominately in green tea leaves (*Camellia sinensis*) and has been associated with an array of health benefits that include reductions in the risk for some forms of cancer, cardiovascular disease, type 2 diabetes mellitus, and osteoporosis. EGCG is highly susceptible to degradation in the intestinal milieu and via oxidative processes (Mochizuki et al. 2002); i.e., 80% of EGCG was degraded after the incubation for 1 h in a simulated intestinal fluid at pH 7.4 (Dube et al. 2010a). Efforts to promote the intake, enhance the stability, and increase bioavailability of EGCG are being explored with the intent to incorporate it into NP for formulation into novel foods. Dube et al. (2010a, 2010b, 2011) conducted a series of studies to evaluate the efficacy of chitosan tripolyphosphate NP (size, 165 nm; zeta potential, 33 mV) in EGCG stability and bioavailability. Dube et al. (2010a) found that EGCG incubated in an alkaline solution (50 mM KH_2PO_4 buffer, pH 7.4), took 10 and 40 min for pure and

chitosan tripolyphosphate EGCG to degrade to 50% of their initial levels, respectively. Using an *ex vivo* mouse jejunum segment mounted in Ussing chambers, Dube et al. (2010b) found that chitosan tripolyphosphate EGCG at 6.2 mg/mL (size, 440 nm; zeta potential, 25 mV) exhibited a 1.8-fold greater absorption rate than the same dose of free EGCG. Using mice, these investigators also examined *in vivo* the absorption of 0.76 mg/kg BW chitosan tripolyphosphate EGC (size, 440 nm) and found that the chitosan-NP increased the relative oral bioavailability by 1.5 fold compared to the same dose of free EGCG (Dube et al. 2011); the C_{max} increased by 1 fold but the T_{max} was not different between the NP and the pure compound. Further, a 2.3-fold increase in the apparent exposure of encapsulated EGCG was evident in the jejunum tissue at 2.5 h compared to free EGCG, however, at 1.5 and 5 h, the concentrations were similar. Nonetheless, the EE of EGCG in this series of experiments was only 0.05%, a concentration that would not be practical for food applications.

Surface modification with chitosan has been shown to enhance absorption via permeation through the paracellular route (George and Abraham 2006). Tang et al. (2012) developed green tea flavanol mixtures (including EGCG, epicatechin gallate, epigallocatechin, and epicatechin) loaded into a poly-(γ-glutamic acid) γ-(PGA)-chitosan NP (size, 140 nm; zeta potential, 33.5 mV) with an EE of 13.8-23.5% and monitored the *in vitro* paracellular permeability through Caco-2 cells. A decrease in transendothelial electrical resistance (TEER), an indicator of monolayer integrity, was utilized as a measure of paracellular permeability. TEER values of Caco-2 cell monolayers incubated for 2 h with free flavanols showed no significant differences when compared to the control group; however, incubation of the encapsulated tea flavanols on the apical side, at pH 6.6 (intestinal pH) for the same duration led to an immediate and pronounced reduction in TEER. After removal of the incubated NP, a gradual increase in TEER

values was observed up to 20 h. Free tea flavanols transported across the Caco-2 cells were ≤6% but incubation with NP lead to enhancement of transported tea catechins to ≈24%. This reduction in TEER followed by an increase in transport with NP incubation (compared to free catechins) suggest that the NP led to an increase in paracellular permeability resulting in an enhancement of transport of the tea flavanols. The gradual increase in TEER subsequent to removal of the NP suggests that the paracellular permeability is reversible.

In addition to enhancing systemic bioavailability, nanoencapsulated EGCG has been shown to provide improved bioactivity. Siddiqui et al. (2009) evaluated the potential of PLA-PEG-NP EGCG (size, 260 nm; zeta potential, -7.92 mV) for the chemoprevention of prostate cancer (androgen -responsive 22rv1 cell xenografts) in athymic nude mice that received 100 µg PLA-PEG EGCG, 1 mg pure EGCG or no treatment 3 times weekly IP. At 45 d post-inoculation, the tumor volume in the control mice was 1.8- and 1.5-fold larger than NP or free EGCG, respectively (P <0.01). In order to achieve comparable tumor growth inhibition, a 10-fold lower dose of NP EGCG was required (compared to free EGCG). The mean serum specific antigen (PSA) level of the control mice was significantly higher, at 3 and 11 fold, compared to the NP and free EGCG groups, respectively.

ii. **Carotenoids**

Carotenoids are a family of fat-soluble pigmented compounds which are ubiquitous in plants foods and display a diverse array of bioactivity, i.e., anti-oxidation and anti-inflammation. While carotenoids are poorly absorbed, due in part to their poor water solubility, the effect of nanoencapsulation on its pharmacokinetic profile *in vivo* has yet to be tested. Yet, in a feeding study with male Swiss albino mice, Arunkumar et al. (2013)

examined the effect, after a single incubation period, of 200 μM lutein (a xanthophyll carotenoid) chitosan triphosphate NP (size, 80-600 nm; EE, 85%) on postprandial lutein levels compared to lutein in mixed micelles. Lutein levels after the oral administration increased in plasma, liver and eye by 53.5, 53.9, and 62.8%, respectively, as compared to the control. Further, Yi et al. (2014) examined the effect of various food protein stabilized solid lipid nanoparticles [sodium caseinate (SC), whey protein isolate (WPI), or soy protein isolate (SPI); size, 75-90 nm; EE, 99%] on the *in vitro* intestinal cellular uptake of 5 μg/ml β-carotene, a carotene carotenoid. Following a 24 h incubation, the cellular uptake of β-carotene by Caco-2 cell monolayers was increased by 2.6, 3.4, and 1.7 fold, respectively, by SC, WPI, and SPI, as compared to the free form. This limited data provides promising evidence that further investigation is needed on the effect of nanoencapsulation on carotenoid bioavailability.

iii. **Curcumin**

Curcumin, found particularly in turmeric (*Curcuma longa*), has been associated with a variety of health benefits that include antioxidant actions to reduce oxidative stress, chemopreventive or cancer therapeutic effects mediated by a capacity for anti-angiogenesis, anti-inflammatory effects associated with the prevention or treatment of chronic conditions including cardiometabolic diseases and acute anti-allergic responses, and enhancement of immune responses to modulate autoimmune disorders. However, as a lipophilic polyphenol, curcumin is poorly absorbed due to its low stability and solubility in the GI tract (Tønnesen 2002). Since the maximum solubility of curcumin in an aqueous buffer (pH 5.0) is 11 ng/mL, several efforts have been undertaken to promote the stability and bioavailability of curcumin with NP formulations.

In a pharmacokinetic study with male Sprague Dawley rats, Shaikh et al. (2009) found that 100 mg/kg body weight (BW) curcumin-PLGA-NP (size, 242 nm; entrapment efficiency (EE), 76.9%; zeta potential, -4.27 mV) increased relative oral bioavailability (AUC/dose) by 25.8 fold (as compared to free curcumin at a dose of 250 mg/kg BW). In addition, the authors reported that the T_{max} and C_{max} of the curcumin NP were increased 4- and 3-fold, respectively. Consistent with the results from Shaikh et al. (2009), Tsai et al. (2011) found the relative oral bioavailability of curcumin-PLGA-NP in the same animal model at a dose of 50 mg/kg BW (size, 158 nm; EE, 46.6%; zeta potential, -12 mV) to be 22.8-fold larger than that of pure curcumin at a 20-fold larger dose. The greater urinary curcumin excretion and a 50% reduction in curcumin elimination in feces in the rats given curcumin-PLGA-NP (as compared to the free form) provided further evidence that NP enhanced curcumin absorption. Interestingly, despite the fact that C_{max} increased 2 fold, T_{max} remained essentially the same. However, Xie et al. (2011) found that 100 mg/kg BW curcumin-PLGA-NP (size, 200 nm; EE, 92.0%), administered to male Sprague Dawley rats, provided greater relative oral bioavailability, compared to free curcumin, but to a markedly lower degree (5.6 fold) compared to that reported by Tsai et al. (2011); T_{max} and C_{max} were increased by 1.2 and 4.4 fold, respectively. While the factors accountable for the discrepancy between studies are unclear, it is unlikely attributed to the size of NP. Recently, Khalil et al. (2013) investigated the effect of surface modified PLGA-PEG-NP on curcumin circulation time in Wistar rats. They observed that both PLGA (size, 161 nm; EE, 77%) and PLGA-PEG (size, 152 nm; EE, 73%) formulations were able to prolong curcumin release in physiological conditions over time. With respect to the efficiency of improving the oral bioavailability of curcumin, PLGA-PEG provided better results in all of the pharmacokinetic parameters compared to PLGA alone. For example, compared to 50 mg/kg BW free curcumin provided in an

aqueous solution, the PLGA and PLGA-PEG-NP at the same dose increased the relative oral bioavailability of curcumin by 15.6 and 51.6 fold, respectively; the T_{max} was extended by 4 and 6 fold and the C_{max} was increased by 3 and 7.5 fold, respectively. These differences in pharmacokinetics between the PLGA and PLGA-PEG NP may have resulted from the longer time of systemic circulation. Further research is required to evaluate the comparative efficacy of PLGA and PLGA-PEG for other polyphenols.

In addition to improving the pharmacokinetic profile, polymeric NP has been shown to improve the bioactivity of curcumin. Yallapu et al. (2010) found 2- and 6-fold increases in the cellular uptake of 2-8 μM doses of curcumin-PLGA-NP (size, 76.2 nm; EE, 89%; zeta potential, 0.06 mV) in cisplatin-resistant A2780CP ovarian and metastatic MDA-MB-231 breast cancer cells, respectively, as compared to the same dose of free curcumin. NP-curcumin, when compared to the free form, also demonstrated superior efficacy in inhibiting proliferation and promoting apoptosis of these two cancer cells *in vitro*. For example, treatment with NP-curcumin resulted in a higher number of cells (5- and 8-fold increases in A2780CP and MDA-MB-231 cells, respectively) that were positive for Annexin V staining (an indicator of cell death) compared to those treated with free curcumin. Similarly, Anand et al. (2010) found that curcumin encapsulated in PLGA-PEG-NP (size, 80.9 nm; EE, 97.5%) was taken up by KBM-5 human chronic myeloid leukemia cells *in vitro* in 5 min as compared to 30 min for the free form. The authors also noted that NP-curcumin was comparable or more potent than free curcumin in inducing apoptosis in leukemic cells and in suppressing proliferation of breast, colorectal, esophageal, and prostate cancer cell lines. NP-curcumin was also more potent than free curcumin in suppressing tumor necrosis factor-induced nuclear factor (NF) κB activation and subsequent NFκB-regulated responses, including cell proliferation (cyclin D1), invasion (matrix metallopeptidase-9), and angiogenesis (vascular endothelial growth

factor). Similarly, Mukerjee and Vishwanatha (2009) reported that PLGA-NP encapsulation (size, 45 nm; EE, 90%) enhanced curcumin uptake into various prostate cancer cells and arrested cell growth and inhibited NFκB activation when compared to free curcumin. These *in vitro* results demonstrate the potential for PLGA-NP as carriers for the oral delivery of curcumin in cancer therapy. However, *in vivo* research will be necessary to confirm the therapeutic efficacy of curcumin encapsulated in PLGA-PEG-NP.

iv. **Quercetin**

Quercetin, a semi-lipophilic flavonol, is ubiquitous in plant foods. Like most flavonoids, quercetin is extensively transformed via phase II metabolism for elimination from the body (Manach et al. 1998). To date, only one pharmacokinetic study is available that examines the efficacy of a non-polymeric NP to improve the oral bioavailability of quercetin. Following oral administration of 50 mg/kg BW quercetin to male Wistar rats, Li et al. (2009) reported that solid lipid (soya lecithin, Tween-80, and PEG) NP (size, 155 nm; EE, 91%; zeta potential, -32 mV) increased the relative oral bioavailability of quercetin by 5.7 fold as compared to free form. The C_{max} and T_{max} of the quercetin NP increased by 2 and 1.6 fold, respectively. Since the bioactivity of quercetin is largely dependent on its metabolites, further research is warranted to evaluate the effect of quercetin encapsulation on its biotransformation in the GI tract and other in other tissues.

While limited information is available on the oral bioavailability of quercetin in polymeric NP, the effect of nanoencapsulation on its antioxidant and anti-inflammatory action has been examined in several studies. Wu et al. (2008) prepared a quercetin NP system with aminoalkyl methacrylate copolymers as a carrier (size, 82 nm; EE, 99%).

They found that the radical scavenging activity of quercetin-NP toward DPPH radicals and superoxide anion was enhanced *in vitro* by 883 and 1377 fold as compared to free form. The quercetin NP was also 59-fold more effective in inhibiting lipid peroxidation reactions. Similarly, Pool et al. (2012) reported that quercetin encapsulated within PLGA (1 and 5 μM) displayed a more potent antioxidant action against peroxyl radical-induced lipid peroxidation and a greater capacity for chelating activity toward transient metals than free quercetin. Ghosh et al. (2009) evaluated the antioxidant activity of a single pretreatment of 2.71 mg/kg BW quercetin-PLGA administered orally to female rats in protecting against injury from reactive oxygen species (ROS) produced in liver and brain tissue 90 min after a subcutaneous injection of arsenite. Oxidative damage was assessed by glutathione, glutathione peroxidase, glutathione transferase, catalase, glucose-6-dehydrogenase, mitochondrial microviscosity, and lipid peroxidation 24 h after the arsenite injection. Quercetin-PLGA provided full protection against the arsenite-induced ROS injury while free quercetin was ineffective. The protection of quercetin-PLGA was ascribed primarily to sequestration of ≥60% of the arsenite deposited in mitochondria of the tissues. The same laboratory reported a synergy between quercetin and meso-2,3-dimercaptosuccinic acid (a hydrophilic arsenic chelator) with respect to protection against arsenic-induced damage in the same animal model when they were encapsulated together in PLGA (Ghosh et al. 2011).

In a rat model, Chakraborty et al. (2012) examined the effectiveness of a single dose of 2.5 mg/kg BW quercetin-PLGA (size, 15 nm; EE, 66%) administered orally prior to an alcohol-induced gastric ulcer in protecting against oxidative damage, mitochondrial integrity, and the up-regulation of matrix metallopeptidase-9 and inducible nitric oxide synthase. The authors reported that quercetin-PLGA prevented 90% of alcohol-induced ulceration as compared to 20% by free quercetin at the same dose. Quercetin-PLGA

maintained the biomarkers of oxidative damage and inflammatory responses in gastric mucosa induced by alcohol at the same level as the negative control. These preclinical findings suggest that the potential therapeutic efficacy of quercetin can be enhanced by nanoencapsulation. More research is necessary to establish the mechanism(s) by which PLGA nanoencapsulation increases quercetin bioactivity, i.e., by protecting quercetin against degradation in acidic environments, increasing overall bioavailability, and/or modifying its metabolite distribution or profile.

v. **Resveratrol**

Resveratrol, a lipophilic stilbene found predominantly in grapes and red wine, displays a diverse array of bioactivity, i.e., chemoprevention or cancer treatment via its roles in cell cycle arrest, differentiation, and apoptosis; anti-inflammation; putative benefits on risk factors for cardiovascular disease and type 2 diabetes mellitus; and “anti-aging” effects. While resveratrol is poorly absorbed, due in part to its low water solubility and unstable chemical nature, the effect of nanoencapsulation on its pharmacokinetic profile *in vivo* has yet to be tested. Using an *in vitro* simulation of GI conditions (an initial 3-h incubation at 37°C in a pH 1.2 buffer, followed by a 33 h incubation at pH 7.4) Neves et al. (2013) tested the concept that resveratrol loaded in a non-polymeric NP [solid lipid NP (cetyl palmitate and polysorbate 60) or a nanostructured lipid carrier (cetyl palmitate, polysorbate 60, and the liquid lipid miglyol-812); size, ~170 nm; EE, ~72%; zeta potential, ~-30 mV] would maintain its chemical integrity in GI tract environment. They found that ≤24% resveratrol in the NP leached in to the GI mimic buffers.

While no pharmacokinetic experiments have been conducted with NP resveratrol, several studies have examined whether polymeric nanoencapsulation enhances its therapeutic potential. Using lipophilic PCL-PEG as a carrier, Lu et al.

(2009) examined the effect of resveratrol-NP (size, 100 nm; EE, 89%) on cell viability, ROS production, and activation of caspase-3 activity (apoptosis) in rat adrenal pheochromocytoma (PC12) cells treated with β-amyloid peptide, an inducer of an Alzheimer's disease model. They found that pretreatment with resveratrol-NP at 10 μM for 12 h provided a significant protection against β-amyloid peptide-induced toxicity while free resveratrol exaggerated the toxicity. The authors postulated that nanoencapsulation facilitated internalization of resveratrol via endocytosis so that resveratrol would not accumulate in the cell membrane where it could induce lipid peroxidation and its sequelae. Similarly, Shao et al. (2009) observed resveratrol encapsulated in m-PEG-PCL copolymer NP (size, 87 nm; EE, 90%; zeta potential, -5.6 mV) was more effective to induce cytotoxicity of rat C6 glioma cancer cells than free resveratrol at the same doses (2-32 μM). The induction of cytotoxicity was in parallel with intracellular ROS generation (determined by a H_2DCFDA dye) and was diminished by the co-treatment of vitamin E as its addition decreased ROS generation. It is worth noting the discrepancy in the effect of resveratrol on ROS production with inhibition in the formal study and promotion in the latter study, probably due to the use of the ROS inducer in the former study and difference in cell lines. These *in vitro* data appear to support application of nanoencapsulation to magnify therapeutic efficacy of resveratrol and decrease its potential toxicity to normal cells.

Conclusion

Research reports from efforts to enhance the bioavailability of dietary phytochemicals provide encouraging evidence for the feasibility of utilizing nanoencapsulation technology. While there is value in carefully characterizing the transport of nanoparticles *in vitro*, potential applications require substantiation of their efficacy and safety *in vivo*.

To date only a limited number of studies using animal models have demonstrated the benefits of nanoencapsulation on absorption, distribution, metabolism, and elimination of phytochemicals. Some studies have demonstrated that increasing the absorption and systemic distribution of bioactives within nanoparticles is associated with higher concentrations within target tissues and/or larger bioactivity. However, the results obtained vary by specific compound and the type and characteristics of the nanoparticle (including its ability to achieve effective entrapment efficiency). Given that a majority of the bioactive constituents studied with NP to date has been water soluble, future studies are warranted to enhance an understanding and application of the properties of more fat-soluble nutrients. Successful "nanonutrient" applications should allow for the development of innovative foods and beverages with a variety of health-promoting and therapeutic functional properties.

References

Acosta E. Bioavailability of nanoparticles in nutrient and nutraceutical delivery. Curr Opin Colloid Interface Sci. 1995; 14:3-15.

Ader P, Wessmann A, Wolffram S. Bioavailability and metabolism of the flavonol quercetin in the pig. Free Radic Biol Med. 2000; 28:1056-1067.

Alexis F, Pridgen E, Molnar LK, Farokhzad OC. Factors affecting the clearance and biodistribution of polymeric nanoparticles. Mol Pharm. 2008; 5:505-515.

Anand P, Nair HB, Sung B, Kunnumakkara AB, Yadav VR, Tekmal RR, Aggarwal BB. Design of curcumin-loaded PLGA nanoparticles formulation with enhanced cellular uptake, and increased bioactivity in vitro and superior bioavailability in vivo. Biochem Pharmacol. 2010; 79:330-338.

Anderson JM. Molecular structure of tight junctions and their role in epithelial transport. News Physiol Sci. 2001; 16:126-130.

Arunkumar R, Harish Prashanth KV, Baskaran V. Promising interaction between nanoencapsulated lutein with low molecular weight chitosan: Characterization and bioavailability of lutein in vitro and in vivo. Food Chem. 2013; 141:327-337.

Bazzano LA, Serdula MK, Liu S. Dietary intake of fruits and vegetables and risk of cardiovascular disease. Curr Atheroscler Rep. 2003; 5:492-499.

Beckman CH. Phenolic-storing cells: keys to programmed cell death and periderm formation in wilt disease resistance and in general defense responses in plants? Physiol. Mol. Plant Pathol. 2000; 57:101-110.

Behrens I, Pena AI, Alonso MJ, Kissel T. Comparative uptake studies of bioadhesive and non-bioadhesive nanoparticles in human intestinal cell lines and rats: the effect of mucus on particle adsorption and transport. Pharm Res. 2002; 19:1185-1193.

Bennet D, Kang SC, Gang J, Kim S. Photoprotective effects of apple peel nanoparticles. Int J Nanomedicine. 2014; 9:93-108.

Bermúdez-Soto MJ, Tomás-Barberán FA, García-Conesa MT. Stability of polyphenols in chokeberry (Aronia melanocarpa) subjected to in vitro gastric and pancreatic digestion. Food Chem. 2007; 102:865-874.

Bernkop-Schnürch A. Mucoadhesive polymers: strategies, achievements and future challenges. Adv Drug Deliv Rev. 2005; 57:1553-1555.

Biesalski HK, Chichili GR, Frank J, von Lintig J, Nohr D. Conversion of beta-carotene to retinal pigment. Vitam Horm. 2007; 75:117-130.

Bohn T. Dietary factors affecting polyphenol bioavailability. Nutr Rev. 2014; Eprint.

Bonifácio BV, Silva PB, Ramos MA, Negri KM, Bauab TM, Chorilli M. Nanotechnology-based drug delivery systems and herbal medicines: a review. Int J Nanomedicine. 2014; 9:1-15.

Brand W, Padilla B, van Bladeren PJ, Williamson G, Rietjens IM. The effect of co-administered flavonoids on the metabolism of hesperetin and the disposition of its metabolites in Caco-2 cell monolayers. Mol Nutr Food Res. 2010; 54:851-860.

Brannon-Peppas L. Recent advances on the use of biodegradable microparticles and nanoparticles in controlled drug delivery. Intern J Pharm. 1995; 116:1-9.

Bravo L. Polyphenols: chemistry, dietary sources, metabolism, and nutritional significance. Nutr Rev. 1998; 56:317-333.

Britton G. Structure and properties of carotenoids in relation to function. FASEB J. 1995; 9:1551-1558.

Brown MJ, Ferruzzi MG, Nguyen ML, Cooper DA, Eldridge AL, Schwartz SJ, White WS. Carotenoid bioavailability is higher from salads ingested with full-fat than with fat-reduced salad dressings as measured with electrochemical detection. Am J Clin Nutr. 2004; 80:396-403.

Campbell DR, Gross MD, Martini MC, Grandits GA, Slavin JL, Potter JD. Plasma carotenoids as biomarkers of vegetable and fruit intake. Cancer Epidemiol Biomarkers Prev. 1994; 3:493-500.

Cartiera MS, Johnson KM, Rajendran V, Caplan MJ, Saltzman WM. The uptake and intracellular fate of PLGA nanoparticles in epithelial cells. Biomaterials. 2009;30:2790-2798.

Castenmiller JJ, West CE, Linssen JP, van het Hof KH, Voragen AG. The food matrix of spinach is limiting factor in determining the bioavailability of beta-carotene and to a lesser extent of lutein in humans. J Nutr. 1999; 129:349-355.

Chae SY, Jang MK, Nah JW. Influence of molecular weight on oral absorption of water soluble chitosans. J Control Release. 2005; 102:383-394.

Chakraborty S, Stalin S, Das N, Choudhury ST, Ghosh S, Swarnakar S. The use of nano-quercetin to arrest mitochondrial damage and MMP-9 upregulation during prevention of gastric inflammation induced by ethanol in rat. Biomaterials. 2012; 33:2991-3001.

Chatterjee M, Roy K, Janarthan M, Das S, Chatterjee M. Biological activity of carotenoids: its implications in cancer risk and prevention. Curr Pharm Biotechnol. 2012; 13:180-190.

Chen ML, Shah V, Patnaik R, Adams W, Hussain A, Conner D, Mehta M, Malinowski H, Lazor J, Huang SM, Hare D, Lesko L, Sporn D, Williams R. Bioavailability and bioequivalence: an FDA regulatory overview. Pharm Res. 2001; 18:1645-1650.

Chitchumroonchokchai C, Schwartz SJ, Failla ML. Assessment of lutein bioavailability from meals and a supplement using simulated digestion and caco-2 human intestinal cells. J Nutr. 2004; 134:2280-2286.

Chun OK, Chung SJ, Song WO. Estimated dietary flavonoid intake and major food sources of U.S. adults. J Nutr. 2007; 137:1244-1252.

Chung HY, Rasmussen HM, Johnson EJ. Lutein bioavailability is higher from lutein-enriched eggs than from supplements and spinach in men. J Nutr. 2004; 134:1887-1893.

Cui J, Yu B, Zhao Y, Zhu W, Li H, Lou H, Zhai G. Enhancement of oral absorption of curcumin by self-microemulsifying drug delivery systems. Int J Pharm. 2009; 371:148-155.

D'Archivio M, Filesi C, Varì R, Scazzocchio B, Masella R. Bioavailability of the polyphenols: status and controversies. Int J Mol Sci. 2010; 11:1321-1342.

Dauchet L, Amouyel P, Hercberg S, Dallongeville J. Fruit and vegetable consumption and risk of coronary heart disease: a meta-analysis of cohort studies. J Nutr. 2006; 136:2588-2593.

de Moura FF, Ho CC, Getachew G, Hickenbottom S, Clifford AJ. Kinetics of 14C distribution after tracer dose of 14C-lutein in an adult woman. Lipids. 2005; 40:1069-1073.

Deming DM, Erdman JW. Mammalian carotenoid absorption and metabolism. Pure Appl Chem. 1999; 71:2213-2223.

des Rieux A, Fievez V, Garinot M, Schneider YJ, Préat V. Nanoparticles as potential oral delivery systems of proteins and vaccines: a mechanistic approach. J Control Release. 2006; 116:1-27.

des Rieux A, Fievez V, Théate I, Mast J, Préat V, Schneider YJ. An improved in vitro model of human intestinal follicle-associated epithelium to study nanoparticle transport by M cells. Eur J Pharm Sci. 2007; 30:380-391.

des Rieux A, Ragnarsson EG, Gullberg E, Préat V, Schneider YJ, Artursson P. Transport of nanoparticles across an in vitro model of the human intestinal follicle associated epithelium. Eur J Pharm Sci. 2005; 25:455-465.

Desai MP, Labhasetwar V, Amidon GL, Levy RJ. Gastrointestinal uptake of biodegradable microparticles: effect of particle size. Pharm Res. 1996; 13:1838-1845.

Dube A, Nicolazzo JA, Larson I. Chitosan nanoparticles enhance the intestinal absorption of the green tea catechins (+)-catechin and (-)-epigallocatechin gallate. Eur J Pharm Sci. 2010b; 41:219-225.

Dube A, Nicolazzo JA, Larson I. Chitosan nanoparticles enhance the plasma exposure of (-)-epigallocatechin gallate in mice through an enhancement in intestinal stability. Eur J Pharm Sci. 2011; 44:422-426.

Dube A, Ng K, Nicolazzo JA, Larson I. Effective use of reducing agents and nanoparticle encapsulation in stabilizing catechins in alkaline solution. Food Chem. 2010a;122:662-667.

FDA. (2011) Considering Whether an FDA-Regulated Product Involves the Application of Nanotechnology, Retrieved June 4 2014, [http://www.fda.gov/ScienceResearch/SpecialTopics/Nanotechnology/ucm257926.htm]

Fiedor J, Burda K. Potential role of carotenoids as antioxidants in human health and disease. Nutrients. 2014; 6:466-488.

Foged C, Brodin B, Frokjaer S, Sundblad A. Particle size and surface charge affect particle uptake by human dendritic cells in an in vitro model. Int J Pharm. 2005; 298:315-322.

Frijlink HW, Eissens AC, Hefting NR, Poelstra K, Lerk CF, Meijer DK. The effect of parenterally administered cyclodextrins on cholesterol levels in the rat. Pharm Res. 1991; 8:9-16.

Galindo-Rodriguez SA, Allemann E, Fessi H, Doelker E. Polymeric nanoparticles for oral delivery of drugs and vaccines: a critical evaluation of in vivo studies. Crit Rev Ther Drug Carrier Syst. 2005; 22:419-464.

Gao X, Cassidy A, Schwarzschild MA, Rimm EB, Ascherio A. Habitual intake of dietary flavonoids and risk of Parkinson disease. Neurology. 2012; 78:1138-1145.

Garrett DA, Failla ML, Sarama RJ. Development of an in vitro digestion method to assess carotenoid bioavailability from meals. J Agric Food Chem. 1999; 47:4301-4309.

George M, Abraham TE. Polyionic hydrocolloids for the intestinal delivery of protein drugs: alginate and chitosan--a review. J Control Release. 2006; 114:1-14.

Geybels MS, Verhage BA, Arts IC, van Schooten FJ, Goldbohm RA, van den Brandt PA. Dietary flavonoid intake, black tea consumption, and risk of overall and advanced stage prostate cancer. Am J Epidemiol. 2013; 177:1388-1398.

Ghosh A, Mandal A, Sarkar S, Panda S, Das N. Nanoencapsulation of quercetin enhances its dietary efficacy in combating arsenic-induced oxidative damage in liver and brain of rats. Life Sci. 2009; 84:75-80.

Ghosh S, Dungdung SR, Chowdhury ST, Mandal AK, Sarkar S, Ghosh D, Das N. Encapsulation of the flavonoid quercetin with an arsenic chelator into nanocapsules enables the simultaneous delivery of hydrophobic and hydrophilic drugs with a synergistic effect against chronic arsenic accumulation and oxidative stress. Free Radic Biol Med. 2011; 51:1893-1902.

Goltz SR, Campbell WW, Chitchumroonchokchai C, Failla ML, Ferruzzi MG. Meal triacylglycerol profile modulates postprandial absorption of carotenoids in humans. Mol Nutr Food Res. 2012; 56:866-877.

Gurley BJ. Emerging technologies for improving phytochemical bioavailability: benefits and risks. Clin Pharmacol Ther. 2011; 89:915-919.

Gyémánt N, Tanaka M, Molnár P, Deli J, Mándoky L, Molnár J. Reversal of multidrug resistance of cancer cells in vitro: modification of drug resistance by selected carotenoids. Anticancer Res. 2006; 26:367-374.

He K, Hu FB, Colditz GA, Manson JE, Willett WC, Liu S. Changes in intake of fruits and vegetables in relation to risk of obesity and weight gain among middle-aged women. Int J Obes Relat Metab Disord. 2004; 28:1569-1574.

He W, Lu Y, Qi J, Chen L, Hu F, Wu W. Nanoemulsion-templated shell-crosslinked nanocapsules as drug delivery systems. Int J Pharm. 2013; 445:69-78.

Heaney RP. Factors influencing the measurement of bioavailability, taking calcium as a model. J Nutr. 2001;131:1344S-1348S.

Hendrich S. Bioavailability of isoflavones. J Chromatogr B Analyt Technol Biomed Life Sci. 2002; 777:203-210.

Herron KL, McGrane MM, Waters D, Lofgren IE, Clark RM, Ordovas JM, Fernandez ML. The ABCG5 polymorphism contributes to individual responses to dietary cholesterol and carotenoids in eggs. J Nutr. 2006; 136:1161-1165.

Hillery AM, Jani PU, Florence AT. Comparative, quantitative study of lymphoid and non-lymphoid uptake of 60 nm polystyrene particles. J Drug Target. 1994;2:151-156.

Huang Y, Leobandung W, Foss A, Peppas NA. Molecular aspects of muco- and bioadhesion: tethered structures and site-specific surfaces. J Control Release. 2000; 65:63-71.

Hung HC, Joshipura KJ, Jiang R, Hu FB, Hunter D, Smith-Warner SA, Colditz GA, Rosner B, Spiegelman D, Willett WC. Fruit and vegetable intake and risk of major chronic disease. J Natl Cancer Inst. 2004; 96:1577-1584.

Jani P, Halbert GW, Langridge J, Florence AT. Nanoparticle uptake by the rat gastrointestinal mucosa: quantitation and particle size dependency. J Pharm Pharmacol. 1990;42:821-826.

Jomova K, Valko M. Health protective effects of carotenoids and their interactions with other biological antioxidants. Eur J Med Chem. 2013; 70:102-110.

Jung T, Kamm W, Breitenbach A, Kaiserling E, Xiao JX, Kissel T. Biodegradable nanoparticles for oral delivery of peptides: is there a role for polymers to affect mucosal uptake? Eur J Pharm Biopharm. 2000; 50:147-160.

Khachik F. Partial synthesis of serum carotenoids and their metabolites. Acta Biochim Pol. 2012; 59:75-78.

Khalil NM, do Nascimento TC, Casa DM, Dalmolin LF, de Mattos AC, Hoss I, Romano MA, Mainardes RM. Pharmacokinetics of curcumin-loaded PLGA and PLGA-PEG blend nanoparticles after oral administration in rats. Colloids Surf B Biointerfaces. 2013; 101:353-360.

Kimmons J, Gillespie C, Seymour J, Serdula M, Blanck HM. Fruit and vegetable intake among adolescents and adults in the United States: percentage meeting individualized recommendations. Medscape J Med. 2009; 11:26.

Kotake-Nara E, Nagao A. Absorption and metabolism of xanthophylls. Mar Drugs. 2011; 9:1024-1037.

Krook MA, Hagerman AE. Stability of Polyphenols Epigallocatechin Gallate and Pentagalloyl Glucose in a Simulated Digestive System. Food Res Int. 2012;49:112-116.

Kumari A, Yadav SK, Yadav SC. Biodegradable polymeric nanoparticles based drug delivery systems. Colloids Surf B Biointerfaces. 2010; 75:1-18.

Kurilich AC, Britz SJ, Clevidence BA, Novotny JA. Isotopic labeling and LC-APCI-MS quantification for investigating absorption of carotenoids and phylloquinone from kale (Brassica oleracea). J Agric Food Chem. 2003; 51:4877-4883.

Lai SK, Wang YY, Hanes J. Mucus-penetrating nanoparticles for drug and gene delivery to mucosal tissues. Adv Drug Deliv Rev. 2009; 61:158-171.

Lakshminarayana R, Raju M, Keshava Prakash MN, Baskaran V. Phospholipid, oleic acid micelles and dietary olive oil influence the lutein absorption and activity of antioxidant enzymes in rats. Lipids. 2009; 44:799-806.

Lakshminarayana R, Raju M, Krishnakantha TP, Baskaran V. Lutein and zeaxanthin in leafy greens and their bioavailability: olive oil influences the absorption of dietary lutein and its accumulation in adult rats. J Agric Food Chem. 2007; 55:6395-6400.

Lam WH, Kazi A, Kuhn DJ, Chow LM, Chan AS, Dou QP, Chan TH. A potential prodrug for a green tea polyphenol proteasome inhibitor: evaluation of the peracetate ester of (-)-epigallocatechin gallate [(-)-EGCG]. Bioorg Med Chem. 2004; 12:5587-5593.

Lambert JD, Hong J, Kim DH, Mishin VM, Yang CS. Piperine enhances the bioavailability of the tea polyphenol (-)-epigallocatechin-3-gallate in mice. J Nutr. 2004; 134:1948-1952.

Lesser S, Cermak R, Wolffram S. Bioavailability of quercetin in pigs is influenced by the dietary fat content. J Nutr. 2004; 134:1508-1511.

Li H, Zhao X, Ma Y, Zhai G, Li L, Lou H. Enhancement of gastrointestinal absorption of quercetin by solid lipid nanoparticles. J Control Release. 2009; 133:238-244.

Lienau A, Glaser T, Tang G, Dolnikowski GG, Grusak MA, Albert K. Bioavailability of lutein in humans from intrinsically labeled vegetables determined by LC-APCI-MS. J Nutr Biochem.
2003; 14:663-670.

Lindqvist A, Andersson S. Biochemical properties of purified recombinant human beta-carotene 15,15'-monooxygenase. J Biol Chem. 2002; 277:23942-23948.

Liu RH. Health benefits of fruit and vegetables are from additive and synergistic combinations of phytochemicals. Am J Clin Nutr. 2003; 78:517S-520S.

Liu RH. Potential synergy of phytochemicals in cancer prevention: mechanism of action. J Nutr. 2004; 134:3479S-3485S.

Lu Z, Ji C, Xu H, Ding H, Ye M, Zhu Z, Ding D, Jiang X, Ding X, Guo X. Resveratrol-loaded polymeric micelles protect cells from Aβ- induced oxidative stress. Inter J Pharm. 2009; 375:89-96.

Ma Y, Zhao X, Li J, Shen Q. The comparison of different daidzein-PLGA nanoparticles in increasing its oral bioavailability. Int J Nanomedicine. 2012; 7:559-570.

Mamatha BS, Baskaran V. Effect of micellar lipids, dietary fiber and β-carotene on lutein bioavailability in aged rats with lutein deficiency. Nutrition. 2011; 27:960-966.

Manach C, Morand C, Crespy V, Demigné C, Texier O, Régérat F, Rémésy C. Quercetin is recovered in human plasma as conjugated derivatives which retain antioxidant properties. FEBS Lett. 1998; 426:331-336.

Manach C, Williamson G, Morand C, Scalbert A, Rémésy C. Bioavailability and bioefficacy of polyphenols in humans. I. Review of 97 bioavailability studies. Am J Clin Nutr. 2005; 81:230S-242S.

Mangels AR, Holden JM, Beecher GR, Forman MR, Lanza E. Carotenoid content of fruits and vegetables: an evaluation of analytic data. J Am Diet Assoc. 1993; 93:284-296.

Mares-Perlman JA, Fisher AI, Klein R, Palta M, Block G, Millen AE, Wright JD. Lutein and zeaxanthin in the diet and serum and their relation to age-related maculopathy in the third national health and nutrition examination survey. Am J Epidemiol. 2001; 153:424-432.

McClean S, Prosser E, Meehan E, O'Malley D, Clarke N, Ramtoola Z, Brayden D. Binding and uptake of biodegradable poly-DL-lactide micro- and nanoparticles in intestinal epithelia. Eur J Pharm Sci. 1998; 6:153-163.

McCullough ML, Peterson JJ, Patel R, Jacques PF, Shah R, Dwyer JT. Flavonoid intake and cardiovascular disease mortality in a prospective cohort of US adults. Am J Clin Nutr. 2012; 95:454-464.

Meyers KJ, Mares JA, Igo RP Jr, Truitt B, Liu Z, Millen AE, Klein M, Johnson EJ, Engelman CD, Karki CK, Blodi B, Gehrs K, Tinker L, Wallace R, Robinson J, LeBlanc ES, Sarto G, Bernstein PS, SanGiovanni JP, Iyengar SK. Genetic evidence for role of carotenoids in age-related macular degeneration in the Carotenoids in Age-Related Eye Disease Study (CAREDS). Invest Ophthalmol Vis Sci. 2014; 55: 587-599.

Milbury PE, Vita JA, Blumberg JB. Anthocyanins are bioavailable in humans following an acute dose of cranberry juice. J Nutr. 2010; 140:1099-1104.

Mochizuki M, Yamazaki S, Kano K, Ikeda T. Kinetic analysis and mechanistic aspects of autoxidation of catechins. Biochim Biophys Acta. 2002; 1569:35-44.
Monsen ER. Dietary reference intakes for the antioxidant nutrients: vitamin C, vitamin E, selenium, and carotenoids. J Am Diet Assoc. 2000; 100:637-640.
Mu X, Zhong Z. Preparation and properties of poly(vinyl alcohol)-stabilized liposomes. Int J Pharm. 2006; 318:55-61.
Mukerjee A, Vishwanatha JK. Formulation, characterization and evaluation of curcumin-loaded PLGA nanospheres for cancer therapy. Anticancer Res. 2009; 29:3867-3875.
Musthaba SM, Baboota S, Ahmed S, Ahuja A, Ali J. Status of novel drug delivery technology for phytotherapeutics. Expert Opin Drug Deliv. 2009; 6:625-637.
Nair HB, Sung B, Yadav VR, Kannappan R, Chaturvedi MM, Aggarwal BB. Delivery of antiinflammatory nutraceuticals by nanoparticles for the prevention and treatment of cancer. Biochem. Pharmacol. 2010; 80:1833-1843.
Narushima K, Takada T, Yamanashi Y, Suzuki H. Niemann-pick C1-like 1 mediates alpha-tocopherol transport. Mol Pharmacol. 2008; 74:42-49.
Neves AR, Lúcio M, Martins S, Lima JL, Reis S. Novel resveratrol nanodelivery systems based on lipid nanoparticles to enhance its oral bioavailability. Int J Nanomedicine. 2013; 8:177-187.
Nijveldt RJ, van Nood E, van Hoorn DE, Boelens PG, van Norren K, van Leeuwen PA. Flavonoids: a review of probable mechanisms of action and potential applications. Am J Clin Nutr. 2001; 74:418-425.
Novotny JA, Kurilich AC, Britz SJ, Clevidence BA. Plasma appearance of labeled beta-carotene, lutein, and retinol in humans after consumption of isotopically labeled kale. J Lipid Res. 2005; 46:1896-1903.
Owens DE 3rd, Peppas NA. Opsonization, biodistribution, and pharmacokinetics of polymeric nanoparticles. Int J Pharm. 2006; 307:93-102.
Pietzonka P, Rothen-Rutishauser B, Langguth P, Wunderli-Allenspach H, Walter E, Merkle HP. Transfer of lipophilic markers from PLGA and polystyrene nanoparticles to caco-2 monolayers mimics particle uptake. Pharm Res. 2002; 19:595-601.
Pool H, Quintanar D, de Dios Figueroa J, Mano CM, Bechara JEH, Godínez LA, Mendoza S. Antioxidant effects of quercetin and catechin encapsulated into PLGA nanoparticles. J Nanomaterials. 2012; 2012:1-12.
Pralhad T, Rajendrakumar K. Study of freeze-dried quercetin-cyclodextrin binary systems by DSC, FT-IR, X-ray diffraction and SEM analysis. J Pharm Biomed Anal. 2004;34:333-339.
RaghuramTC, Krishnaswamy K. Basic concepts of clinical pharmacokinetics. J Assoc Physicians India. 1992; 40:29-35.
Reboul E, Borel P. Proteins involved in uptake, intracellular transport and basolateral secretion of fat-soluble vitamins and carotenoids by mammalian enterocytes. Prog Lipid Res. 2011; 50:388-402.
Reboul E. Absorption of vitamin A and carotenoids by the enterocyte: focus on transport proteins. Nutrients. 2013; 5:3563-3581.
Reix N, Parat A, Seyfritz E, Van der Werf R, Epure V, Ebel N, Danicher L, Marchioni E, Jeandidier N, Pinget M, Frère Y, Sigrist S. In vitro uptake evaluation in Caco-2 cells and in vivo results in diabetic rats of insulin-loaded PLGA nanoparticles. Int J Pharm. 2012; 437:213-220.
Richer S, Stiles W, Statkute L, Pulido J, Frankowski J, Rudy D, Pei K, Tsipursky M, Nyland J. Double-masked, placebo-controlled, randomized trial of lutein and antioxidant supplementation in the intervention of atrophic age-related macular

degeneration: the Veterans LAST study (Lutein Antioxidant Supplementation Trial). Optometry. 2004; 75:216-230.

Roodenburg AJ, Leenen R, van het Hof KH, Weststrate JA, Tijburg LB. Amount of fat in the diet affects bioavailability of lutein esters but not of alpha-carotene, beta-carotene, and vitamin E in humans. Am J Clin Nutr. 2000; 71:1187-1193.

Scalbert A, Johnson IT, Saltmarsh M. Polyphenols: antioxidants and beyond. Am J Clin Nutr. 2005;81:215S-217S.

Scalbert A, Williamson G. Dietary intake and bioavailability of polyphenols. J Nutr. 2000; 130:2073S-2085S.

Scheepens A, Tan K, Paxton JW. Improving the oral bioavailability of beneficial polyphenols through designed synergies. Genes Nutr. 2010; 5:75-87.

Shaikh J, Ankola DD, Beniwal V, Singh D, Kumar MN. Nanoparticle encapsulation improves oral bioavailability of curcumin by at least 9-fold when compared to curcumin administered with piperine as absorption enhancer. Eur J Pharm Sci. 2009; 37:223-230.

Shakweh M, Ponchel G, Fattal E. Particle uptake by Peyer's patches: a pathway for drug and vaccine delivery. Expert Opin Drug Deliv. 2004; 1:141-163.

Shao J, Li X, Lu X, Jiang C, Hu Y, Li Q, You Y, Fu Z. Enhanced growth inhibition effect of resveratrol incorporated into biodegradable nanoparticles against glioma cells is mediated by the induction of intracellular reactive oxygen species levels. Colloids Surf B Biointerfaces. 2009; 72:40-47.

Siddiqui IA, Adhami VM, Bharali DJ, Hafeez BB, Asim M, Khwaja SI, Ahmad N, Cui H, Mousa SA, Mukhtar H. Introducing nanochemoprevention as a novel approach for cancer control: proof of principle with green tea polyphenol epigallocatechin-3-gallate. Cancer Res. 2009; 69:1712-1716.

Sila A, Nasri M, Bougatef A. Isolation and characterisation of carotenoproteins from deep-water pink shrimp processing waste. Int J Biol Macromol. 2012; 51:953-959.

Smith J, Wood E, Dornish M. Effect of chitosan on epithelial cell tight junctions. Pharm Res. 2004; 21:43-49.

Smith-Warner SA, Spiegelman D, Yaun SS, Albanes D, Beeson WL, van den Brandt PA, Feskanich D, Folsom AR, Fraser GE, Freudenheim JL, Giovannucci E, Goldbohm RA, Graham S, Kushi LH, Miller AB, Pietinen P, Rohan TE, Speizer FE, Willett WC, Hunter DJ. Fruits, vegetables and lung cancer: a pooled analysis of cohort studies. Int J Cancer. 2003; 107:1001-1011.

Sonaje K, Chuang EY, Lin KJ, Yen TC, Su FY, Tseng MT, Sung HW. Opening of epithelial tight junctions and enhancement of paracellular permeation by chitosan: microscopic, ultrastructural, and computed-tomographic observations. Mol Pharm. 2012; 9:1271-1279.

Sonaje K, Lin YH, Juang JH, Wey SP, Chen CT, Sung HW. In vivo evaluation of safety and efficacy of self-assembled nanoparticles for oral insulin delivery. Biomaterials. 2009; 30:2329-2339.

Soppimath KS, Aminabhavi TM, Kulkarni AR, Rudzinski WE. Biodegradable polymeric nanoparticles as drug delivery devices. J Control Release. 2001; 70:1-20.

Spencer JP. Metabolism of tea flavonoids in the gastrointestinal tract. J Nutr. 2003; 133:3255S-3261S.

Srinivasan VS. Bioavailability of nutrients: a practical approach to in vitro demonstration of the availability of nutrients in multivitamin-mineral combination products. J Nutr. 2001; 131:1349S-1350S.

Stahl W, Sies H. Antioxidant activity of carotenoids. Mol Aspects Med. 2003; 24:345-351.

Stahl W, Sies H. β-Carotene and other carotenoids in protection from sunlight. Am J Clin Nutr. 2012; 96:1179S-1184S.

Sy C, Gleize B, Dangles O, Landrier JF, Veyrat CC, Borel P. Effects of physicochemical properties of carotenoids on their bioaccessibility, intestinal cell uptake, and blood and tissue concentrations. Mol Nutr Food Res. 2012; 56:1385-1397.

Tan C, Xia S, Xue J, Xie J, Feng B, Zhang X. Liposomes as vehicles for lutein: preparation, stability, liposomal membrane dyanamics, and structure. J Agri Food Chem. 2013; 61:8175-8184.

Tang DW, Yu SH, Ho YC, Huang BQ, Tsai GJ, Hsieh HY, Sung HW, Mi FL. Characterization of tea catechins-loaded nanoparticles prepared from chitosan and an edible polypeptide. Food Hydrocolloids. 2012; 30:33-41.

Thanou M, Verhoef JC, Junginger HE. Chitosan and its derivatives as intestinal absorption enhancers. Adv Drug Deliv Rev. 2001; 50:S91-101.

Thomas VH, Bhattachar S, Hitchingham L, Zocharski P, Naath M, Surendran N, Stoner CL, El-Kattan A. The road map to oral bioavailability: an industrial perspective. Expert Opin. Drug Metab. Toxicol. 2006; 2:591-608.

Tobío M, Sánchez A, Vila A, Soriano II, Evora C, Vila-Jato JL, Alonso MJ. The role of PEG on the stability in digestive fluids and in vivo fate of PEG-PLA nanoparticles following oral administration. Colloids Surf B Biointerfaces. 2000; 18:315-323.

Tønnesen HH. Solubility, chemical and photochemical stability of curcumin in surfactant solutions. Studies of curcumin and curcuminoids, XXVIII. Pharmazie. 2002; 57:820-824.

Tsai YM, Jan WC, Chien CF, Lee WC, Lin LC, Tsai TH. Optimised nano-formulation on the bioavailability of hydrophobic polyphenol, curcumin, in freely-moving rats. Food Chem. 2011; 127:918-925.

van der Merwe SM, Verhoef JC, Verheijden JH, Kotzé AF, Junginger HE. Trimethylated chitosan as polymeric absorption enhancer for improved peroral delivery of peptide drugs. Eur J Pharm Biopharm. 2004; 58:225-235.

van Het Hof KH, West CE, Weststrate JA, Hautvast JG. Dietary factors that affect the bioavailability of carotenoids. J Nutr. 2000; 130:503-6.

Vasir JK, Labhasetwar V. Quantification of the force of nanoparticle-cell membrane interactions and its influence on intracellular trafficking of nanoparticles. Biomaterials. 2008; 29:4244-4252.

Verhagen H, Coolen S, Duchateau G, Hamer M, Kyle J, Rechner A. Assessment of the efficacy of functional food ingredients-introducing the concept "kinetics of biomarkers". Mutat Res. 2004; 551:65-78.

Vila A, Sánchez A, Tobío M, Calvo P, Alonso MJ. Design of biodegradable particles for protein delivery. J Control Release. 2002; 78:15-24.

Wedick NM, Pan A, Cassidy A, Rimm EB, Sampson L, Rosner B, Willett W, Hu FB, Sun Q, van Dam RM. Dietary flavonoid intakes and risk of type 2 diabetes in US men and women. Am J Clin Nutr. 2012; 95:925-933.

Weissenboeck A, Bogner E, Wirth M, Gabor F. Binding and uptake of wheat germ agglutinin-grafted PLGA-nanospheres by caco-2 monolayers. Pharm Res. 2004; 21:1917-1923.

Windrum P, Morris TC, Drake MB, Niederwieser D, Ruutu T; EBMT Chronic Leukaemia Working Party Complications Subcommittee. Variation in dimethyl sulfoxide use in

stem cell transplantation: a survey of EBMT centres. Bone Marrow Transplant. 2005; 36:601-603.

Wu TH, Yen FL, Lin LT, Tsai TR, Lin CC, Cham TM. Preparation, physicochemical characterization, and antioxidant effects of quercetin nanoparticles. Int J Pharm. 2008; 346:160-168.

Xie X, Tao Q, Zou Y, Zhang F, Guo M, Wang Y, Wang H, Zhou Q, Yu S. PLGA nanoparticles improve the oral bioavailability of curcumin in rats: characterizations and mechanisms. J Agric Food Chem. 2011; 59:9280-9289.

Yallapu MM, Gupta BK, Jaggi M, Chauhan SC. Fabrication of curcumin encapsulated PLGA nanoparticles for improved therapeutic effects in metastatic cancer cells. J Colloid Interface Sci. 2010; 351:19-29.

Yeum KJ, Russell RM. Carotenoid bioavailability and bioconversion. Annu Rev Nutr. 2002; 22:483-504.

Yi J, Lam TI, Yokoyama W, Cheng LW, Zhong F. Cellular uptake of beta-carotene from protein stabilized solid lipid nanoparticles prepared by homogenization-evaporation method. J Agri Food Chem. 2014; 62:1096-1104.

Yin Y, Chen D, Qiao M, Wei X, Hu H. Lectin-conjugated PLGA nanoparticles loaded with thymopentin: ex vivo bioadhesion and in vivo biodistribution. J Control Release. 2007; 123:27-38.

Yoncheva K, Guembe L, Campanero MA, Irache JM. Evaluation of bioadhesive potential and intestinal transport of pegylated poly(anhydride) nanoparticles. Int J Pharm. 2007; 334:156-165.

Yonekura L, Kobayashi M, Terasaki M, Nagao A. Keto-carotenoids are the major metabolites of dietary lutein and fucoxanthin in mouse tissues. J Nutr. 2010; 140:1824-1831.

Yuan ZP, Chen LJ, Fan LY, Tang MH, Yang GL, Yang HS, Du XB, Wang GQ, Yao WX, Zhao QM, Ye B, Wang R, Diao P, Zhang W, Wu HB, Zhao X, Wei YQ. Liposomal quercetin efficiently suppresses growth of solid tumors in murine models. Clin Cancer Res. 2006; 12:3193-3199.

Yue ZG, Wei W, Lv PP, Yue H, Wang LY, Su ZG, Ma GH. Surface charge affects cellular uptake and intracellular trafficking of chitosan-based nanoparticles. Biomacromolecules. 2011; 12:2440-2446.

Zhang L, Sun M, Guo R, Jiang Z, Liu Y, Jiang X, Yang C. Chitosan surface-modified hydroxycamptothecin loaded nanoparticles with enhanced transport across Caco-2 cell monolayer. J Nanosci Nanotechnol. 2006; 6:2912-2920.

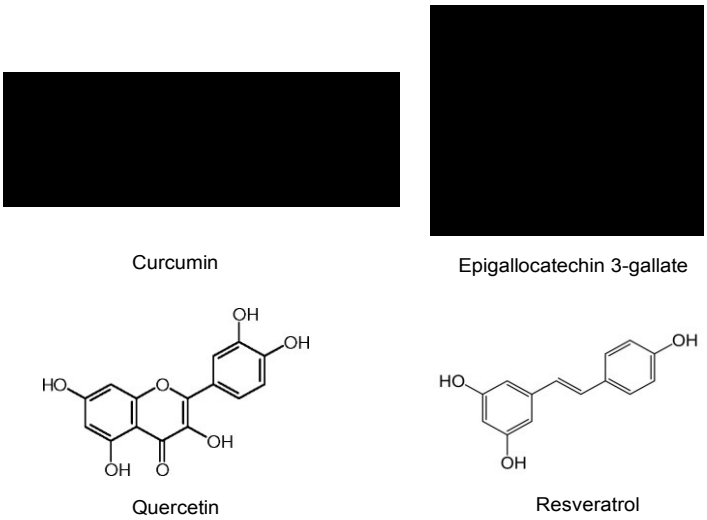

Fig. 1. Chemical structure of selected polyphenols

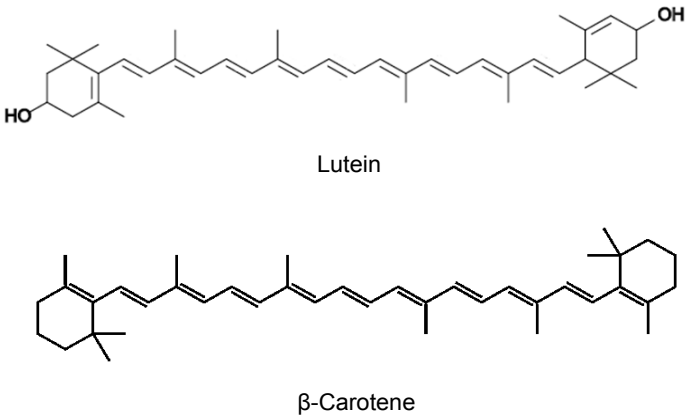

Fig. 2. Chemical structure of selected carotenoids

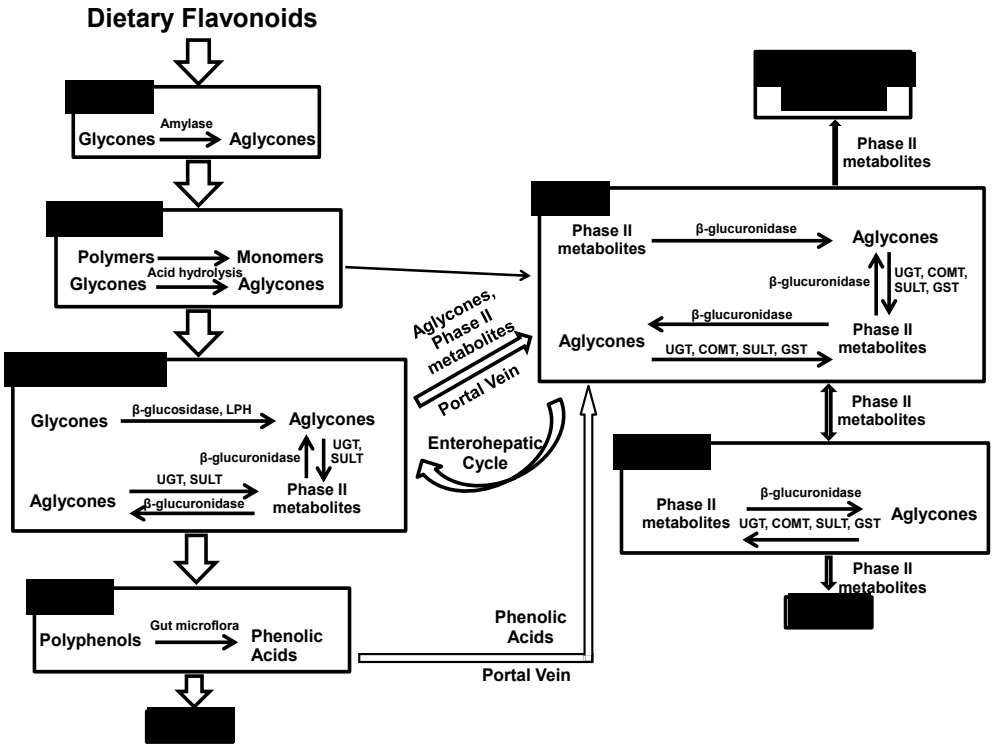

Fig. 3. Absorption, distribution, metabolism, and excretion of dietary flavonoids. Size of arrows proportional to percent distribution from consumption to excretion. Abbreviations: UGT, UDP-glucuronosyltransferase; COMT, catechol-*O*-methyltransferase; SULT, sulfotransferase; GST, glutathione S-transferase; LPH, lactase-phlorizin hydrolase (Spencer 2003; Bohn 2014).

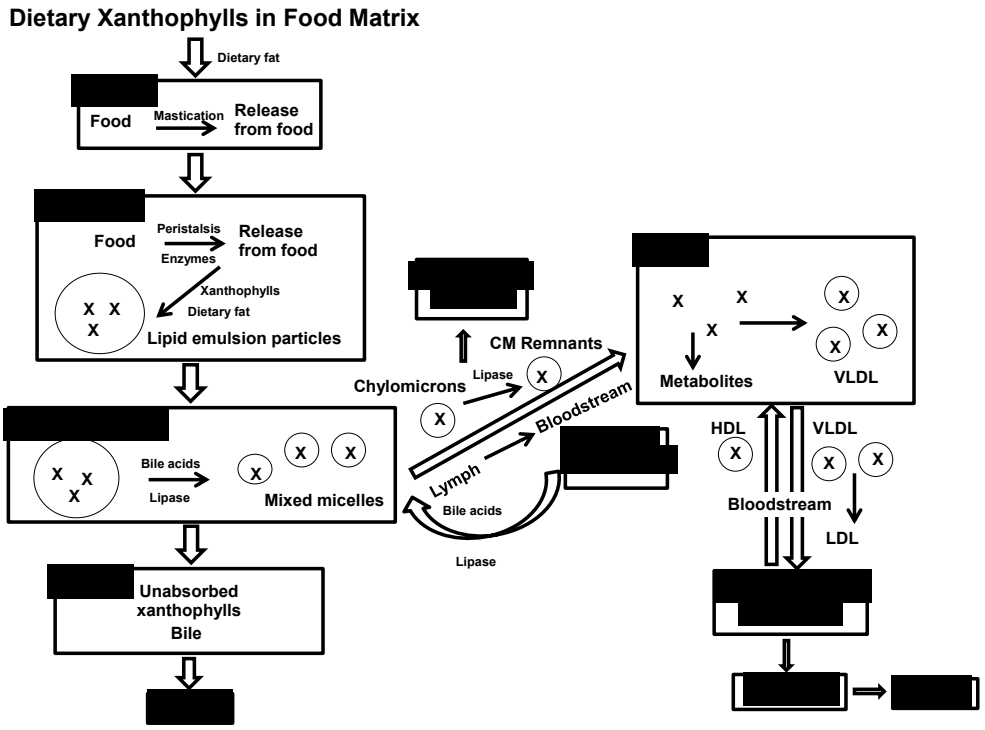

Fig. 4. Absorption, distribution, metabolism, and excretion of dietary xanthophylls. Size of arrows proportional to percent distribution from consumption to excretion. Abbreviations: X, xanthophylls; VLDL, very low density lipoprotein; LDL, low density lipoprotein; HDL, high density lipoprotein (Deming and Erdman 1999).

Table 1. Examples of *in vivo* oral pharmacokinetic studies (polymeric NP vs. free phytochemical) in animal models

Studies	Animal	Formulation/Dose (per BW)	Time points	C_{max} (μg/mL)	T_{max} (min)	AUC (min*μg/mL)
EGCG						
Dube et al. 2011	Swiss Outbred Mice	• CS: 0.76 mg/kg • Free: 0.76 mg/kg	0-5 h	Free EGCG: 0.016 ± 0.004 vs. 0.015 ± 0.002 Total EGCG (free + phase II conjugates): 0.017 ± 0.003 vs. 0.016 ± 0.001	90 for all	Free EGCG: 4.57 ± 0.33 vs. 3.15 ± 0.11 Total EGCG (free + phase II conjugates): 4.93 ± 0.3 vs. 3.19 ± 0.11
Curcumin						
Tsai et al. 2011	SD Rat	• PLGA (50:50)-PVA (20%): 50 mg/kg • Free: 1 g/kg	0-6 h	0.044 ± 0.004 vs. 0.022 ± 0.002 *P* <0.05	~30 vs. ~45	7.32 ± 0.8 vs. 6.44 ± 2.0
Xie et al. 2011	SD Rat	• PLGA (50:50)-PVA (1%): 100 mg/kg • Free: 100 mg/kg	0-12 h	6.75 ± 1.54 vs. 1.55 ± 0.21 *P* <0.01	120 ± 0 vs. 102±16 *P* <0.01	2066 ± 332 vs. 367 ± 21 *P* <0.01
Khalil et al. 2013	Wistar Rat	• PLGA (50:50)-PVA (0.5%): 50 mg/kg • PLGA-PEG: 50 mg/kg	0-24 h	0.012 ± 0.0005 vs. 0.030 ± 0.005	120 vs. 180	8.04 ± 0.21 vs. 26.87 ± 3.84

Studies	Animal	Formulation/Dose (per BW)	Time points	C_{max} (µg/mL)	T_{max} (min)	AUC (min*µg/mL)
Quercetin						
Li et al. 2009	Wistar rat	• SLN: 50 mg/kg • Free: 50 mg/kg	0-48 h	12.22 ± 2.15 vs. 5.90 ± 1.24	480 vs. 300	19,440 ± 2,481 vs. 3,403.8 ± 553.8

[1]All data are expressed as mean ± SD

[2]Abbreviations: AUC, area under the curve of time and concentration; C_{max}, maximum concentration; T_{max}, time to C_{max}; SD, Sprague Dawley; Cur, curcumin; NP, Nanoparticle; PLGA, poly(lactic-co-glycolytic acid); PVA, polyvinyl alcohol; PEG, polyethylene glycol; CS, chitosan; SLN, solid lipid nanoparticles.

III. Preliminary Data

Epigallocatechin gallate (EGCG), a water-soluble flavanol found in green tea, was initially selected to test the hypothesis that nanoencapsulation will improve the bioavailability of phytochemicals. Thus, a series of pilot experiments were performed to establish the lowest EGCG dose required to achieve a detectable concentration of EGCG in rat plasma. The objective of this study was to demonstrate the feasibility of entrapping EGCG in polymeric nanoparticles (NP) at a level optimal for a bioavailability study in rats.

Methods: EGCG (Sigma-Aldrich, St Louis, MO, USA) was administered by intragastric gavage at a dose of 1 mg/kg body weight (BW) purified and in poly(lactic-co-glycolic acid) (PLGA)-NP [entrapment efficiency (EE) of 0.4%]; no EGCG was detected in plasma. We subsequently sought to establish the lowest dose of EGCG necessary to achieve a detectable concentration of EGCG in rat plasma. EGCG [in water with 0.2 mg/mL ascorbic acid (pH 3.6)] was gavaged to male Fischer 344 rats at a dose of 25, 37.5, 50, 100, or 150 mg/kg BW (n = 1/dose). Blood was collected 2 h subsequent to the gavage (according to the anticipated T_{max} of EGCG in plasma) and plasma was analyzed using a HPLC- electrochemical detection.

Results: The EGCG concentration in plasma of rats gavaged with 25, 37.5, 50, 100, and 150 mg/kg BW was 170, 10, 20, 2,600, and 500 ng/mL, respectively. Given the wide variation in the bioavailability of EGCG between rats, we estimated that an oral dose of EGCG at 50 mg/kg BW would be the lowest dose that could be reliably detected in plasma. Based on the need to provide a dose of 50 mg/kg BW and the EE of 0.4% obtained from the current production protocol, we estimated a required dose 2.5 g of PLGA-NP EGCG/rat. Due to the solubility of PLGA-NP EGCG, delivering this dose

would not be feasible unless the EE for EGCG could be increased to 8%. Thus, we refocused our investigation on lutein which has a NP EE of ~75%.

Chapter 1: Development of a Cell Culture Model to Examine Fat-Soluble Nutrient Absorption *In Vitro*

Abstract

Permeable supports (PS) are employed in *in vitro* nutrient absorption studies but data are absent on their efficacy compared to the conventional system (CONV). The *in vivo* absorption of fat soluble nutrients is influenced by its delivery vehicle, yet a fundamental understanding of the influence of vehicle on cells in culture is also lacking. We used Caco-2 cells to compare the efficacy of lutein absorption in CONV and PS systems and to examine the role of micelles, the physiological vehicle within one's small intestine. After plating for 2 and 21 d to attain confluence and differentiation in CONV and PS, respectively, cells were treated with lutein in micelles or ethanol. After incubation, lutein in cell lysate as well as apical and basolateral mediums were quantified by HPLC-UV. After 24 h, the lutein in the cells in CONV was at least 460 and 8% greater in ethanol and micelle, respectively, than in PS. Yet, the intracellular AUC over time was only different for ethanol ($P \leq 0.05$). In PS, 0.15% of micellized lutein was secreted to the basolateral medium while only 0.016% of lutein in ethanol was secreted. The absorption of lutein (uptake + secretion), independent of vehicle, in CONV increased linearly with dose (0.35 to 4 or to 14.6 μg/mL for ethanol or micelle, respectively), while that in PS peaked at 1.18 μg/mL. With Caco-2 cells cultured in PS reliably grown to display phenotypes and functions of enterocytes in the small intestine, this *in vitro* platform enables the generation of information that is closer to the physiology of the absorptive enterocytes. However, although the CONV has the physiology of colonic tissue, it appears to display a greater efficacy for lutein uptake by Caco-2 cells which can provide a rapid, preliminary tool for methodology development for nutrient absorption studies.

Introduction

In vitro models present a useful approach to studying mechanisms of intestinal nutrient transport. The human intestinal Caco-2 cell line has been used extensively as an *in vitro* model of absorptive enterocytes (Delie and Rubas 1997; Le Ferrec et al. 2001; Sambruy et al. 2001). Caco-2 cells originate from human colonic carcinoma, and after differentiation, exhibit morphological and functional characteristics comparable to those of differentiated epithelial cells that line the mucosa of the small intestine. They spontaneously differentiate to an enterocyte-like phenotype when they grow to confluency in conventional monolayer culture conditions (Ferruzza et al. 2012; Sambruy et al. 2005; Reisher et al. 1993). During the early phases of differentiation, the cells express both colonocyte and enterocyte-specific proteins, such as surfactant protein A and α-1 antitrypsin, respectively (Engle et al. 1998). As differentiation proceeds, colonocyte-specific gene expression decreases and morphological and biochemical characteristics of enterocytes develop (such as tight junctions, microvilli, enzymes and transport systems).

Caco-2 cells are cultured on permeable cell culture supports (PS) or conventional tissue culture treated plastic plates (CONV) for absorption experiments of nutrients (and also pharmacological agents). Caco-2 cells differentiate more efficiently on PS than on CONV because Caco-2 cells remain in a proliferative stage due to constant cell detachment resulting from intracellular fluid being transported to the basolateral space of cells (Perdikis et al. 1997, Cereijido et al. 1978). The PS also facilitates investigation of cell permeability and transepithelial transport because of establishment of functional tight junctions between cells (Sambruy et al. 2005). The apical and basolateral surfaces of cells face the upper and lower compartments, which correspond to the intestinal lumen

side and serosal side, respectively. Yet, data are absent on whether the PS generates more efficient intestinal absorption and more valid information than the CONV approach.

The absorption of fat-soluble vitamins and carotenoids *in vivo* is influenced by the vehicle that carries the nutrient to the apical membrane of the enterocytes. During digestion, fat soluble nutrients are released from their food matrix and transferred to mixed micelles or, to a lesser extent, to vesicles such as liposomes (Borel 2003; Noy et al. 1995) or associated with proteins such as β-lactoglobulin (Pérez and Calvo 1995). Once solubilized, uptake into the intestinal mucosa involves passive diffusion or facilitated transport through cholesterol transporters (Reboul and Borel 2011; Narushima et al. 2008; Reboul 2013). The final step in absorption is assimilation into chylomicrons and secretion into the lymph for systemic distribution. Aside from the major physiological vehicle, the mixed micelle, fat soluble nutrients have also been delivered to a variety of cell types in culture incorporated both liposomes and water-miscible beadlets (Garrett et al. 1999; Reboul et al. 2007; Shahrhad et al. 2002; Lancrajan et al. 2001). The organic solvents tetrahydrofuran (THF), dimethylsulfoxide (DMSO), and ethanol have also been frequently employed as delivery vehicles (O'Sullivan et al. 2004; Zhang and Omaye 2001; Liu et al. 2004; El-Metwally and Adrian 1999), but with numerous limitations that include instability, insolubility and cytotoxicity. Nonetheless, a fundamental understanding of the influence of vehicle on cells in culture remains lacking.

The efficacy of nutrient intestinal absorption *in vitro* using Caco-2 cell monolayers grown in CONV and PS system has not been systemically compared. Thus, we have examined the absorption efficacy of lutein since its putative health benefits have been established (Tapiero et al. 2004; Krinsky and Johnson 2005; Johnson 2002). Lutein, a fat-soluble xanthophyll carotenoid, is commonly present in dark green leafy vegetables,

corn, avocados, and egg yolks. We also tested 2 delivery vehicles that were employed to solubilize lutein, i.e., a synthetically prepared micelle that models the physiological vehicle within the small intestine and the organic solvent ethanol, which despite its intermediate solubility, is safe and commonly consumed in humans (Craft and Soares 1992). A better understanding of the properties of CONV vs. PS and the type of delivery vehicle therein will provide practical guidelines regarding *in vitro* approaches to the study of nutrient absorption.

Materials and Methods

Chemicals and materials

β-Cryptoxanthin (BC, 97%), 1-oleoyl-*rac*-glycerol [Monoolein (MO), 99%], 2-oleoyl-1-palmitoyl-*sn*-glycero-3-phosphocholine (PC, 99%), 1-palmitoyl-*sn*-glycero-3-phosphocholine [Lysolecithin, (LC), 99%], sodium glycodeoxycholate (GDC, 97%), sodium taurodeoxycholate hydrate (TDC, 97%), taurocholic acid sodium salt hydrate (TC, 95%), sodium oleate (OA, 99%) and bovine serum albumin (97%) were purchased from Sigma-Aldrich (St. Louis, MO). Advanced Dulbecco's Modified Eagle Medium (DMEM), 200 mM L-glutamine, Penicillin-Streptomycin (10,000 U/mL) were purchased from Gibco, Life Technologies Inc. (Grand Island, NY). Hyclone phosphate buffer saline (PBS) without Ca^{2+} or Mg^{2+}, Pierce RIPA buffer, and Pierce bicinchoninic acid (BCA) protein assay were purchased from Thermo Fischer Scientific (Rockford, IL). Multi-well tissue culture treated plates, Transwell® permeable supports, cell culture treated flasks, and sterile filters (0.22 μM pores) were purchased from Corning Life Sciences (Tewksbury, MA). Caco-2 cells, fetal bovine serum and trypsin-EDTA (0.25%) were

purchased from ATCC (Manassas, VA). All other solvents were of HPLC grade and purchased from Sigma-Aldrich (St. Louis, MO). Purified lutein (70-75%) was a gift from Kemin Industries Inc. (Des Moines, IO).

Preparation of lutein

Unmodified pure lutein in ethanol was added directly to serum-free medium, vortexed, and sonicated at room temperature for 2 min. Micelles containing lutein were prepared according to Chitchumroonchokchai et al. (2004). Briefly, MO, PC, and LC in chloroform (500, 200, and 200 μM, respectively), OA (1500 μM) in methanol, and lutein in ethanol were added to a conical glass tube and dried under N_2 gas at room temperature. Filtered sterilized (0.22 μM pores) serum–free medium containing 800, 450, and 750 μM GDC, TDC, and TC, respectively, were added to the glass tube, and the mixture was sonicated for 30 min at room temperature under red light.

In the time course experiment, one lutein concentration (4 and 14.6 μg/mL for ethanol and micelles, respectively) was employed to evaluate the effects of vehicle and cell culture models on absorption. The pharmacologic concentration of 14.6 μg/mL of lutein (~5 mg/d) was selected for micelles based on the consideration that it would be an adequate dose to quantify absorption. Further, this concentration was calculated based on the assumption of a mean dietary intake of 1 mg lutein (Monsen 2000) and delivery of 2-3 L of water to the small intestine per day. Lutein at 4 μg/mL (~1.3 mg/d) was selected for testing with ethanol to assure lutein solubility and cell viability. Although the solubility of lutein in ethanol has been shown to be 300 μg/mL (Craft and Soares 1992), we were not able to successfully prepare lutein in ethanol above 4 μg/mL. Further, viability of

Caco-2 cells in ethanol has been shown to decrease if exposed to ethanol concentrations >7% (Park et al. 2012). In the dose response experiment, the lutein concentration in the medium for ethanol was 0.35, 1.18, and 4 µg/mL which are equivalent to a low to average daily lutein intake (~0.11, 0.39, and 1.3 mg in 3 L intestinal water). The lutein concentration in medium for micelle was increased to include these doses plus 14.6 µg/mL which are equivalent to a low to high average daily lutein intake (~0.11, 0.39, 1.3, and 5 mg in 3 L intestinal water).

Cell culture

Caco-2 cells were maintained in advanced DMEM supplemented with 10% fetal bovine serum and 1% L-glutamine and the absence of antibiotics in a humidified incubator (Thermo Scientific Series 7000) at 37°C and 5% CO_2. Cells between the 12 and 27th passages were used for all experiments.

To examine the uptake of lutein in a CONV system, cells in medium in the absence of antibiotics were seeded at a density of 7 x 10^4 cells/well on 24-well tissue culture treated plates (1.9 cm^2 growth area/well). Cells were grown for 48 h to attain confluence of 75-85%. At the beginning of each experiment, serum-containing media was removed and replaced with 1 mL of lutein enriched serum-free media. Since cells do not adhere tightly to the plates, washing of the cells with PBS to remove any serum was avoided. Serum-free media was utilized to remove any variability in performance (Ferruzza et al. 2012). The range of the time course (0-48 h) was selected based on the data of pilot experiments of maximal cell uptake, which showed that maximal uptake was not yet reached by 24 h but plateaued by 48 h (results not shown). It is noteworthy that

lutein in medium was tested for stability in the CONV for at least 48 h. At the end of the selected incubation times, medium was collected. Cells remaining on the tissue culture plates were washed twice with PBS containing 2 mg/mL bovine serum albumin to remove residual lutein adhering to the apical face of the cell surface. Cell samples were incubated with 300 µl RIPA buffer for 5 min on ice for lysis and removal. All samples were collected in 2 mL Eppendorf™ tubes, flushed with N_2 gas, wrapped in parafilm, and stored at -80°C until further analysis. All experiments and analyses were conducted under red light.

To examine the uptake and secretion of lutein in a PS system, cells in medium supplemented with 1% antibiotics (penicillin-streptomycin) were seeded at a density of 5 x 10^4 cells/well on collagen-coated Transwell® permeable filters (12 well plate, 0.9 cm^2 growth area, 3 µm pore size). Cells were grown for 21 d (medium changed every 2-3 d) to attain complete differentiation and monolayer integrity when biomarkers, i.e., trans-epithelial electrical resistance (TEER) and alkaline phosphatase activity, reached a plateau (Ferruzza et al. 2012). TEER, reflective of monolayer integrity, was measured using a voltohmmeter equipped with a chopstick electrode (EVOHM2, World Precision Instruments, Sarasota, FL). Alkaline phosphatase activity, an index of differentiation, was measured spectrophometrically using p-nitrophenyl-phosphate as an enzyme substrate, according to the manufacturer's instructions (Sigma-Aldrich, St. Louis, MO). The cell lysate was collected using 210 µL 0.16% digitonin in 2 mM EDTA solution at 37°C and utilized to measure protein content and reflect cell count.

At the beginning of each PS experiment, the apical side of Caco-2 cells was washed with PBS twice to remove any serum containing media and replaced with 0.5 mL of lutein enriched serum-free media. The basolateral compartment was filled with 1.5

mL serum-free media. The range of the time course (0-48 h) was selected based on the data of pilot experiments of chylomicron production and secretion to the basolateral compartment. Results showed a 50% increase in apo-lipoprotein-B (apo-B) production between 6 and 16 h yet a steady state was not yet reached 36-48 h (data not shown). Apo-B was quantified using an ELISA kit (Antiobodies-Online.com, Product # ABIN612664) after isolation using a gradient ultracentrifugation (Luchoomun and Hussain 1999). At the end of selected incubation times, media from each side of the membrane were collected. Cells remaining on the permeable filters were washed twice with PBS containing 2 mg/mL bovine serum albumin, incubated with 350 µL above and 600 µL below with 0.25% trypsin-EDTA solution for 30 min at 37°C to remove cells from the membrane filters, and then lysed with RIPA buffer for 5 min on ice. All samples were collected in Eppendorf™ tubes, flushed with N_2 gas, wrapped in parafilm, and stored at -80°C until analysis. All experiments and analysis were conducted under red light.

To determine the proportion of free intracellular lutein in cell lysate, which was not attached to cell membranes, additional cell samples were collected at T_{max} (determined from kinetic experiments) and combined in duplicate (all treatments for CONV and lutein in micelle for PS) or quadruplet (lutein in ethanol for PS) to guarantee adequate quantification.

Lutein extraction and analysis

Apical and basolateral medium and cell lysates (sample size of 3-4 wells) were thawed and briefly vortexed. Cell lysates were sonicated for 30 sec at room temperature. To determine the proportion of intracellular lutein, cell lysate samples were further

centrifuged at 14,000 rpm for 30 min to collect cell pellets and supernatant. Lutein and β-cryptoxanthin (internal standard) in the samples were quantified according to the method of Yeum et al. (1995) with slight modifications. Briefly, the samples were extracted sequentially with FOLCH solution (chloroform/methanol: 2/1) and hexane. The organic layer was removed, combined, evaporated to dryness under N_2 gas, reconstituted in 100 µL acetone, and analyzed by reverse phase HPLC-UV. Carotenoids were separated by a ProntoSIL C30 column (4.6 x 150 nm, 3.0 µm, MAC-MOD Analytical, Inc., Chadds Ford, PA). Lutein and β-cryptoxanthin were monitored at 443 and 450 nm, respectively. Their concentrations were calculated using standard curves constructed with authenticated lutein and β-cryptoxanthin. The limit of detection and quantification for lutein was 0.63 and 1.0 ng on column, respectively. The recovery rate for the internal standard, calculated from 57 samples, was 71.8 $\pm$ 19.4%. The protein content of cell lysates was determined using a BCA protein assay kit (Thermo Fischer Scientific, Rockford, IL) and was used to reflect cell count.

Statistics

All data are expressed as mean $\pm$ SD (n = 3-4 wells). The peak concentration of cell lysate and plateauing basolateral medium (C_{max}) and the time to reach C_{max} (T_{max}) were determined. The area under the curve (AUC) of apical, cell lysate and basolateral concentrations vs. time curve (0-48 h) were calculated from random complete time course curves using the linear trapezoidal integrations (Nielson et al. 2006). The differences between means of cell culture models (CONV and PS) were analyzed using Student's t-test while the differences between doses in cell culture models were

analyzed by one-way ANOVA, followed by post hoc Tukey-Kramer honestly significant difference (HSD) test. Pearson's correlation test (r value) was employed to analyze the correlation of concentrations between parameters. Simple linear regression test (r^2 value) was employed to analyze the dose response of absorption between cell culture models. Three-way ANOVA was performed to test statistical significance of dose, vehicle and cell culture model. Differences with $P \leq 0.05$ were considered significant. The JMP IN 4 statistical software package (SAS Institute, NC) was used to perform all statistical analyses.

Results

The influence of delivery vehicle on the time course of lutein uptake by undifferentiated Caco-2 cells grown in CONV system

The effect of time course on the cell uptake of lutein and its pharmacokinetic parameters for CONV are presented in **Fig. 1** and **Table 1**. The uptake of lutein in ethanol by the cell lysate reached its C_{max} at 39 $\pm$ 6 h (**Table 1**). The uptake of lutein by the cell lysate was not linear, increasing more gradually up until 24 h followed by a spike and plateau at 36 h (**Fig 1a**). Simultaneously, there was an increase of 27% in the concentration of lutein within the apical medium from 0-4 h followed by a sharp decrease which leveled off as the cell uptake reached its C_{max}. There was no correlation over time between lutein concentrations within the cell lysate and that within the apical medium. The uptake of lutein in micelles by the cell lysate followed a similar trend as that of lutein in ethanol (**Fig. 1b**). The uptake also increased gradually up until 24 h reaching its C_{max} at 42 $\pm$ 7 h (**Table 1**). Lutein in the apical medium decreased as the uptake by cells increased

which also reached a steady state as the cell uptake reached its C_{max}. Unlike lutein in ethanol, there was a medium correlation between the concentrations within the cell lysate and that within the apical medium (r = -0.54, *P* = 0.0013).

The influence of delivery vehicle on the time course of lutein uptake and secretion by differentiated Caco-2 cells grown in PS system

The effect of time course on the cell uptake and secretion of lutein and its pharmacokinetic parameters for PS are presented in **Fig. 2** and **Table 1**. The uptake of lutein in ethanol by the cell lysate reached its C_{max} at 12 $\pm$ 10.6 h (**Table 1**). Simultaneously, the concentration of lutein in the apical medium decreased by 24% over 8 h also followed by no further decrease thereafter up to 48 h (**Fig. 2a**). Further, the secretion of lutein in ethanol increased sharply once the cell lysate reached its C_{max} at 0.016% of dose with no further increase thereafter up to 48 h. Although the concentrations within the basolateral medium were strongly correlated over time with that within the apical medium (r = -0.81, *P* <0.0001), there was no correlation between that within the cell lysate and the other compartments. The uptake of lutein in micelle by the cell lysate reached its C_{max} at 8 h followed by a subsequent decrease gradually thereafter towards its starting concentration at the 2 h time point (**Fig. 2b**). Simultaneously, the concentration of lutein in the apical medium decreased over time as the cell lysate reached its C_{max} followed by a more gradual decrease up to 48 h. Furthermore, the concentrations within the cell lysate were strongly correlated with that within the apical media (r = -0.82, *P* = 0.001). The secretion of lutein in micelle increased linearly starting at 4 h and reached its plateau at 0.15% of the dose after 36 h (**Fig. 2b**).

Similarly, the concentrations within the cell lysate as well as within the apical medium were strongly correlated with that within the basolateral medium (r = 0.91, *P* = 0.0006 and r = -0.97, *P* <0.0001, respectively).

The influence of the cell culture model on the time course and dose response of lutein uptake and percent absorption

The effect of cell culture model on the time course of lutein cell uptake and pharmacokinetic parameters are presented in **Fig. 3** and **Table 1**. After 2 h, the uptake of lutein in ethanol by cell lysate using PS was 299% greater than using CONV. Yet, after 24 h, the uptake using CONV was 214% greater than using PS (*P* <0.05, **Fig. 3a**). Further, the C_{max} for CONV was 460% greater than that for PS, T_{max} was delayed by ~27 h, and the AUC was 156% greater (*P* <0.05). In comparison to lutein in ethanol, the effect of cell culture model on the uptake of lutein in micelle was similar. After 8 h, the uptake of lutein in micelle by cell lysate using PS was 178% greater than using CONV. Yet, after 24 h, the uptake using CONV was at least 81% greater than using PS. Further, the C_{max} for CONV was 277% greater than that for PS and the T_{max} was ~34 h delayed (*P* <0.05), yet the AUCs were not statistically different. The percent of lutein uptake at T_{max} which was estimated to be free within the cytosol and not attached to cell membrane was not affected by cell culture model but by delivery vehicle (**Table 2**). The amount of lutein free within cells was 154% greater for lutein delivered in ethanol than in micelles. It shall be noted that in CONV the concentrations within the cell lysate of ethanol was correlated with that of micelle (r = 0.97, *P* <0.0001), yet there was no correlation between the apical mediums. Further, in PS the concentrations within the

basolateral and apical mediums of ethanol were correlated with that of micelle (r = 0.75, *P* <0.0001 and r = 0.76, *P* <0.0001, respectively), yet there was no correlation between the cell lysates.

The influence of cell culture model on the effect of dose on the percent lutein absorption (cell uptake and secretion, % of dose) at a fixed incubation time of 36 h is presented in **Fig. 4**. Using CONV, there was a dose response relationship for lutein in ethanol absorption from 0.35 to 4 μg/mL (r^2 = 0.73, *P* = 0.0028), although with a linear increase in response not statistically different until reaching the highest dose (*P* <0.05). Similarly, there was also a dose response relationship using PS from 0.35 to 4 μg/mL, which reached a peak in absorption at 1.18 μg/mL (r^2 = 0.99, *P* <0.0001). Furthermore, in 2 out of the 3 doses, the percent of dose absorbed using CONV was at least 422% greater than that using PS (17-45% vs. 0.69-13.6%, *P* <0.05). Similar to lutein in ethanol, using CONV, there was also a dose response relationship for lutein in micelle absorption from 0.35 to 14.6 μg/mL (r^2 = 0.57, *P* = 0.0156), also with a linear increase in response not statistically different until reaching the highest dose (*P* <0.05). There was also a dose response relationship using PS from 0.35 to 14.6 μg/mL, which also reached a peak in absorption between 1.18 and 4 μg/mL (r^2 = 0.86, *P* = 0.0026). Yet unlike lutein in ethanol, only 1 out of 4 doses, the percent of dose absorbed using CONV was 319% greater than using PS (79.2% vs. 18.9%, *P* <0.05). It is noteworthy that despite these differences the variation in absorption for both vehicles using CONV appears to be at least 252% greater than that using PS. It also shall be noted that within each cell culture model, the difference in percent of dose absorbed between vehicles was not statistically different.

Discussion

In this study, we found that compared to PS, the CONV displayed the larger efficacy of lutein uptake by Caco-2 cells over time in terms of C_{max}, independent of delivery vehicle. Yet, in terms of AUC for uptake over time, the difference between the 2 systems was only significantly different for ethanol. The absorption (uptake + secretion) of lutein, independent of delivery vehicle, by Caco-2 cells grown in CONV increased linearly with dose (0.35 to 4 or to 14.6 μg/mL for ethanol or micelle, respectively), while that in PS reached a peak at 1.18 μg/mL. Lastly, compared to the organic solvent ethanol, the micelle increased the efficacy of secretion by Caco-2 cells in PS, as well as led to stronger correlations for concentrations between cell culture compartments.

Several studies have explored the intestinal uptake of carotenoids delivered in organic solvents using the CONV system, yet the results suggest the percent of dose taken up by cells to be lower than our observations for doses of 0.35 to 4 μg/mL whose uptake was between 17 and 45% after 36 h. Liu et al. (2004) characterized the intestinal uptake of lutein (2.3 μg/mL) in the organic solvent dimethylsulfoxide (DMSO) by Caco-2 cells grown for 2 and 14 d. The time course and dose responses were shown to be independent of the age of the cultured cells, with uptake after 3-4 h at 8% of dose. Further, O'Sullivan et al. (2004) showed that a variety of carotenoids (5 μM), such as lutein, lycopene, α-carotene, and β-carotene, delivered in the organic solvent tetrahydrofuran (THF) to a Caco-2 cell monolayer grown for 21-22 d were undetectable within the cells after 24 h. Yi et al. (2014) reported that the uptake of β-carotene (5 μg/mL) in a THF-dimethylsulfoxide (DMSO) co-solvent mixture by Caco-2 cells grown for 5 d was 3% of dose after 24 h. Potential reasons for the discrepancies could be due in part to differences in the organic solvents utilized for carotenoid delivery and the age of

cultured cells. Future investigations would benefit from exploring the effect of varying organic solvents on carotenoid absorption.

Our observations for lutein in synthetic micelles using the CONV system at percent of dose (0.35 to 14.6 µg/mL) taken up by the cells between 7.8 and 79.2% after 36 h are similar to that reported in the literature. Garrett et al. (1999) characterized the intestinal uptake of lutein, lycopene, α-carotene, and β-carotene (0.83, 1.95, 0.93, and 1.96 µg/mL, respectively) isolated and micellized from carotenoid rich baby foods after the *in vitro* mimic digestion simulating the gastric and small intestinal phases of digestion. They reported that the uptake by Caco-2 cells grown for 11-14 d increased linearly over time up to 28-46% of dose after 6 h. Further, Chitchumroonchokchai et al. (2004) conducted a comparison of the intestinal uptake between lutein from spinach puree micellized by the *in vitro* digestion method and that of the pure compound solubilized in a synthetic micelle similar to the preparation conducted in our investigation. They showed that the uptake of lutein (0.5 µg/mL) by Caco-2 cells grown for 11-14 d of lutein either micellized synthetically or by *in vitro* digestion increased over time reaching 35 or 67% of dose, respectively after 20 h. However, it shall be noted that the doses investigated in these earlier studies were 7.5 to 29.2% lower than our highest dose.

Studies investigating the intestinal absorption of carotenoids in organic solvents using the PS system are lacking. Yet, previous studies investigating the absorption of lutein in micelle are consistent with our observations. In our time course study, the percentage of dose (14.6 µg/mL) taken up by the cell lysate at the T_{max} at 16-34% after 8 h falls within the range of previous *in vitro* results between 18-36% after 3 to 16 h (Chitchumroonchokchai et al. 2004; Sy et al. 2012; O'Sullivan et al. 2007; During et al. 2002). Further, given the inconsistencies in the literature related to the degree of

secretion into the basolateral medium, the percent secretion in our study of <1% falls within the range of 0-10% reported in these earlier studies. It is expected that the secretion out of the intestinal cells in our study for lutein in ethanol was minimal as bile salts and phospholipids have been shown to stimulate synthesis and secretion of chylomicrons (Luchoomun and Hussain 1999; Traber et al. 1987). Although the degree of absorption reported in the literature (Chitchumroonchokchai et al. 2004; Sy et al. 2012; O'Sullivan et al. 2007; During et al. 2002) are consistent to our observations, the kinetic responses in the time course experiments are dissimilar. Unlike previous investigations which never reached its C_{max} for cell lysate within a 16 to 20 h incubation period, our results show a peak concentration within 8 h. It is difficult to compare our time course response for secretion, given that cultures from previous experiments were incubated for only 16 to 20 h, a duration which does not suffice for optimal lutein assimilation to chylomicrons and subsequent secretion (Luchoomun and Hussain 1999; Traber et al. 1987). Potential reasons for the discrepancies in response could be due in part to inconsistencies in vehicles used for carotenoid delivery. For example, tween-40 micelles, which are commonly used for carotenoid delivery, do not include bile salts and fatty acids required for chylomicron production. Future investigation could explore the influence of different micelle formulations utilized to deliver carotenoids on absorption.

Compared to the PS system, the greater uptake of lutein by the CONV system over time may be explained by the influence of differentiation on the behavior of the cells. Hence, it is possible that lutein is able to move into a colonic cell grown to confluence similarly or more efficiently than a differentiated colonic cell expressing an enterocyte-like phenotype. Intracellular levels of β-carotene have been reported in a variety of colonic cell models yet *in vivo* evidence remains lacking. Franseen-van Hal et

al. (2005) examined difference in cellular uptake of β-carotene (1 μM) in presence of THF and α-linoleic acid in 5 human cell lines, i.e., 3 colorectal carcinoma cell lines (Caco-2, HT-29, and HT29D4), a SV40 transformed colon cell line (CCD 841 CoTr), and a small intestinal carcinoma cell line (HuTu 80) after they were all grown to confluence. They found that Caco-2, HT-29, and HT29D4 had low intracellular levels of β-carotene (2-8 pmol/10^6 cells), while CCD 841 CoTr and HuTu 80 had medium levels (50-300 pmol/10^6 cells). However, the extent of secretion was not investigated. Since nondifferentiated Caco-2 cells do not synthesize sufficient apo-B for lipoprotein assembly (Dashti et al. 1990; Reisher et al. 1993; Wagner et al. 1992), future investigations are warranted to explore the extent of carotenoid secretion from undifferentiated colonic cells grown in the PS system.

Despite the widespread use and acceptability of the Caco-2 cell model to investigate nutrient absorption, this model suffers from significant shortcomings that render it less relevant to *in vivo* absorption. The Caco-2 cell model is composed of solely absorptive cells whereas the intestinal epithelium is a conglomerate of absorptive enterocytes and other cells such as goblet cells, endocrine cells, and microfold (M) cells. Several modifications have been made to more closely mimic the heterogeneity of the intestinal epithelium. Co-culturing Caco-2/HT29 introduces the presence of mucin-secreting goblet cells as an additional transport barrier (Hilgendorf et al. 2000; Mahler et al. 2009; Nollevaux et al. 2006). Co-culturing Caco-2/Raji B lymphocytes develops a model of the follicle-associated epithelium of the Peyer's patches containing M cells (des Rieux et al. 2005; Kadiyala et al. 2010; Gullberg et al. 2000). Recently, Antunes et al. (2013) co-cultured Caco-2, HT29, and Raji B together to closely resemble the intestinal mucosa. Thus, more research is needed for the development of reliable and replicable

methodology before it can become a relatively rapid and reliable experimental tool for nutrient absorption studies.

There is a limitation to this investigation that could be further explored. In the time course experiment, a lower dose than that used in micelles was selected for ethanol to assure solubility and cell viability. This limitation did not have much influence on the results of the time course study as the kinetic patterns within each cell culture model are similar given that the T_{max} between vehicles were close. Further, in the CONV system there was a correlation between the effect of vehicle on the time course in cell lysate and in the PS system there was a correlation between the effect of vehicle on the time course in the basolateral and apical mediums.

In summary, the cell culture model has an influence on lutein uptake by Caco-2 cells and micelle components appear to facilitate more effective intestinal secretion of lutein. With Caco-2 cells cultured in the PS system reliably grown to display phenotypes and functions of enterocytes in the small intestine, this *in vitro* platform enables the generation of information that is closer to the physiology of the absorptive enterocytes. However, although the CONV system has the physiology of a colonic tissue, it appears to display a larger efficacy of lutein uptake by Caco-2 cells which can provide a rapid, preliminary tool for methodology development for nutrient absorption studies. The results of this study will help to provide practical guidelines regarding *in vitro* approaches to the study of nutrient absorption.

Reference

Antunes F, Andrade F, Araújo F, Ferreira D, Sarmento B. Establishment of a triple co-culture in vitro cell models to study intestinal absorption of peptide drugs. Eur J Pharm Biopharm. 2013; 83:427-435.

Borel P. Factors affecting intestinal absorption of highly lipophilic food microconstituents (fat-soluble vitamins,carotenoids and phytosterols). Clin Chem Lab Med. 2003; 41:979-994.

Cereijido M, Robbins ES, Dolan WJ, Rotunno CA, Sabatini DD. Polarized monolayers formed by epithelial cells on a permeable and translucent support. J Cell Biol. 1978; 77:853-880.

Chitchumroonchokchai C, Schwartz SJ, Failla ML. Assessment of lutein bioavailability from meals and a supplement using simulated digestion and caco-2 human intestinal cells. J Nutr. 2004; 134:2280-2286.

Craft NE, Soares JH. Relative solubility, stability, and absorptivity of lutein and β-carotene in organic solvents. J Agri Food Chem. 1992; 40:431-434.

Dashti N, Smith EA, Alaupovic P. Increased production of apolipoprotein B and its lipoproteins by oleic acid in Caco-2 cells. J Lipid Res. 1990; 31:113-123.

Delie F, Rubas W. A human colonic cell line sharing similarities with enterocytes as a model to examine oral absorption: advantages and limitations of the Caco-2 model. Crit Rev Ther Drug Carrier Syst. 1997; 14:221-286.

des Rieux A, Ragnarsson EG, Gullberg E, Préat V, Schneider YJ, Artursson P. Transport of nanoparticles across an in vitro model of the human intestinal follicle associated epithelium. Eur J Pharm Sci. 2005; 25:455-465.

During, A., Hussain, M., Morel, D., Harrison, E. (2002). Carotenoid uptake and secretion by CaCo-2 cells: beta-carotene isomer selectivity and carotenoid interactions. J Lipid Res. 43, 1086-1095.

El-Metwally TH, Adrian TE. Optimization of treatment conditions for studying the anticancer effects of retinoids using pancreatic adenocarcinoma as a model. Biochem Biophys Res Commun. 1999; 257:596-603.

Engle MJ, Goetz GS, Alpers DH. (Caco-2 cells express a combination of colonocyte and enterocyte phenotypes. J Cell Physiol. 1998; 174:362-369.

Ferruzza S, Rossi C, Scarino ML, Sambuy Y. A protocol for differentiation of human intestinal Caco-2 cells in asymmetric serum-containing medium. Toxicol In Vitro. 2012; 26: 1252-1255.

Franssen-van Hal NL, Bunschoten JE, Venema DP, Hollman PC, Riss G, Keijer J. Human intestinal and lung cell lines exposed to beta-carotene show a large variation in intracellular levels of beta-carotene and its metabolites. Arch Biochem Biophys. 2005; 439: 32-41.

Garrett DA, Failla ML, Sarama RJ. Development of an in vitro digestion method to assess carotenoid bioavailability from meals. J Agric Food Chem. 1999; 47:4301-4309.

Gullberg E, Leonard M, Karlsson J, Hopkins AM, Brayden D, Baird AW, Artursson P. Expression of specific markers and particle transport in a new human intestinal M-cell model. Biochem Biophys Res Commun. 2000; 279:808-813.

Hilgendorf C, Spahn-Langguth H, Regårdh CG, Lipka E, Amidon GL, Langguth P. Caco-2 versus Caco-2/HT29-MTX co-cultured cell lines: permeabilities via diffusion, inside- and outside-directed carrier-mediated transport. J Pharm Sci. 2000; 89:63-75.

Johnson EJ. The role of carotenoids in human health. Nutr Clin Care. 2002; 5:56-65.
Kadiyala I, Loo Y, Roy K, Rice J, Leong KW. Transport of chitosan-DNA nanoparticles in human intestinal M-cell model versus normal intestinal enterocytes. Eur J Pharm Sci. 2010; 39:103-109.
Krinsky NI, Johnson EJ. Carotenoid actions and their relation to health and disease. Mol. Aspects Med. 2005; 26:459-516.
Lancrajan I, Diehl HA, Socaciu C, Engelke M, Zorn-Kruppa M. Carotenoid incorporation into natural membranes from artificial carriers: liposomes and beta-cyclodextrins. Chem Phys Lipids. 2001; 112:1-10.
Le Ferrec E, Chesne C, Artusson P, Brayden D, Fabre G, Gires P, Guillou F, Rousset M, Rubas W, Scarino ML. In vitro models of the intestinal barrier. The report and recommendations of ECVAM Workshop 46. European Centre for the Validation of Alternative methods. Altern Lab Anim. 2001; 29:649-668.
Liu CS, Glahn RP, Liu RH. Assessment of carotenoid bioavailability of whole foods using a Caco-2 cell culture model coupled with an in vitro digestion. J Agric Food Chem. 2004; 52:4330-4337.
Luchoomun J, Hussain MM. Assembly and secretion of chylomicrons by differentiated Caco-2 cells. Nascent triglycerides and preformed phospholipids are preferentially used for lipoprotein assembly. J Biol Chem. 1999; 274:19565-19572.
Mahler GJ, Shuler ML, Glahn RP. Characterization of Caco-2 and HT29-MTX cocultures in an in vitro digestion/cell culture model used to predict iron bioavailability. J Nutr Biochem. 2009; 20:494-502.
Monsen ER. Dietary reference intakes for the antioxidant nutrients: vitamin C, vitamin E, selenium, and carotenoids. J Am Diet Assoc. 2000; 100:637-640.
Narushima K, Takada T, Yamanashi Y, Suzuki H. (2008). Niemann-pick C1-like 1 mediates alpha-tocopherol transport. Mol Pharmacol. 2008; 74:42-49.
Nielsen IL, Chee WS, Poulsen L, Offord-Cavin E, Rasmussen SE, Frederiksen H, Enslen M, Barron D, Horcajada MN, Williamson G. Bioavailability is improved by enzymatic modification of the citrus flavonoid hesperidin in humans: a randomized, double-blind, crossover trial. J Nutr.2006; 136:404-408.
Nollevaux G, Devillé C, El Moualij B, Zorzi W, Deloyer P, Schneider YJ, Peulen O, Dandrifosse G. Development of a serum-free co-culture of human intestinal epithelium cell-lines (Caco-2/HT29-5M21). BMC Cell Biol. 2006; 7:20-31.
Noy N, Kelleher DJ, Scotto AW. Interactions of retinol with lipid bilayers: studies with vesicles of different radii. J Lipid Res. 1995; 36:375-382.
O'Sullivan SM, Woods JA, O'Brien NM. Use of Tween 40 and Tween 80 to deliver a mixture of phytochemicals to human colonic adenocarcinoma cell (CaCo-2) monolayers. Br J Nutr. 2004; 91:757-764.
O'Sullivan L, Ryan L, O'Brien N. Comparison of the uptake and secretion of carotene and xanthophyll carotenoids by Caco-2 intestinal cells. Br J Nutr. 2007; 98:38-44.
Park SC, Lim JY, Jeen YT, Keum B, Seo YS, Kim YS, Lee SJ, Lee HS, Chun HJ, Um SH, Kim CD, Ryu HS, Sul D, Oh E. Ethanol-induced DNA damage and repair-related molecules in human intestinal epithelial Caco-2 cells. Mol Med Rep. 2012; 5:1027-1032.
Perdikis DA, Basson MN. Basal nutrition promotes human intestinal epithelial (Caco-2) proliferation, brush border enzyme activity, and motility. Crit Care Med. 1997; 25:159-165.

Pérez MD, Calvo M. Interaction of beta-lactoglobulin with retinol and fatty acids and its role as a possible biological function for this protein: a review. J Dairy Sci. 1995; 78:978-988.

Reboul E. Absorption of vitamin A and carotenoids by the enterocyte: focus on transport proteins. Nutrients. 2013; 5:3563-3581.

Reboul E, Thap S, Perrot E, Amiot MJ, Lairon D, Borel P. Effect of the main dietary antioxidants (carotenoids, gamma-tocopherol, polyphenols, and vitamin C) on alpha-tocopherol absorption. Eur J Clin Nutr. 2007; 61:1167-1173.

Reboul E, Borel P. Proteins involved in uptake, intracellular transport and basolateral secretion of fat-soluble vitamins and carotenoids by mammalian enterocytes. Prog Lipid Res. 2011; 50:388-402.

Reisher SR, Hughes TE, Ordovas JM, Schaefer EJ, Feinstein SI. Increased expression of apolipoprotein genes accompanies differentiation in the intestinal cell line Caco-2. Proc Natl Acad Sci U S A. 1993; 90:5757-5761.

Sambruy Y, Ferruzza S, Ranaldi G, De Angelis I. Intestinal cell culture models: applications in toxicology and pharmacology. Cell Biol Toxicol. 2001; 17:301-317.

Sambruy Y, De Angelis I, Ranaldi G, Scarino ML, Stammati A, Zucco F. The Caco-2 cell line as a model of the intestinal barrier: influence of cell and culture-related factors on Caco-2 cell functional characteristics. Cell Biol Toxicol. 2005; 21:1-26.

Shahrzad S, Cadenas E, Sevanian A, Packer L. Impact of water-dispersible beadlets as a vehicle for the delivery of carotenoids to cultured cells. Biofactors. 2002; 16:83-91.

Sy C, Gleize B, Dangles O, Landrier JF, Veyrat CC, Borel P. Effects of physicochemical properties of carotenoids on their bioaccessibility, intestinal cell uptake, and blood and tissue concentrations. Mol Nutr Food Res. 2012; 56:1385-97.

Tapiero H, Townsend DM, Tew KD. The role of carotenoids in the prevention of human patholiges. Biomed. Pharmacother. 2004; 58:100-110.

Traber MG, Kayden HJ, Rindler MJ. Polarized secretion of newly synthesized lipoproteins by the Caco-2 human intestinal cell line. J Lipid Res. 1987; 28:1350-1363.

Wagner RD, Krul ES, Moberly JB, Alpers DH, Schonfeld G. Apolipoprotein expression and cellular differentiation in Caco-2 intestinal cells. Am J Physiol. 1992; 263:E374-E382.

Yeum KJ, Taylor A, Tang G, Russell RM. Measurement of carotenoids, retinoids, and tocopherols in human lenses. Invest Ophthalmol Vis Sci. 1995; 36:2756-2761.

Yi J, Lam TI, Yokoyama W, Cheng LW, Zhong F. (2014). Cellular uptake of beta-carotene from protein stabilized solid lipid nano-particles prepared by homogenization-evaporation method. J Agri. Food Chem. 2014; 62:1096-1104.

Zhang P, Omaye ST. Antioxidant and prooxidant roles for beta-carotene, alpha-tocopherol and ascorbic acid in human lung cells. Toxicol In Vitro. 2001; 15:13-24.

Table 1. Pharmacokinetic parameters of cell lysate from CONV and PS incubated with lutein in ethanol as well as in micelle.

	C_{max} (µg/mg pro)		T_{max} (h)		AUC (h*ng/mg pro)	
Vehicle	**CONV**	**PS**	**CONV**	**PS**	**CONV**	**PS**
Ethanol	2.8 ± 0.5	0.5 ± 0.3 *	39 ± 6	12 ± 10.6 *	41 ± 16	16 ± 6.7 *
Micelle	13.2 ± 3.9	3.5 ± 1.5 *	42 ± 7	8 *	178 ± 59	130 ± 180

Values are mean ± SD, n = 3 and 4 wells for PS and CONV, respectively. Percentage C_{max} free in cell indicates proportion of C_{max} within cytosol and not attached to cell membranes. *Means between the vehicles in the same row differ, tested by Students' t-test (P <0.05).

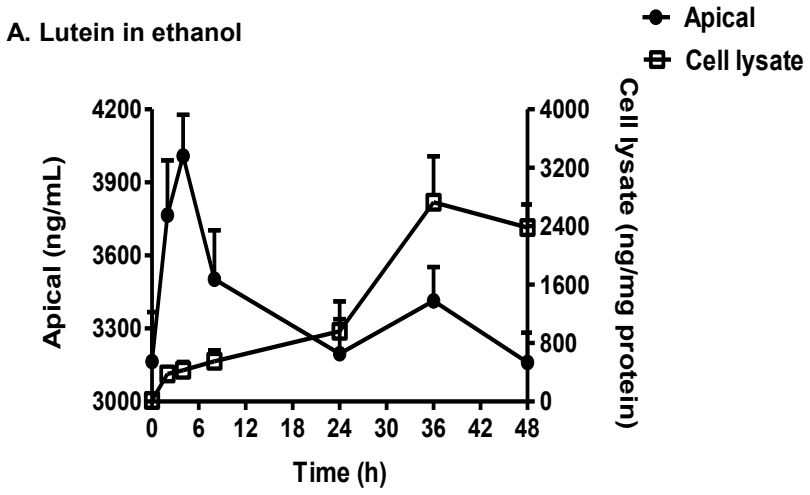

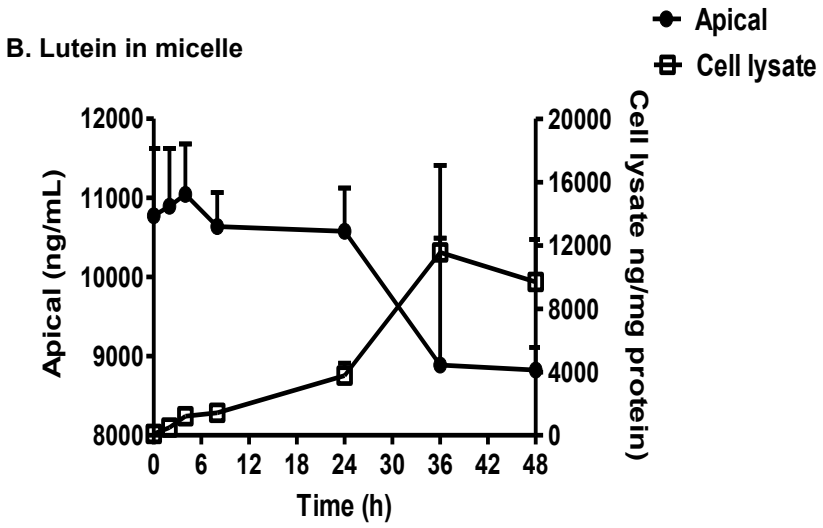

Fig. 1. Effect of time course on lutein uptake by undifferentiated Caco-2 cells grown in CONV system. (A) Cells treated with lutein in ethanol at dose of 4 µg/mL and (B) with lutein in micelle at dose of 14.6 µg/mL. Values are mean ± SD, n = 4 wells.

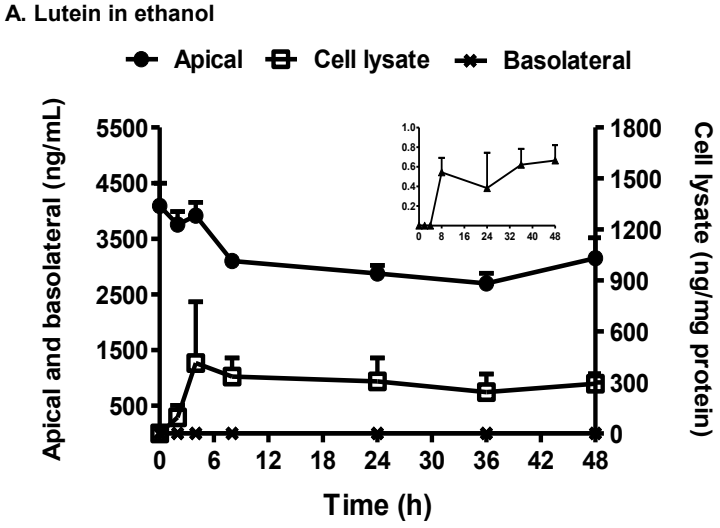

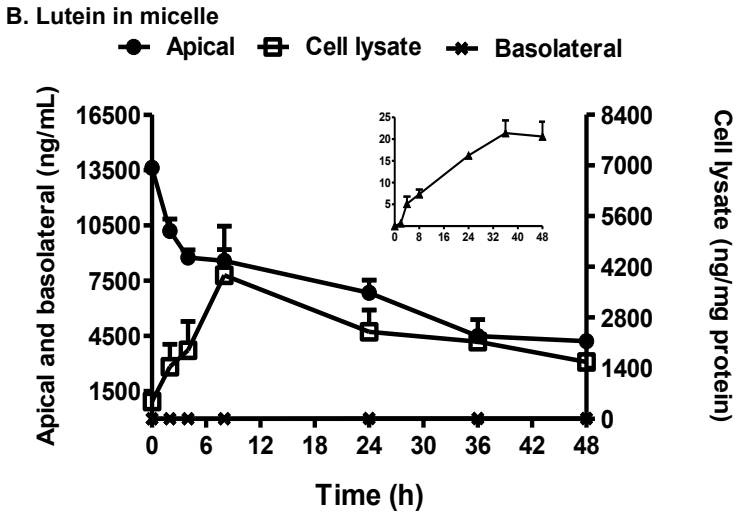

Fig. 2. Effect of time course on lutein uptake and secretion by differentiated Caco-2 cells grown in PS system. (A) Cells treated with lutein in ethanol at dose of 4 µg/mL and (B) with lutein in micelle at dose of 14.6 µg/mL. Values are mean ± SD, n = 4 wells.

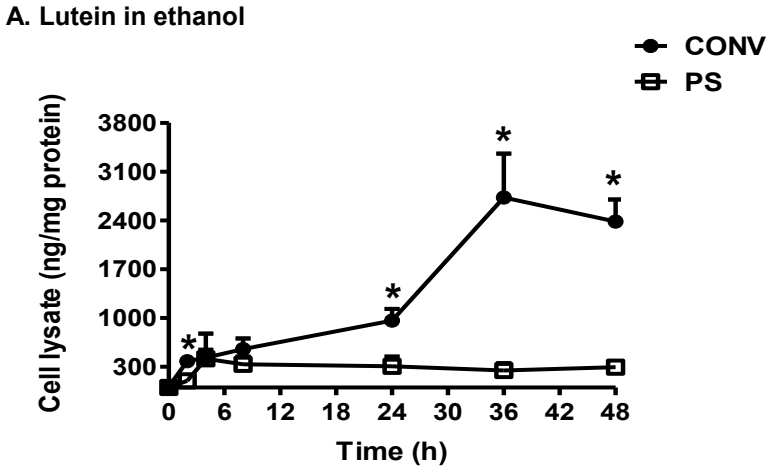

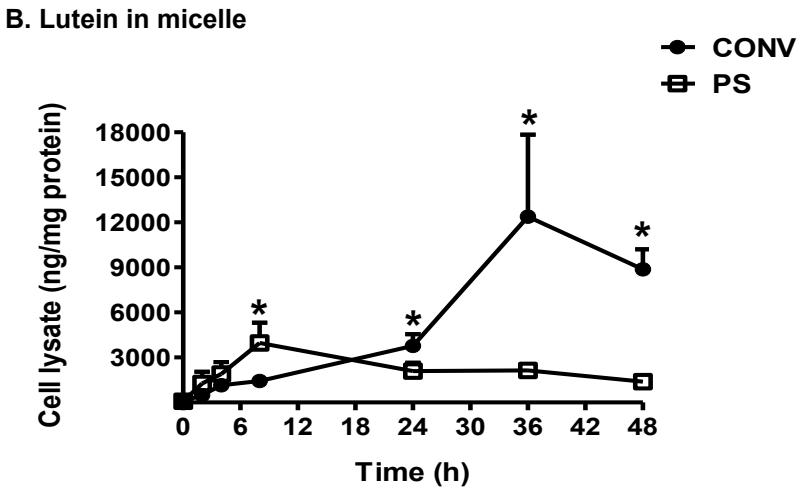

Fig. 3. Effect of cell culture model on the time course of lutein uptake. (A) Cells treated with lutein in ethanol at dose of 4 μg/mL and (B) with lutein in micelle at dose of 14.6 μg/mL. Values are mean ± SD, n = 3 and 4 wells for PS and CONV, respectively. *Means between cell culture models in the same time point differ, tested by Students' t-test (P <0.05).

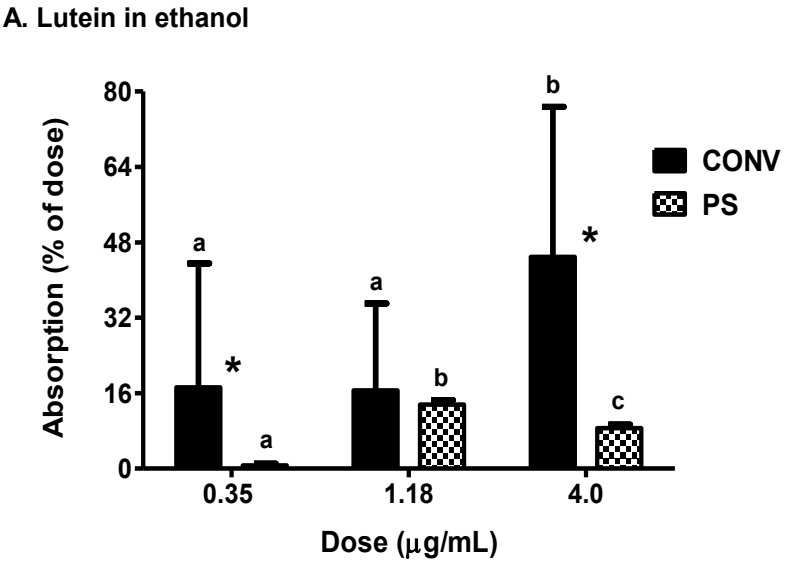

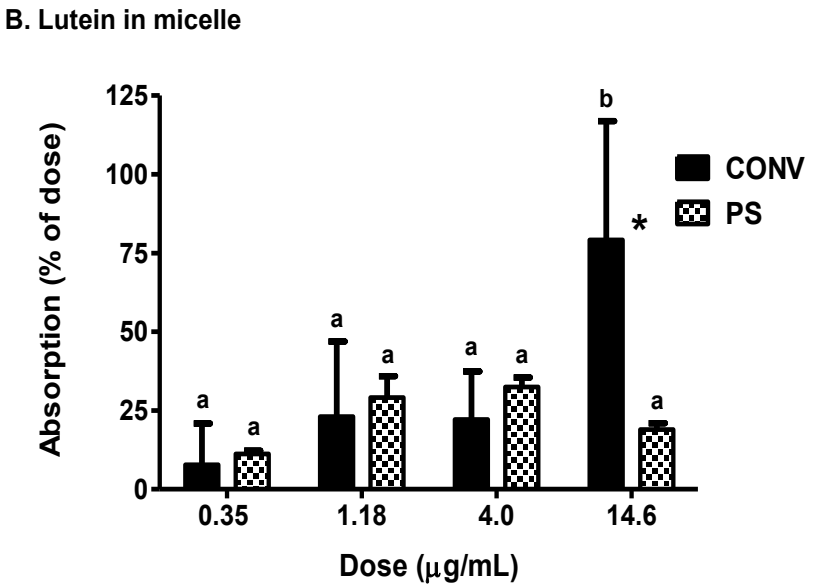

Fig. 4. Effect of dose and influence of cell culture model on lutein absorption in Caco-2 cells at a fixed incubation time of 36 h. (A) Cells treated with lutein in ethanol and (B) with lutein in micelle. Values are mean ± SD, n = 3 and 4 wells for PS and CONV, respectively. *Means between cell culture models in the same dose differ, tested by Students' t-test (P <0.05). [ab]Means between dose in the same model differ, assessed by one-way ANOVA, followed by with Tukey's HSD test (P <0.05).

Chapter 2: The Divergent Impact of Polymeric Nanoparticles on the Bioavailability of Lutein *In Vivo* and *In Vitro*

Abstract

Lutein, a fat-soluble xanthophyll, contributes partially to the health benefits from consuming plant foods. Like all dietary carotenoids, lutein has a low bioavailability. In addition to increasing the intake of lutein-rich foods to enhance lutein status, polymeric nanoencapsulation presents a novel approach to enhancing lutein bioavailability. We evaluated the impact of polymeric nanoencapsulation with poly(lactic-co-glycolic acid) (PLGA) on lutein bioavailability *in vitro* and *in vivo*. We also explored the effect of micelle components on the absorption of PLGA-NP lutein. The bioavailability of free lutein and PLGA-NP-lutein was assessed *in vivo* in rats by examining plasma pharmacokinetics and lutein deposition in selected tissues. Lutein uptake and secretion was assessed *in vitro* in Caco-2 cell grown in a permeable support system. Lutein in samples was quantified by HPLC-UV. Compared to free lutein, PLGA nanoencapsulation increased maximal plasma concentration and area under the time course curve in rats by 54.5 and 77.6 fold, respectively, while in general promoting tissue accumulation in mesenteric adipose and spleen instead of the liver. In comparison to micellized lutein, nanoencapsulation improved the maximal concentration of lutein in rat plasma by 15.6 fold and in selected tissues by $\geq$3.8 fold. In contrast, PLGA-NP lutein decreased the uptake and secretion of lutein in Caco-2 cells by 10.0 and 50.5 fold, respectively, compared to micellized lutein. This effect on cell uptake and secretion of PLGA-NP lutein was moderated (6 and 18.5 fold of reduction) by the addition of micelle components. In conclusion, polymeric nanoencapsulation appears a promising approach to improve the bioavailability of lutein *in vivo*.

Introduction

The consumption of plant based foods and beverages have been associated with reduced risk of chronic disease (Dauchet et al. 2006; He et al. 2004; Smith-Warner et al. 2003). Carotenoids in fruits and vegetables appear to contribute to health promotion through an array of putative bioactions, i.e., antioxidation, anti-inflammation, and modulation of cell signal transduction (Stahl and Sies 2003; Chatterjee et al. 2012). Lutein is a fat-soluble xanthophyll primarily present in dark green leafy vegetables. Its intake and blood status are inversely associated with the risk of age-related macular degeneration, cataracts, cognitive dysfunction, and some forms of cancer (Johnson 2004; Granado et al. 2003). The absorption of lutein in the small intestine depends on several critical steps, including incorporation into micelles, uptake into intestinal cells, and integration into chylomicrons to facilitate luminal secretion. Like all other carotenoids, the bioavailability of lutein is relatively low at ~2.0-9.4% (de Moura et al. 2005; Lienau et al. 2003). In addition, *in vitro* Caco-2 cell culture studies have shown that although 7-35% of micellized lutein was uptaken into intestinal cells, $\leq$6% was secreted to the basolateral side (Sy et al. 2012; Chitchumroonchokchai et al. 2004).

Increasing the bioavailability of certain phytochemicals can be accomplished by preparing foods rich in these ingredients in optimal ways. For example, chopping and sautéing will augment the release of lutein from chloroplasts and tissues of vegetables, and co-consumption with lipids improves the efficiency of micellarization in the small intestine (Yeum and Russell 2002). Recently, nanoencapsulation has been presented as a novel approach for enhancing the bioavailability of poorly absorbed nutrients. Vishwanathan et al. (2009) demonstrated in a human study that nanoemulsions of lutein, mimicking a synthetic micelle with a greater surface to volume ratio, significantly improved its bioavailability. Using an *in vitro* model, Yi et al. (2014) reported that solid

lipid nanoencapsulation of β-carotene significantly improved cellular uptake in Caco-2 cells. In addition to nanoencapsulation using lipid-like ingredients, water-soluble polymeric nanoparticles (NP), such as chitosan and poly(lactic-co-glycolic acid) (PLGA), have emerged as an alternative and promising approach to enhance the bioavailability of poorly absorbed nutrients via their large nutrient loading capacity and greater stability (He et al. 2013). Arunkumar et al. (2013) found that lutein nanocapsulated in chitosan displayed higher bioavailability than unmodified lutein in mice. PLGA has been adopted as a preferred NP because of its well-established safety (Semete et al. 2010) and stability in intestinal environments (Murugeshu et al. 2011), as well as its effectiveness as a carrier of hydrophobic compounds in Caco-2 cells (Derakhshandeh et al. 2010; Gang et al. 2013) and in rats (Tsai et al. 2011; Khalil et al. 2013). A better understanding of the bioavailability of dietary xanthophylls nanoencapsulated in a water-soluble polymer matrix such as PLGA could provide information relevant to its application to formulate novel food products.

Both *in vitro* and *in vivo* models are common and useful approaches to the study of bioavailability. *In vitro* models are utilized as simple, inexpensive, and reproducible tools to predict bioavailability in conjunction with several factors, i.e., digestive stability, micellarization, intestinal transport, and metabolism (Garrett et al. 1999; Sugawara et al. 2001; Chitchumroonchokchai et al. 2004). However, several food- and host-related factors that are capable of influencing bioavailability at different anatomical locations cannot be fully examined in *in vitro* platforms (West and Castenmiller 1998). Information on comparison of the bioavailability of polymeric NPs using both *in vitro* and *in vivo systems* is limited. In the current study, we examined the impact of polymeric PLGA nanoencapsulation on lutein bioavailability and pharmacokinetics in rats. We also investigated the effect of PLGA-NP on the uptake of lutein into intestinal cells compared

to a physiologically relevant vehicle, the micelle. Furthermore, we explored the need of additional micelles for the absorption of lutein loaded in a water soluble NP.

Materials and Methods

Chemicals and materials

β-Cryptoxanthin (BC, 97%), chlorophyll-a (CA, from *Anacystis nidulans* algae), 1-oleoyl-*rac*-glycerol [Monoolein (MO), 99%], 2-oleoyl-1-palmitoyl-*sn*-glycero-3-phosphocholine (PC, 99%), 1-palmitoyl-*sn*-glycero-3-phosphocholine [Lysolecithin, (LC), 99%], sodium glycodeoxycholate (GDC, 97%), sodium taurodeoxycholate hydrate (TDC, 97%), taurocholic acid sodium salt hydrate (TC, 95%), sodium oleate (OA, 99%) and bovine serum albumin (97%) were purchased from Sigma-Aldrich (St. Louis, MO). Advanced Dulbecco's Modified Eagle Medium (DMEM), 200 mM L-glutamine, Penicillin-Streptomycin (10,000 U/mL) were purchased from Gibco, Life Technologies Inc. (Grand Island, NY). Hyclone phosphate buffer saline (PBS) without Ca^{2+} or Mg^{2+}, Pierce RIPA buffer, and Pierce bicinchoninic acid (BCA) protein assay were purchased from Thermo Fischer Scientific (Rockford, IL). Multi-well tissue culture treated plates, Transwell® permeable supports, cell culture treated flasks, and sterile filters (0.22 μM pores) were purchased from Corning Life Sciences (Tewksbury, MA). Caco-2 cells, fetal bovine serum and trypsin-EDTA (0.25%) were purchased from ATCC (Manassas, VA). All other solvents were of HPLC grade and purchased from Sigma-Aldrich (St. Louis, MO). Purified lutein (70-75%) was a gift from Kemin Industries Inc. (Des Moines, IA). Olive oil and refined flour were obtained from Bertolli's and local supermarket respectively. All solvents were of HPLC grade and purchased from Sigma-Aldrich (St. Louis, MO).

Preparation of polymeric NP containing lutein

The polymeric PLGA-NP containing lutein was synthesized by Cristina Sabliov in the College of Agriculture at Louisiana State University using the emulsion evaporation technique (Astete and Sabliov 2006). Briefly, 400 mg polymer PLGA, 50:50 with a molecular weight (MW) of 30-60 kDa (Sigma-Aldrich, St. Louis, MO) was dissolved in 8 mL of ethyl acetate and 40 mg lutein was added after polymer dissolution, creating the organic phase. The organic phase was mixed with 60 mL of 2% polyvinyl alcohol (PVA, MW 30 kDa; Sigma-Aldrich, St. Louis, MO) in water (aqueous phase) under strong stirring for 5 min at room temperature. The suspension was microfluidized (Microfluidics Inc., Westwood, MA) at 25,000 psi 4 times in an ice bath. The resulting mixture was placed in a Buchi R-124 Rotovapor and dried under N_2 gas for approximately 30 min. The particles were then dialyzed for 48 h (water was replaced every 8 h) using a Spectra/Por CE cellulose ester membrane with 100 kDa molecular weight cut off (Spectrum Rancho, Dominquez, CA) to remove PVA. Finally, trehalose (Sigma-Aldrich, St. Louis, MO) was added in an 1 to 1 theoretical ratio before freezing the NP suspension, and the sample was freeze-dried for 40 h using a Freezone 2.5 Plus freeze-drier (Labconco, Kansas City, MO).

Nanoparticle Characterization: The morphology of PLGA-NP was studied with transmission electron microscopy (TEM) using a JEOL 100-CX system (JEOL USA Inc., Peabody, MA). One droplet of the NP suspension was placed on a polymer-coated copper grid of 400 mesh with a carbon film, and the excess sample was removed with filter paper. PLGA-NP was tested for size, polydispersity index (PI), and zeta potential by dynamic light scattering (DLS) using the Malvern Zetasizer Nano ZS (Malvern Instruments Inc., Southborough, MA). The NP size was 124 $\pm$ 4 nm with a PI of 0.11 $\pm$

0.09, zeta potential of -5.3 ± 1.9 mV, pH of 6.5, and entrapment efficiency of 52 ± 3%. Lutein concentration in PLGA-NP varied by 1.5% between batches.

Preparation of synthetic micelles containing lutein

Micelles containing lutein were prepared for cell culture experiments and an animal pilot study according to Chitchumroonchokchai et al. (2004). For the cell culture study, MO, PC, and LC in chloroform (500, 200, and 200 μM, respectively), OA (1500 μM) in methanol, and lutein in ethanol were added to a conical glass tube and dried under N_2 gas at room temperature. Filtered, sterilized (0.22 μM pores) serum–free medium containing 800, 450, and 750 μM GDC, TDC, and TC, respectively, were added to the glass tube, and the resulting mixture was sonicated for 30 min at room temperature under red light. For the animal pilot study, the components used to prepare mixed micelles were scaled up 3-fold, and serum–free medium was replaced with PBS.

Bioavailability of lutein in animal model

Male Fischer 344 rats [mean body weight (BW) of 238 ± 8.0 g] were obtained from Charles River Laboratories (Wilmington, MA) and housed individually in wire cages at 25°C with a 12 h light:dark cycle. After they were fed *ad libitum* with a lutein-free AIN-93G semi-purified diet (Teklad, Madison, WI) for 2 wk, 96 rats were randomly assigned to one of two lutein treatment groups, unmodified (free) and PLGA-NP, with 8 rats each in 6 time points. The time points were chosen based on the results of pilot studies (results not shown). An additional 8 rats were randomly assigned to serve as negative controls for the flour-oil slurry and *ad libitum* diet and were shown to have no lutein in

plasma and selected tissues. Following an overnight 18-h fast, lutein at 10 mg/kg BW (~2.38 mg per rat) was delivered in 1.0 mL of 30% olive oil + 70% flour slurry (0.3 g flour in 1 mL H_2O) via gastric gavage. The olive oil + flour slurry was employed as a delivery vehicle as olive oil has been shown to influence absorption of lutein (Lakshminarayana et al. 2007) and the slurry mixture mimics a food-like mixture. The dose was selected based on detectability of tissue lutein in pilot studies (results not shown) and the feasibility of the NP production capacity. Rats were anesthetized at their assigned time points with 5% isoflurane (Aerrane™, Baxter, Deerfield, IL) and blood from each rat was collected via the orbital sinus through heparin coated micro-hematocrit tubes and transferred to tubes with ETDA as an anticoagulant. Subsequently, organs were harvested and snap frozen in liquid nitrogen. Plasma was collected after whole blood was centrifuged at 2500 x *g* for 10 min at 4°C. All collected samples were stored at -80°C until analysis. As a comparison to the main absorption study, we conducted a pilot study to examine bioavailability of 10 mg/kg BW lutein in micelle solution utilized employed in the Caco-2 cell experiments as described below. Three rats each were randomly assigned to 4 time points (chosen from NP study results, Fig. 1). The study protocol was compliant with all the provisions of the *Guide for the Care and Use of Laboratory Animals* (National Research Council, NIH) and approved by the Tufts University Institutional Animal Care and Use Committee. All experiments and analysis were conducted under red light to protect lutein from photooxidation.

Intestinal absorption of lutein in Caco-2 cell monolayers

Caco-2 cells were maintained in advanced DMEM supplemented with 10% fetal bovine serum and 1% L-glutamine and the absence of antibiotics in a humidified incubator (Thermo Scientific Series 7000) at 37°C and 5% CO_2. Cells between the 12 and 27th passages were used for all experiments.

The uptake and secretion of lutein was tested in three vehicles: (i) micelle, (ii) PLGA-NP, and (iii) PLGA-NP plus additional micelle components. Cells were maintained in medium supplemented with 1% antibiotics (Penicillin-Streptomycin) and seeded at a density of 5 x 10^4 cells/well on collagen coated Transwell® permeable filters (12 well plate, 0.9 cm^2 growth area, 3 µm pore size). Cells were grown for 21 d (with medium changed every 2-3 d) to attain complete differentiation and monolayer integrity when biomarkers [i.e., trans-epithelial electrical resistance (TEER) and alkaline phosphatase activity], reached a plateau (Ferruzza et al. 2012). TEER, reflective of monolayer integrity, was measured using a voltohmmeter equipped with a chopstick electrode (EVOHM2, World Precision Instruments, Sarasota, FL). Alkaline phosphatase activity, an index of differentiation, was measured spectrophometrically using *p*-nitrophenyl-phosphate as an enzyme substrate, according to the manufacturer's instructions (Sigma-Aldrich, St. Louis, MO). The cell lysate was collected using 210 µL of 0.16% digitonin in 2 mM EDTA solution at 37°C and utilized to measure protein content that reflected cell count. In the time course experiment, lutein concentration of 14.6 µg/mL was employed to examine the effect of vehicle. The concentration of 14.6 µg/mL of lutein (~5 mg/d) was selected based on the consideration that it would be an adequate dose to quantify absorption. This concentration was calculated based on the assumption of a mean dietary intake of 1 mg/d lutein (Monsen 2000) and delivery of 2-3 L of water to the small

intestine per day. In the dose response experiment, the lutein concentration in the medium was 0.35, 1.18, 4, and 14.6 µg/mL, which are equivalent to a low to high average lutein intake per day (~0.11, 0.39, 1.3, and 5 mg in 3 L intestinal water).

At the beginning of each experiment, the apical side of Caco-2 cells was washed with PBS twice to remove any serum containing media and replaced with 0.5 mL of lutein enriched serum-free media. The basolateral compartment was filled with 1.5 mL serum-free media. The range of the time course (0-48 h) was selected based on the data of pilot experiments of chylomicron production and secretion to the basolateral compartment. Results showed a 50% increase in apo-lipoprotein-B (apo-B) production between 6 and 16 h yet a steady state was not yet reached 36-48 h (data not shown). Lutein in medium was stable in the culturing conditions for ≥48 h. Apo-B was quantified using an ELISA kit (Antiobodies-Online.com, Product # ABIN612664) after chylomicron isolation using a gradient ultracentrifugation (Luchoomun and Hussain 1999). In the dose response experiment, one incubation time (micelle: 36 h, PLGA-NP and PLGA-NP + micelle: 84 h) was employed to examine the effect of vehicle on lutein uptake and was selected based on the time required to reach a plateau in lutein secretion to basolateral medium. At the end of selected incubation times, media from each side of the membrane was collected. Cells remaining on the permeable filters were washed twice with PBS containing 2 mg/mL bovine serum albumin, incubated with 350 µL above and 600 µL below with 0.25% trypsin-EDTA solution for 30 min at 37°C to detach cells from the membrane filters, and then lysed with 300 µL RIPA buffer for 5 min on ice. All samples were collected in Eppendorf™ tubes, flushed with N_2 gas, wrapped in parafilm, and stored at -80°C until analysis. All experiments and analysis were conducted under red light.

Lutein extraction and analysis

Lutein was extracted primarily from plasma, liver, and mesenteric adipose tissue. Lutein was further extracted from non-accumulating tissues such as spleen and lung for selected time points displaying peak lutein levels determined from the primary tissues. The tissues analyzed were selected as they have been reported to contain the highest tissue accumulation of lutein (Itagaki et al. 2006; Jenkins et al. 2000). Aliquots of pulverized tissue were weighed and homogenized with 0.8, 2.3, and 2.3 mL of 0.9% saline (~80 mg liver, 50 mg spleen, and 50 mg lung) or 0.875 mL methanol (~50 mg adipose tissue) using T25 digital Ultra-Turrax homogenizer (IKA Works, Inc, Wilmington, NC). Aliquots of plasma samples (350 µL), apical and basolateral mediums, and cell lysates (n = 3-4 wells) were briefly vortexed. Cell lysates were sonicated 30 sec at room temperature.

Lutein in the samples was quantified according to the method of Yeum et al. (1995) with slight modifications. β-Cryptoxanthin was used as the internal standard for plasma, adipose tissue, and cell culture and cholorphyll-a was used for liver, spleen, and lung because β-cryptoxanthin was coeluted with unknown compound(s) in the tissues. Briefly, the samples were extracted sequentially with FOLCH solution (chloroform/methanol: 2/1) and hexane while adipose tissue was extracted twice with hexane. The organic layer was removed, combined, evaporated to dryness under N_2 gas, reconstituted in 100 µl acetone, and analyzed by a reverse phase HPLC-UV method. Carotenoids were separated by a ProntoSIL C30 column (4.6 x 150 nm, 3.0 µm, MAC-MOD Analytical, Inc., Chadds Ford, PA, USA). Lutein, β-Cryptoxanthin, and chlorophyll-a were monitored at 443, 450, and 660 nm, respectively. Their concentrations were calculated using standard curves constructed with authenticated

standards. The limit of detection and quantification for lutein was 0.63 and 1 ng on column, respectively. The inter-day and intra-day coefficients of variation (CV) of lutein in plasma, liver, and mesenteric adipose tissue were 6.2, 6.4, and 4.8 and 7.5, 6.4 and 4.1%, respectively. The recovery rate for the internal standards in plasma, liver, and mesenteric adipose tissue calculated from 104 samples was 84 $\pm$ 11, 83 $\pm$ 8, 63 $\pm$ 8% while that in cell culture samples from 57 samples was 72 $\pm$ 19%. The protein content of cell lysates was determined using a BCA protein assay kit (Thermo Fischer Scientific, Rockford, IL) and was used to reflect cell count.

Statistics

All data are expressed as mean $\pm$ SD. The peak lutein concentration (C_{max}), the time to reach C_{max} (T_{max}), and area under concentration vs. time curve (AUC) of plasma and tissues were obtained from complete time course plots that were constructed with randomly selected rats in each time points. The AUC was also calculated using the linear trapezoidal integrations (Nielson et al. 2006). Intestinal absorption (total uptake) is of the sum of lutein in cell lysate and basolateral medium. Differences between means of treatments in the rat study were analyzed by Students' t-test while those in cell culture samples were analyzed by one-way ANOVA, followed by post hoc Tukey-Kramer honestly significant difference (HSD) test. Simple linear regression test (r^2 value) was employed to analyze the dose response of absorption between treatments. Differences with $P \leq 0.05$ were considered significant. The JMP IN 4 statistical software package (SAS Institute, NC, USA) was used to perform all statistical analyses.

Results

Bioavailability of lutein in animal model

In the pharmacokinetics experiment, rats were orally gavaged with 10 mg/kg BW lutein free and PLGA-NP for up to 4.2 h. (**Fig. 1**). Free lutein was not detected in the plasma at 4 time points before the T_{max} of 2.2 h, with a maximum concentration (C_{max}) of 1.7 $\pm$ 1.4 ng/mL (**Fig. 1a**). It shall be noted that lutein was not detected in 3 out of 8 rats at the T_{max}. Lutein was not detected at 4.2 h. When PLGA-NP lutein was administered, lutein was detected in plasma at 50 min yet with a large variability at 56.3 $\pm$ 149.5 ng/mL due to one rat with 426 ng/mL. Plasma lutein level between rats became consistent at 1.2 h with a mean concentration being 56-fold greater than free lutein (**Fig. 1a**, P <0.05). The lutein concentration increased to 90.2 $\pm$ 18.1 ng/mL, C_{max}, at 2.2 h. Despite the same T_{max}, the maximum concentration was 54.5-fold greater than free lutein (P <0.05) (**Table 1**). PLGA-NP lutein was still detected at 4.2 h with its concentration being 28-fold greater than free lutein (**Fig. 1a**, P <0.05). Further, the bioavailability of PLGA-NP lutein (AUC) was 77.6-fold greater than free lutein (**Table 1**, P <0.05). Micellized lutein was detected in the plasma at 40 min in 1 out of the 3 rats (2.9 ng/mL) which increased with a large variability to its maximum concentration of 5.8 $\pm$ 8.5 ng/mL in 2 out of the 3 rats at 4.2 h (**Fig. S1**). Hence, the maximum plasma concentration for micellized lutein which was delayed 2 h was 3.4-fold greater and 15.6-fold less than the C_{max} for free and PLGA-NP lutein.

During the first 1.2 h, free lutein was distributed to the liver with a large variation of concentration between rats from 0 to 2.3 μg/g (**Fig. 1b**). PLGA-NP lutein was delayed the first 1.2 h approaching the mean concentration of free lutein by 3.5 h with a smaller

variability between rats. Although the C_{max} for free lutein was 3.6-fold greater than PLGA NP (**Table** 1, *P* <0.05), its earlier T_{max} at 1.6 h and 1.7-fold greater AUC were not statistically different. The distribution of PLGA-NP lutein to the mesenteric adipose was also delayed the first 30 min reaching a peak concentration between 50 and 70 min with a large variation between rats from 0 to 1.6 μg/g (**Fig. 1c**) which was cleared at 4.2 h. Free lutein was delayed an additional 1.2 h also with a large variation over the time course between 0 and 532 ng/g. Further, although the C_{max} and AUC for PLGA-NP lutein was 3.9- and 4.4-fold greater than free lutein, none of the pharmacokinetic parameters were statistically different (**Table 1**). Similar to the liver, the tissue distribution of PLGA-NP lutein in spleen increased over time reaching a maximum concentration of 363 $\pm$ 192.7 ng/g at 4.2 h which was 19.1-fold greater than free lutein (**Fig. 1d**, *P* <0.05). Similar to the distribution of free lutein in liver, lutein in either treatment was delivered to the lung in the first 10 min with a maximum concentration at this time at 242.7 $\pm$ 214.1 ng/g and also with a large variation which was cleared at 4.2 h (**Fig. 1e**). The pharmacokinetic profiles of micellized lutein within the selected tissues were similar to that of free lutein, yet the apparent maximum concentrations were 27-, 3.5-, 2.4-, and 3.5-fold lower in liver, mesenteric adipose, spleen and lung (**Fig. S1**). Micellized lutein was also 7.5-, 13.5-, 30.4-, and 3.8-fold lower in the aforementioned tissues, respectively, than PLGA-NP lutein.

Intestinal absorption of lutein in Caco-2 cell monolayers

In the time course experiment, Caco-2 cells were treated with 14.6 μg/mL lutein in micelle and PLGA-NP with and without additional micelle components for up to 48 h

(**Fig. 2**). The apparent C_{max} of cell lysate of 4 ± 1.4 µg/mg protein was reached in 8 h after the cells were treated with micellized lutein, followed by a >2-fold reduction from 8 to 24 h post treatment (**Fig. 2a)**. The lutein content of micellized lutein treated cell lysate from 24 to 36 h remained unchanged, and at 48 h post treatment, lutein content was close to that at 2 h (**Fig. 2a**). The lutein content in the apical media followed an opposite trend to that of the cell lysate in the first 8 h post treatment decreasing 1.5-fold as the cell lysate increased toward its T_{max} with a subsequent more gradual decrease by 2.2-fold thereafter up to 48 h post treatment (**Fig. 2b**). The secretion of lutein in micelles increased linearly 4.2 fold starting at 4 h and reached its plateau of 20.6 ± 3.4 ng/mL after 36 h (**Fig. 2c**). The lutein content of PLGA-NP lutein treated cell lysate and secretion in basolateral medium was 10- and 50.5-fold lower, respectively, than that of micellized lutein at 48 h post treatment (P <0.05). With the addition of micelle components to PLGA-NP, the concentration of lutein in cell lysate and secretion in basolateral medium increased 6 and 18.5 fold as compared to PLGA-NP, respectively (P <0.05), yet was still 1.7- and 2.8-fold lower, respectively, than that from micellized lutein (P <0.05). The lutein content of PLGA-NP and PLGA-NP + micelle treated cell lysate and secretion in basolateral medium was monitored up to 96 h but never reached the C_{max} of the micellized lutein and remained at 20.9/3.8- and 8.1/1.9-fold lower for cell lysate and basolateral, respectively.

In the dose-response experiment, Caco-2 cells were treated with 0.35 to 14.6 µg/mL lutein in micelle and PLGA-NP with and without additional micelle components for 48 and 84 h, respectively (**Fig. 3**). There was a dose-response effect on cell uptake and secretion (% of dose as µg) from 0.35 to 14.6 µg/mL lutein which peaked between 1.18 and 4 µg/mL for all three vehicles. Further, the strength and significance of the dose-

response decreased from micelle to PLGA-NP and increased with the addition of micelle components but was still less than micelle (r^2 = 0.88, 0.59, and 0.63 with *P* = 0.0005, 0.0161, and 0.007, respectively). In all doses, the absorption of micellized lutein was at least 4.4-fold greater than PLGA-NP lutein which was improved by the addition of micelle components albeit still about 1.5-fold less than micelles.

Discussion

In the current study, we found that compared to free lutein, nanoencapsulation using PLGA improved the pharmacokinetics (C_{max} and AUC) of lutein in the plasma of rats, while diverting tissue accumulation to mesenteric adipose and spleen instead of the liver. Compared to micellized lutein, nanoencapsulation improved the maximal concentration of lutein in the plasma and selected tissues of rats while decreasing the cell uptake and secretion of lutein in differentiated Caco-2 cells. This contrasting effect on cell uptake and secretion was moderated slightly by the addition of micelle components.

We found that oral administration of lutein free or in PLGA-NP at a dose of 10 mg/kg BW in rats reached its T_{max} at 2.2 h and was essentially eliminated by 4.2 h. In two previous oral pharmacokinetic studies exploring the bioavailability of lutein in Wistar rats over 8-9 h, investigators similarly found the T_{max} in plasma at 2 h (Lakshminarayana et al. 2006; Mamatha and Baskaran 2011). The overall distribution of free lutein in tissues observed in this study was similar to other studies which report that oral as well as intravenous delivery of lutein in Wistar rats over 6 h preferentially accumulated in the liver relative to the spleen and lung (Itagaki et al. 2006; Sato et al. 2011). Further,

although we found the T_{max} of free lutein in the liver was reached at 1.6 $\pm$ 1.8 h, previous research revealed a longer time to maximal plasma concentration at 3-4 h (Lakshminarayana et al. 2006; Itagaki et al. 2006). Acute time course data for distribution of lutein to adipose tissue as well as spleen and lung in rodent models after oral delivery have not been reported in the literature.

Nanoencapsulation has also been shown in a limited number of *in vivo* studies to enhance the bioavailability of lutein in mice as well as humans. Vishwanathan et al. (2009) reported that in humans, nanoemulsions of lutein using the phospholipid Phospholipon 85G, increased mean serum lutein concentrations by approximately 1.3 fold compared to a supplement of lutein in pill form. Similar to our comparison of lutein bioavailability in PLGA-NP and micelle, Arunkumar et al. (2013) found that lutein nanoencapsulated in polymeric chitosan displayed approximately 2-fold greater mean lutein concentrations in plasma, liver and eye in mice at 8 h compared to a micelle vehicle, although a full time course was not studied. Absent other reports about the oral delivery of PLGA carotenoids, it is worth noting that enhanced bioavailability has been demonstrated with other lipophilic phytochemicals, particularly curcumin, in the plasma of rats. Khalil et al. (2013) demonstrated that PLGA-0.5% PVA (size and EE: 161 nm and 73%; polymer MW 10 kDa) improved the plasma AUC of curcumin 15.6 fold over 24 h in Wistar rats compared to the same dose in an aqueous solution. Similarly, Tsai et al. (2011) found that PLGA- 2% PVA (size, EE, and zeta potentials: 158 nm, 46.6%, -12 mV; polymer MW 5-15 kDa) also enhanced the plasma AUC of curcumin 1.1 fold over 2 h in Sprague Dawley rats compared to a 20-fold larger dose in an aqueous solution. In contrast to our observations in plasma and the results of Tsai et al. (2011), Khalil et al. (2013) and others (Mittal et al. 2007; Ma et al. 2012) reported a delay in absorption of PLGA-NPs between 2 and 30 h. While Mitall et al. (2007) and Yallapu et al. (2010)

indicated that an increase in MW, particle size, and percentage of stabilizer may prolong the release behavior of nanosized delivery systems (due in part to an increased lipophilicity, surface to volume ratio and stability) the results of these studies did not follow their suggested principle. Thus, future studies are warranted to explore the effect of all three parameters on compound release.

We found that the overall tissue distribution of PLGA-NP lutein in rats preferentially accumulated in the mesenteric adipose tissue and spleen. Further, PLGA-NP appeared to delay lutein accumulation in liver and spleen. Previous studies exploring the biodistribution of nanoencapsulated hydrophobic compounds delivered orally are limited. As noted, Arunkumar et al. (2013) found that lutein nanoencapsulated in chitosan displayed approximately 2-fold greater mean lutein concentrations in liver and eye in mice at 8 h compared to micelle. Tissue distribution of intravenously delivered PLGA-NP either empty or containing hydrophilic compounds (i.e., the flavonoid breviscapine or the chemotherapy drug docetaxel) have been investigated in rodent models and shown to have the highest deposition in liver followed by spleen (Mohammad and Reineke 2013; Liu et al. 2008; Cheng et al. 2007). Tissues with more porous endothelial walls in blood vessels, such as the liver and spleen, have been shown to have significant uptake of NP. This is due, in part, to the macrophages residing in these tissues also known as the reticulo-enothelial system (Li and Huang 2008; Kumari et al. 2010). Future research exploring the tissue distribution of orally delivered PLGA-NP, especially those containing hydrophobic compounds, is needed to fully understand particle behavior *in vivo*.

In our Caco-2 cell study, the percentage of micellized lutein taken up by the cell lysate at the T_{max} falls within the range of previously reported *in vitro* results at 18-36% (Chitchumroonchokchai et al. 2004; Sy et al. 2012). There are inconsistencies in the

literature related to the degree of lutein secretion from differentiated Caco-2 cells into the basolateral medium. Nonetheless, the <1% percent secretion observed in our experiments falls within the range of 0-10% observed in other *in vitro* studies (Chitchumroonchokchai et al. 2004; Sy et al. 2012). In contrast to our rat study, our Caco-2 cell study demonstrated that, compared to micellized lutein, nanoencapsulation appeared to decrease the cell uptake and secretion of lutein in differentiated Caco-2 cells, which was moderated slightly by the addition of micelle components. Previous *in vitro* investigations exploring the cellular uptake of nanoencapsulated carotenoids are limited. Yi et al. (2014) noted that solid lipid nanoencapsulation of β-carotene with Tween 20, a nonionic synthetic emulsifier, and sodium caseinate, whey protein isolate, or soy protein isolate improved cellular uptake in Caco-2 cells by 2.6, 3.4, and 1.7 fold, respectively, compared to free β-carotene solubilized in organic solvent after 24 h.

Previous studies investigating the cell uptake and secretion of PLGA carotenoids have not been reported. Yet, other *in vitro* studies investigating PLGA nanoencapsulated lipophilic compounds demonstrate conflicting results. In a study on the uptake and transport of furanodiene, a lipophilic extract from *Curcuma wenyujin*, Gang et al. (2013) reported that PLGA nanoencapsulation did not alter uptake, but increased secretion 4 fold after 4 h. Similarly, Derakhshandeh et al. (2010) found that PLGA nanoencapsulation augmented the uptake and secretion of the hydrophobic anti-cancer drug 9-nitrocamptothecin in a dose-independent manner. The lack of improved uptake by the PLGA-NP observed in our study as well as by Gang et al. (2013) may be due in part by varying mechanisms of compound uptake into enterocytes. Lutein is taken up along with micelles by intestinal cells via passive diffusion and facilitated transport through cholesterol transporters, followed by assimilation into chylomicrons for secretion into the lymph system (Reboul and Borel 2011). In contrast, PLGA-NPs are taken up via

a partial energy-dependent endocytosis in the villi, followed by exocytosis into the circulation (Behrens et al. 2002; Reix et al. 2012; McClean et al. 1998). Nevertheless, the amount of PLGA-NPs translocated into Caco-2 cell monolayers appears minimal because of low endocytic capacity (Cartiera et al. 2009; Pietzonka et al. 2002). Our demonstration of improved uptake and secretion of PLGA-NP lutein in Caco-2 cells with the additional of micelle components is consistent with reports that 30% of hydrophobic compounds are released from the NP during the first 2-3 h under simulated gastrointestinal conditions (Gang et al. 2013; Derakhshandeh et al. 2010). Hence, bile salts and phospholipids used for synthesis of chylomicrons appear to facilitate more effective intestinal secretion of PLGA-NP lutein (Luchoomun and Hussain 1999).

There are a number of potential reasons for the inconsistent results between the rat and Caco-2 cell studies. A Caco-2 cell monolayer is composed solely of absorptive cells, whereas the intestinal epithelium is a conglomerate of absorptive enterocytes and other cells such as the mucus secreting goblet cells and microfold (M) cells located in Peyer's patch. A major obstacle affecting the transport of compounds across the intestinal mucosa that was not examined in this study was that of the mucus layer barriers. It is unknown whether the efficacy of absorption of PLGA-NP and synthetic micelles are affected by this mucus layer. In addition, M cells may be a more efficient cellular route of PLGA-NP compared to the micelle since they lack microvilli but possess broader microfolds to transport antigens via endocytosis (des Rieux et al. 2005). Future investigation could utilize inverted co-culture models of Caco-2 cells with goblet and M cell-like cells (Hilgendorf et al. 2000; des Rieux et al. 2005). No one animal completely mimics human absorption and metabolism of carotenoids. Although the rat is a commonly utilized model, carotenoid uptake observed in our study using an epithelial

colorectal adenocarcinoma cell model from humans, did not reflect those anticipated. Future studies could employ alternate animal models (such as the ferret) that may more closely reflect the carotenoid absorbance in humans (Lee et al. 1999; Ribaya-Mercado et al. 1989). Generally, as rats do not efficiently absorb intact carotenoids, high doses, as we did in this study, are fed to rats to achieve an adequate tissue level, which diminishes the relevance to humans. Given that ferrets have been used in many areas of carotenoid research, including absorption and bioavailability, and results generated are similar to those reported in humans (White et al. 1993; Murano et al. 2005) it would informative to examine the bioavailability of PLGA-NP lutein in this animal model and see if these *in vivo* results are more comparable to the *in vitro* results we observed in Caco-2 cells.

There is a limitation to this investigation that should be noted. In the *in vitro* time course experiment, only 3 time points (0, 24, 48 h) were administered for PLGA-NP lutein with and without the additional micelle components due to financial and time constraints. We expect that this limitation should not have marked influence on the time course study as there should not be a change in the kinetic pattern between 0 and 24 h. Given that the secretion of lutein from PLGA-NP and PLGA-NP + micelle in the basolateral medium continued to increase gradually from 0-24 h, there should not be a peak in lutein content in cell lysate within this time period as was observed with the micelle which had a secretion which leveled off between 8 and 24 h.

In summary, using an *in vivo* rat model, polymeric nanoencapsulation appears a promising approach to improving the bioavailability of lutein. However, the inconsistent results between the *in vivo* and *in vitro* models warrant further study to confirm which approach better predicts responses in humans. The results of this study helps build a knowledge base to choose ideal carriers for the oral delivery of lipophilic compounds but

raises issues with regard to the comparability and the predictive value of *in vitro* models to *in vivo* responses.

References

Arunkumar R, Harish Prashanth KV, Baskaran V. Promising interaction between nanoencapsulated lutein with low molecular weight chitosan: Characterization and bioavailability of lutein in vitro and in vivo. Food Chem. 2013; 141:327-337.

Astete CE, Sabliov CM. Synthesis and characterization of PLGA nanoparticles. J Biomater Sci Polym Ed. 2006; 17:247-289.

Behrens I, Pena AI, Alonso MJ, Kissel T. Comparative uptake studies of bioadhesive and non-bioadhesive nanoparticles in human intestinal cell lines and rats: the effect of mucus on particle adsorption and transport. Pharm Res. 2002; 19:1185-1193.

Cartiera MS, Johnson KM, Rajendran V, Caplan MJ, Saltzman WM. The uptake and intracellular fate of PLGA nanoparticles in epithelial cells. Biomaterials. 2009; 30:2790-2798.

Chatterjee M, Roy K, Janarthan M, Das S, Chatterjee M. Biological activity of carotenoids: its implications in cancer risk and prevention. Curr Pharm Biotechnol. 2012; 13:180-190.

Cheng J, Teply BA, Sherifi I, Sung J, Luther G, Gu FX, Levy-Nissenbaum E, Radovic-Moreno AF, Langer R, Farokhzad OC. Formulation of functionalized PLGA-PEG nanoparticles for in vivo targeted drug delivery. Biomaterials. 2007; 28:869-876.

Chitchumroonchokchai C, Schwartz SJ, Failla ML. Assessment of lutein bioavailability from meals and a supplement using simulated digestion and caco-2 human intestinal cells. J Nutr. 2004; 134:2280-2286.

Dauchet L, Amouyel P, Hercberg S, Dallongeville J. Fruit and vegetable consumption and risk of coronary heart disease: a meta-analysis of cohort studies. J Nutr. 2006; 136:2588-2593.

de Moura FF, Ho CC, Getachew G, Hickenbottom S, Clifford AJ. Kinetics of 14C distribution after tracer dose of 14C-lutein in an adult woman. Lipids. 2005; 40:1069-1073.

Derakhshandeh K, Hochhaus G, Dadashzadeh S. In vitro cellular uptake and transport study of 9-nitrocamptothecin PLGA nanoparticles across caco-2 cell monolayer model. Iran J Pharm Res. 2010; 10:425-434.

des Rieux A, Ragnarsson EG, Gullberg E, Préat V, Schneider YJ, Artursson P. Transport of nanoparticles across an in vitro model of the human intestinal follicle associated epithelium. Eur J Pharm Sci. 2005; 25:455-465.

Ferruzza S, Rossi C, Scarino ML, Sambuy Y. A protocol for differentiation of human intestinal Caco-2 cells in asymmetric serum containing medium. Toxicol In Vitro. 2012; 26:1252-1255.

Gang LI, Dong-Hai LIN, Xin-Xin XIE, Li-Fang QIN, Jun-Teng WANG, Ke LIU. Uptake and transport of furanodiene in Caco-2 cell monolayers: a comparison study between furanodiene and furanodiene loaded PLGA nanoparticles. Chin J Nat Med. 2013; 11:49-55.

Garrett DA, Failla ML, Sarama RJ. Development of an in vitro digestion method to assess carotenoid bioavailability from meals. J Agric Food Chem. 1999; 47:4301-4309.

Granado F, Olmedilla B, Blanco I. Nutritional and clinical relevance of lutein in human health. Br J Nutr. 2003; 90:487-502.

He W, Lu Y, Qi J, Chen L, Hu F, Wu W. Nanoemulsion-templated shell-crosslinked nanocapsules as drug delivery systems. Int J Pharm. 2013; 445:69-78.

He K, Hu FB, Colditz GA, Manson JE, Willett WC, Liu S. Changes in intake of fruits and vegetables in relation to risk of obesity and weight gain among middle-aged women. Int J Obes Relat Metab Disord. 2004; 28:1569-1574.

Hilgendorf C, Spahn-Langguth H, Regårdh CG, Lipka E, Amidon GL, Langguth P. Caco-2 versus Caco-2/HT29-MTX co-cultured cell lines: permeabilities via diffusion, inside- and outside-directed carrier-mediated transport. J Pharm Sci. 2000; 89:63-75.

Itagaki S, Ogura W, Sato Y, Noda T, Hirano T, Mizuno S, Iseki K. Characterization of the disposition of lutein after i.v. administration to rats. Biol Pharm Bull. 2006; 29:2123-2125.

Jenkins MY, Mitchell GV, Grundel E. Natural tocopherols in a dietary supplement of lutein affect tissue distribution of tocopherols in young rats. Nutr Cancer. 2000; 37:207-214.

Johnson EJ. A Biological Role of Lutein. Food Rev Intern. 2004; 20:1-16.

Khalil NM, do Nascimento TC, Casa DM, Dalmolin LF, de Mattos AC, Hoss I, Romano MA, Mainardes RM. Pharmacokinetics of curcumin-loaded PLGA and PLGA-PEG blend nanoparticles after oral administration in rats. Colloids Surf B Biointerfaces. 2013; 101:353-360.

Kumari A, Yadav SK, Yadav SC. Biodegradable polymeric nanoparticles based drug delivery systems. Colloids Surf B Biointerfaces. 2010; 75:1-18.

Lakshminarayana R, Raju M, Krishnakantha TP, Baskaran V. Enhanced lutein bioavailability by lyso-phosphatidylcholine in rats. Mol Cell Biochem. 2006; 281:103-110.

Lakshminarayana R, Raju M, Krishnakantha TP, Baskaran V. Lutein and zeaxanthin in leafy greens and their bioavailability: olive oil influences the absorption of dietary lutein and its accumulation in adult rats. J Agric Food Chem. 2007; 55:6395-6400.

Lee CM, Boileau AC, Boileau, TW, Williams, AW, Swanson, KS, Heintz, KA, Erdman JW Jr. Review of animal models in carotenoid research. J Nutr. 1999; 129:2271-2277.

Li SD, Huang L. Pharmacokinetics and Biodistribution of Nanoparticles. Mol Pharm. 2008; 5:496-504

Lienau A, Glaser T, Tang G, Dolnikowski GG, Grusak MA, Albert K. Bioavailability of lutein in humans from intrinsically labeled vegetables determined by LC-APCI-MS. J Nutr Biochem. 2003; 14:663-670.

Liu M, Li H, Luo G, Liu Q, Wang Y. Pharmacokinetics and biodistribution of surface modification polymeric nanoparticles. Arch Pharm Res. 2008; 31:547-554.

Luchoomun J, Hussain MM. Assembly and secretion of chylomicrons by differentiated Caco-2 cells. Nascent triglycerides and preformed phospholipids are preferentially used for lipoprotein assembly. J Biol Chem. 1999; 274, 19565-19572.

Ma Y, Zhao X, Li J, Shen Q. The comparison of different daidzein-PLGA nanoparticles in increasing its oral bioavailability. Int J Nanomedicine. 2012; 7:559-570.

Mamatha BS, Baskaran V. Effect of micellar lipids, dietary fiber and β-carotene on lutein bioavailability in aged rats with lutein deficiency. Nutrition. 2011; 27:960-966.

McClean S, Prosser E, Meehan E, O'Malley D, Clarke N, Ramtoola Z, Brayden D. Binding and uptake of biodegradable poly-DL-lactide micro- and nanoparticles in intestinal epithelia. Eur J Pharm Sci. 1998; 6:153-163.

Mittal G, Sahana DK, Bhardwaj V, Ravi Kumar MN. Estradiol loaded PLGA nanoparticles for oral administration: effect of polymer molecular weight and copolymer composition on release behavior in vitro and in vivo. J Control Release. 2007; 119:77-85.

Mohammad AK, Reineke JJ. Quantitative detection of PLGA nanoparticle degradation in tissues following intravenous administration. Mol Pharm. 2013; 10:2183-2189.

Monsen ER. Dietary reference intakes for the antioxidant nutrients: vitamin C, vitamin E, selenium, and carotenoids. J Am Diet Assoc. 2000; 100:637-640.

Murano I, Morroni M, Zingaretti MC, Oliver P, Sánchez J, Fuster A, Picó C, Palou A, Cinti S. Morphology of ferret subcutaneous adipose tissue after 6-month daily supplementation with oral beta-carotene. Biochim Biophys Acta. 2005; 1740:305-312.

Murugeshu A, Astete C, Leonardi C, Morgan T, Sabliov CM. Chitosan/PLGA particles for controlled release of α-tocopherol in the GI tract via oral administration. Nanomedicine (Lond). 2011; 6:1513-1528.

Nielsen IL, Chee WS, Poulsen L, Offord-Cavin E, Rasmussen SE, Frederiksen H, Enslen M, Barron D, Horcajada MN, Williamson G. Bioavailability is improved by enzymatic modification of the citrus flavonoid hesperidin in humans: a randomized, double-blind, crossover trial. J Nutr.2006; 136:404-408.

Pietzonka P, Rothen-Rutishauser B, Langguth P, Wunderli-Allenspach H, Walter E, Merkle HP. Transfer of lipophilic markers from PLGA and polystyrene nanoparticles to caco-2 monolayers mimics particle uptake. Pharm Res. 2002; 19:595-601.

Reboul E, Borel P. Proteins involved in uptake, intracellular transport and basolateral secretion of fat-soluble vitamins and carotenoids by mammalian enterocytes. Prog Lipid Res. 2011; 50:388-402.

Reix N, Parat A, Seyfritz E, Van der Werf R, Epure V, Ebel N, Danicher L, Marchioni E, Jeandidier N, Pinget M, Frère Y, Sigrist S. In vitro uptake evaluation in Caco-2 cells and in vivo results in diabetic rats of insulin-loaded PLGA nanoparticles. Int J Pharm. 2012; 437:213-220.

Ribaya-Mercado JD, Holmgren SC, Fox JG, Russell RM. Dietary beta-carotene absorption and metabolism in ferrets and rats. J Nutr. 1989; 119:665-668.

Sato Y, Kobayashi M, Itagaki S, Hirano T, Noda T, Mizuno S, Sugawara M, Iseki K. Pharmacokinetic properties of lutein emulsion after oral administration to rats and effect of food intake on plasma concentration of lutein. Biopharm Drug Dispos. 2011; 32:151-158.

Semete B, Booysen L, Lemmer Y, Kalombo L, Katata L, Verschoor J, Swai HS. In vivo evaluation of the biodistribution and safety of PLGA nanoparticles as drug delivery systems. Nanomedicine. 2010; 6:662-671.

Smith-Warner SA, Spiegelman D, Yaun SS, Albanes D, Beeson WL, van den Brandt PA, Feskanich D, Folsom AR, Fraser GE, Freudenheim JL, Giovannucci E, Goldbohm RA, Graham S, Kushi LH, Miller AB, Pietinen P, Rohan TE, Speizer FE, Willett WC, Hunter DJ. Fruits, vegetables and lung cancer: a pooled analysis of cohort studies. Int J Cancer. 2003; 107:1001-1011.

Stahl W, Sies H. Antioxidant activity of carotenoids. Mol Aspects Med. 2003; 24:345-351.

Sugawara T, Kushiro M, Zhang H, Nara E, Ono H, Nagao A. Lysophosphatidylcholine enhances carotenoid uptake from mixed micelles by Caco-2 human intestinal cells. J Nutr. 2001; 131:2921-2927.

Sy C, Gleize B, Dangles O, Landrier JF, Veyrat CC, Borel P. Effects of physicochemical properties of carotenoids on their bioaccessibility, intestinal cell uptake, and blood and tissue concentrations. Mol Nutr Food Res. 2012; 56:1385-1397.

Tsai YM, Jan WC, Chien CF, Lee WC, Lin LC, Tsai TH. Optimised nano-formulation on the bioavailability of hydrophobic polyphenol, curcumin, in freely-moving rats. Food Chem. 2011; 127:918-925.

Vishwanathan R, Wilson TA, Nicolosi RJ. Bioavailability of a nanoemulsion of lutein is greater than a lutein supplement. Nano Biomedicine and Engineering. 2009; 1:38-49.

West CE, Castenmiller, JJ. Quantification of the "SLAMENGHI" factors for carotenoid bioavailability and bioconversion. Int J Vitam Nutr Res. 1998; 68:371-377.

White WS, Peck KM, Ulman EA, Erdman JW Jr. The ferret as a model for evaluation of the bioavailabilities of all-trans-beta-carotene and its isomers. J Nutr. 1993; 123:1129-1139.

Yeum KJ, Russell RM. Carotenoid bioavailability and bioconversion. Annu Rev Nutr. 2002; 22:483-504.

Yeum KJ, Taylor A, Tang G, Russell RM. Measurement of carotenoids, retinoids, and tocopherols in human lenses. Invest Ophthalmol Vis Sci. 1995; 36:2756-2761.

Yi J, Lam TI, Yokoyama W, Cheng LW, Zhong F. Cellular uptake of beta-carotene from protein stabilized solid lipid nano-particles prepared by homogenization-evaporation method. J Agri. Food Chem. 2014; 62: 1096-1104.

Table 1. Pharmacokinetic parameters of plasma and selected tissues after oral administration of 10 mg/kg BW lutein [free or in PLGA nanoparticles (NP)] in rats.

Tissue	C_{max} (ng/mL or g)		T_{max} (h)		AUC (h*ng/mL or g)	
	Free	PLGA-NP	Free	PLGA-NP	Free	PLGA-NP
Plasma	1.7 ± 1.4	90.2 ± 18.1*	2.2	2.2	2.5 ± 1.3	193.9 ± 44.5*
Liver	891.1 ± 243	247.2 ± 42.1*	1.6 ± 1.8	3.2 ± 1.8	846.9 ± 596.2	493.8 ± 109.4
Mesen. Adipose	111.1 ± 129.1	430.1 ± 455.1	2.6 ± 1.8	1.3 ± 0.6	117.9 ± 182.9	519.9 ± 494.6

Values are expressed as mean ± SD, n = 8 rats/time point. *Means between the treatments in the same row differ, tested by Students' t-test (P <0.05).

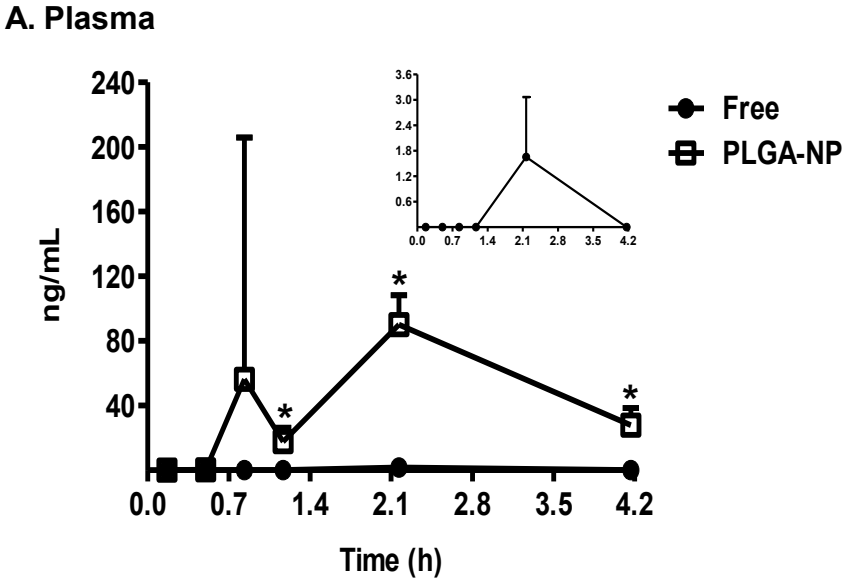

B. Liver

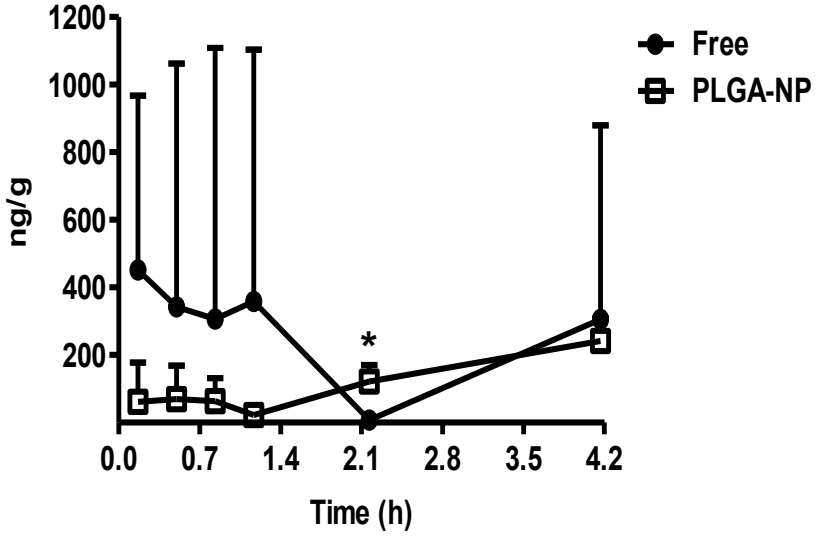

C. Mesenteric Adipose

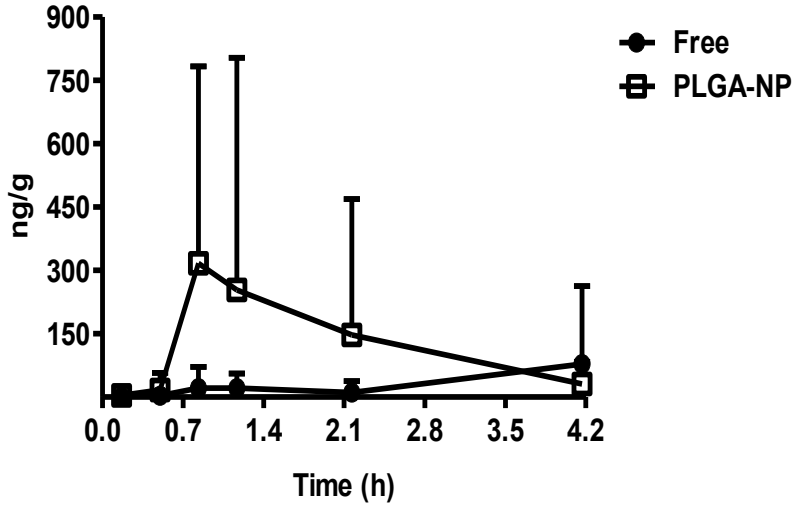

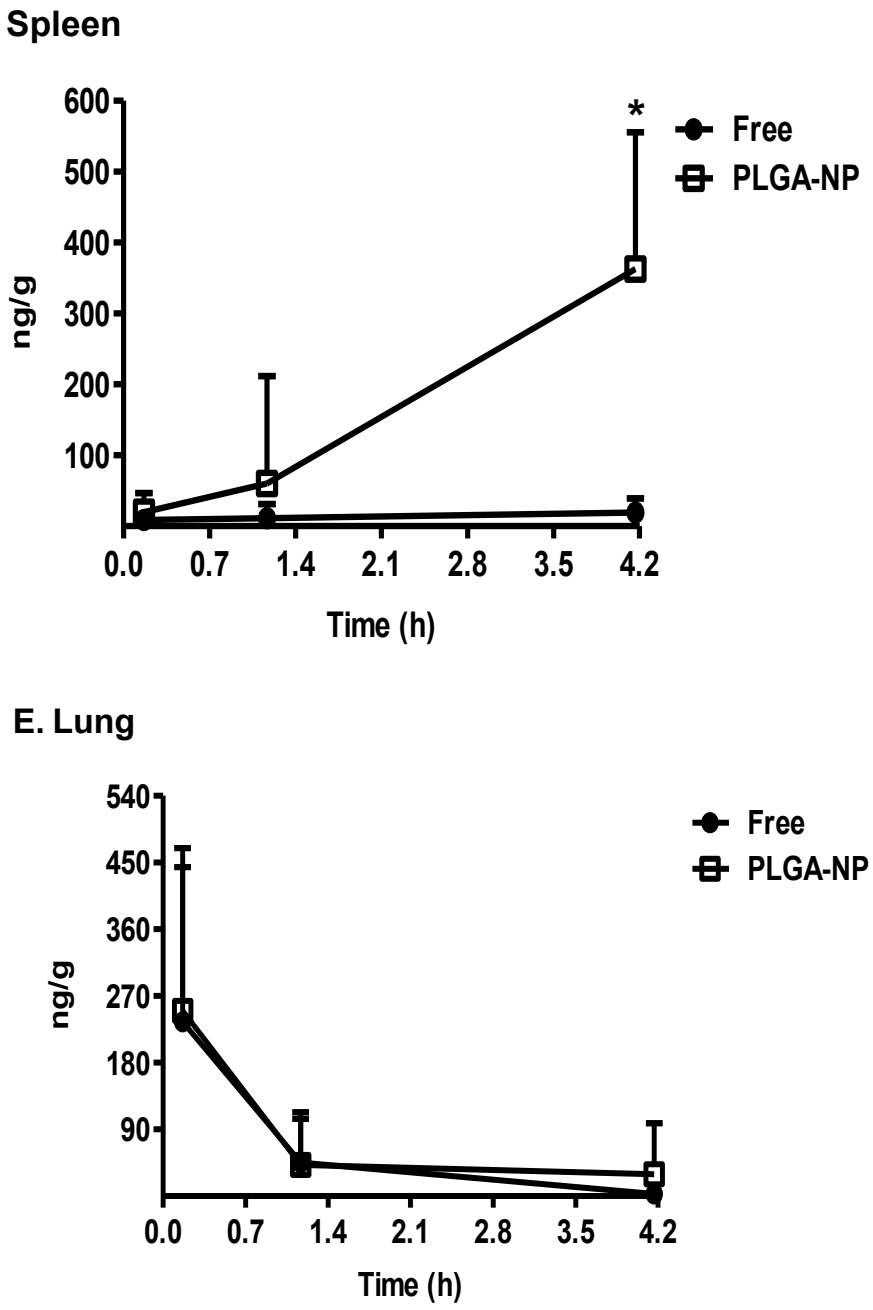

Fig. 1. The effect of polymeric nanoencapsulation on the time profile of lutein in (A) plasma, (B) liver, (C) mesenteric adipose, (D) spleen, and (E) lung after oral administration of 10 mg/kg BW in rats. The insert within (A) is the time profile of free lutein in plasma. Values are expressed as mean $\pm$ SD, n = 8 rats/time point. *Means of the same time points differ, assessed by Students' t-test (P <0.05).

A. Cell lysate

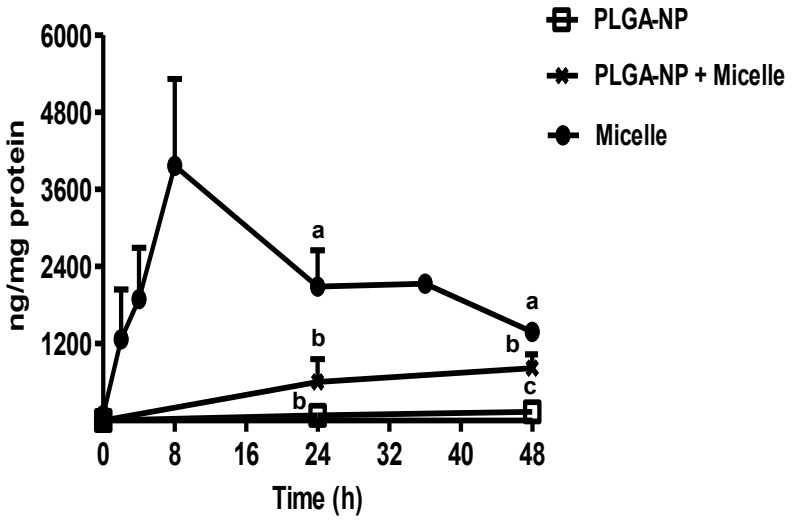

B. Apical

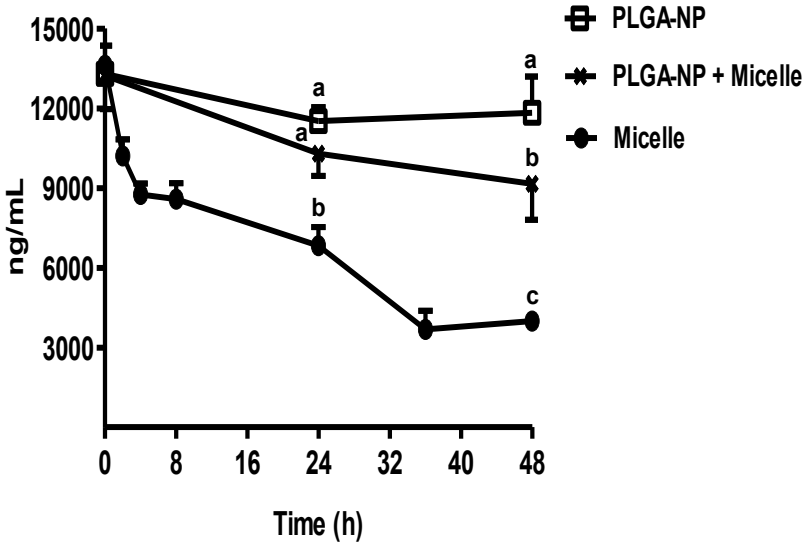

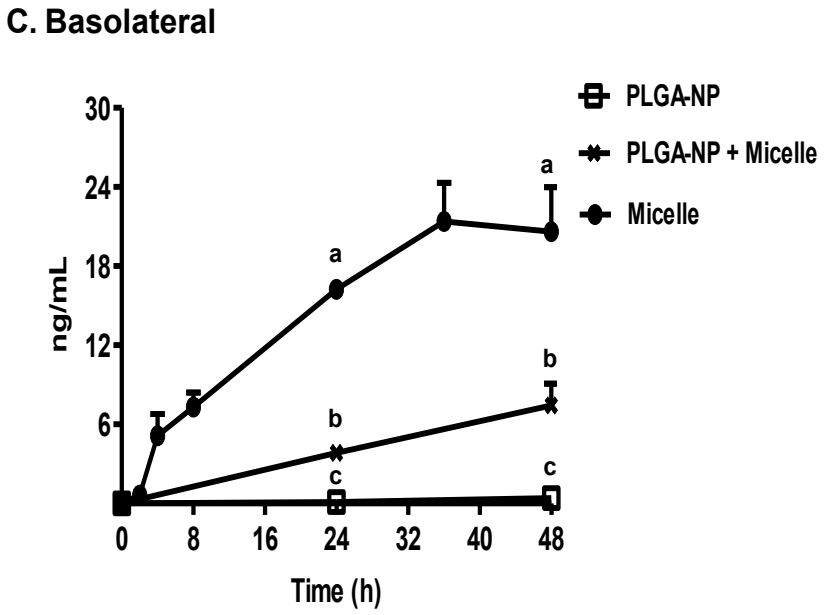

Fig. 2. The effect of polymeric nanoencapsulation with or without additional micelle components on lutein uptake and secretion in differentiated Caco-2 cells treated with 14.6 µg/mL lutein. Values are expressed as mean ± SD, n = 3-4 replicates. [abc]Means of the same time points differ, assessed by one-way ANOVA, followed by with Tukey's HSD test (P <0.05).

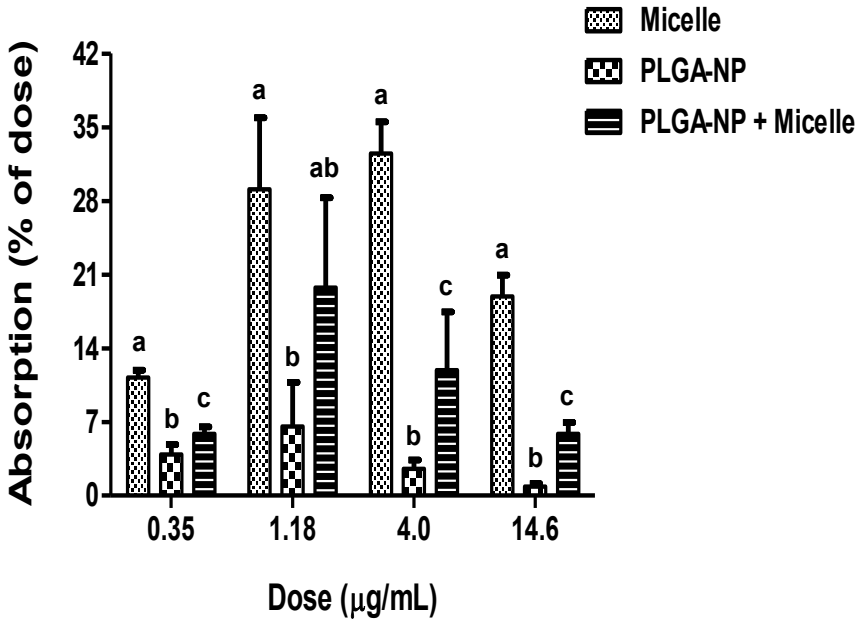

Fig. 3. Effect of polymeric nanoencapsulation with or without additional micelle components on lutein absorption (% of dose) in differentiated Caco-2 cells treated with lutein for 36 h for micelle and 84 h for PLGA-NP and PLGA-NP + micelle. Values are expressed as mean ± SD, n = 3-4 replicates. [abc]Means of the same dose differ, assessed by one-way ANOVA, followed by with Tukey's HSD test (P <0.05).

Appendix

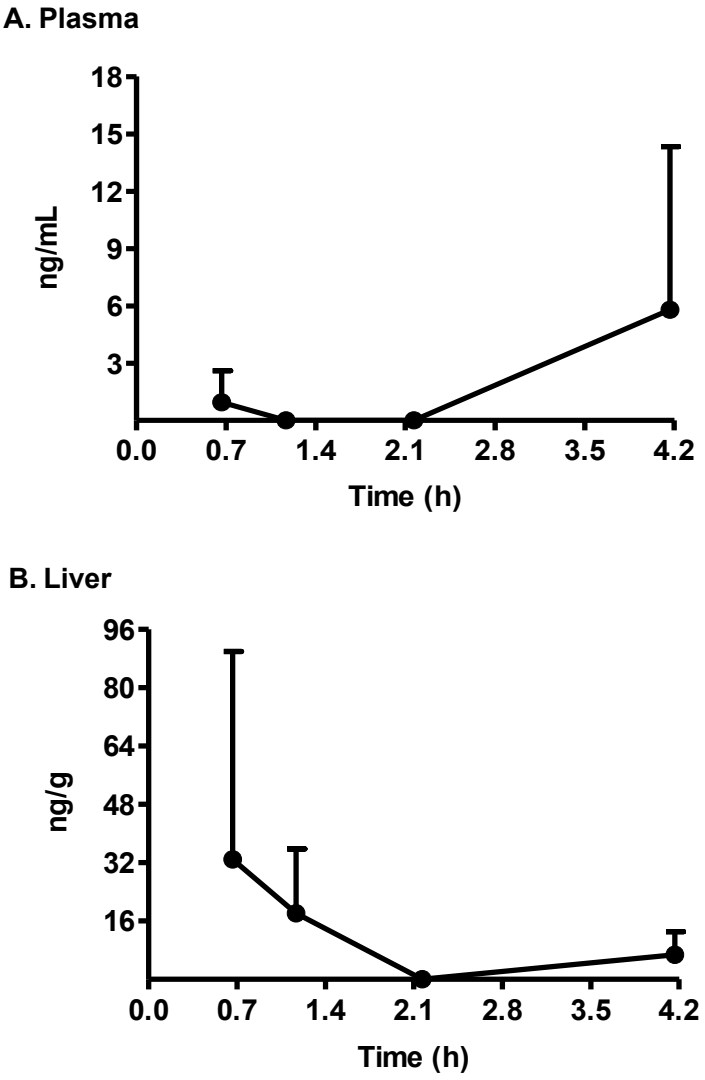

C. Mesenteric Adipose

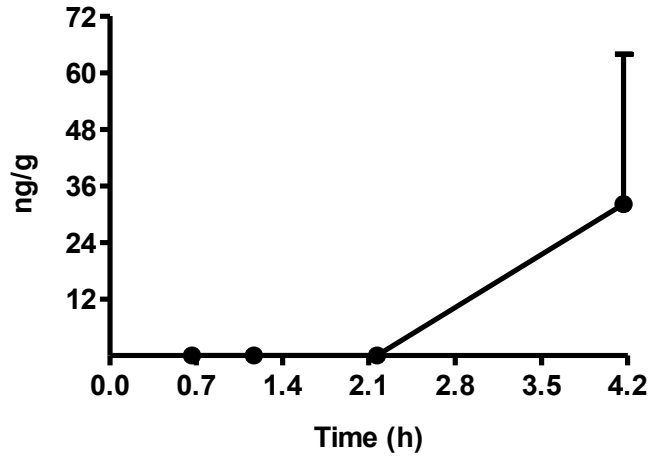

D. Spleen

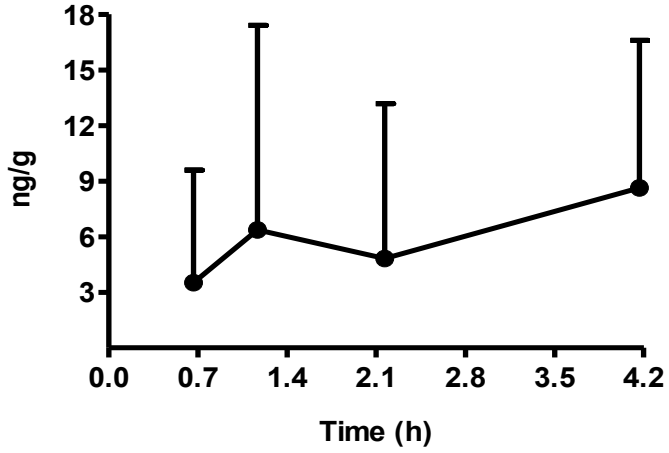

E. Lung

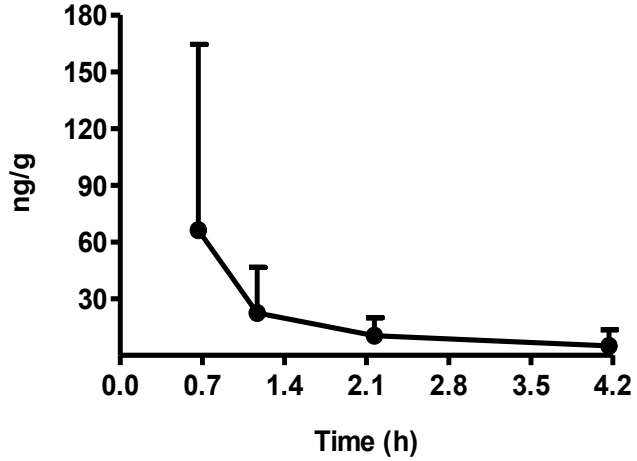

Fig. S1. The effect of micellization on the time profile of lutein in (A) plasma, (B) liver, (C), mesenteric adipose, (D) spleen, and (E) lung after oral administration of 10 mg/kg BW in rats. Values are expressed as mean ± SD, n = 3 rats/time point.

Summary and Discussion

Lutein, a fat-soluble xanthophyll, contributes partially to the health benefits from consuming plant foods. Like all dietary carotenoids, lutein has a low bioavailability. In addition to increasing the intake of lutein-rich foods to enhance lutein status, polymeric nanoencapsulation presents a novel approach to enhancing lutein bioavailability. The overall research objective of this project was to investigate in rats the impact of nanoencapsulation using poly(lactic-co-glycolic acid) (PLGA) on the pharmacokinetics of lutein. We also used an *in vitro* cell culture approach utilizing human epithelial colorectal adenocarcinoma (Caco-2) cells grown in both conventional and permeable support systems to investigate the impact of PLGA on the absorption of lutein in intestinal cells.

The study described in Chapter 1 of this dissertation was the first to systemically compare the efficacy of lutein absorption *in vitro* using Caco-2 cell monolayers grown in conventional (CONV) and permeable support systems (PS). We further examined the role of the micelle, the physiological vehicle within the small intestine, on intestinal absorption *in vitro* in comparison to the organic solvent ethanol, which is safe and commonly consumed by humans. The findings from this study indicated that compared to PS, intracelluar lutein content in CONV was at least 460 and 8% greater in ethanol and micelles, respectively, over 24 h. Yet, the AUC of the intracellular lutein over time was only significantly different for ethanol. Further, the absorption (uptake + secretion) of lutein, independent of delivery vehicle, by Caco-2 cells grown in CONV increased linearly with dose (0.35 to 4 or to 14.6 µg/mL for ethanol or micelle, respectively), while

that in PS reached a peak at 1.18 μg/mL. The greater uptake of lutein by the CONV system over time and dose may be explained by the influence of differentiation on the transport mechanism(s) of the cells. Caco-2 is a cell line originating from human colonic carcinoma that spontaneously differentiates to an enterocyte-like phenotype when monolayers reach confluency and are maintained using conventional monolayer culturing conditions (Ferruzza et al. 2012; Sambruy et al. 2005; Reisher et al. 1993). Hence it is possible that lutein may be able to move into colonic cells grown to confluence more efficiently than a differentiated colonic cell expressing an enterocyte-like phenotype. Lastly, in PS, 0.15% of micellized lutein was secreted to the basolateral medium while only 0.016% was secreted in ethanol, suggesting the necessity of chylomicrons synthesized from micelle components for lutein secretion. In conclusion, these findings suggest lutein uptake by Caco-2 cells is subject to influence of culturing system (CONV vs. PS) and delivery vehicle (ethanol vs. micelle).

The study described in Chapter 2 was the first to examine the impact of polymeric (PLGA) nanoencapsulation on lutein pharmacokinetics in plasma and distribution in selected tissues in rats. We further investigated the effect of PLGA-NP on the absorption of lutein in intestinal cells compared to a more physiological vehicle, the micelle using the permeable support system approach. Additionally, we explored the need of additional micelles for the ultimate absorption of lutein loaded in a water soluble NP. The findings of the rat study indicated that compared to free lutein, PLGA nanoencapsulation increased maximal plasma concentration and area under the time course curve in rats by 54.5 and 77.6 fold, respectively, while in general diverting lutein accumulation to mesenteric adipose and spleen instead of the liver. In comparison to micellized lutein, nanoencapsulation improved the maximal concentration of lutein in rat

plasma 15.6 fold and ≥3.8 fold in selected tissues. In contrast, PLGA-NP lutein decreased the uptake and secretion of lutein in Caco-2 cells by 10.0 and 50.5 fold, respectively, compared to micellized lutein. This effect on cell uptake and secretion of PLGA-NP lutein was moderated (6- and 18.5-fold reductions) by the addition of micelle components. The results of this study suggest that polymeric nanoencapsulation appears a promising approach to improve the bioavailability of lutein in rats. Yet, the inconsistent results between the rat and cell culture models warrant further investigations on which approach better predicts responses in humans. Further, bile salts and phospholipids which are necessary to stimulate synthesis and secretion of chylomicrons appear to facilitate more effective intestinal secretion of PLGA-NP lutein.

In summary, with Caco-2 cells cultured in the PS system reliably grown to display phenotypes and functions of enterocytes in the small intestine, this *in vitro* platform enables the generation of information that is closer to the physiology of the absorptive enterocytes. However, although the CONV system has the physiology of a colonic tissue, it appears to display a larger efficacy of lutein uptake by Caco-2 cells which can provide a rapid, preliminary tool for methodology development for nutrient absorption studies. Further, polymeric nanoencapsulation appears a promising approach to improve the bioavailability of lutein *in vivo* but raises issues with regard to the comparability and the predictive value of *in vitro* models to *in vivo* responses. The results of this dissertation will help provide practical guidelines regarding *in vitro* approaches to the study of nutrient absorption and build the knowledge base to choose ideal carriers for the oral delivery of lipophilic compounds.

Future Directions:

Aim 1: To investigate the extent to which polymeric nanoencapsulation will increase the absorption of lutein in modeled intestinal cells after being subjected to *in vitro* digestion.

Besides the improvement of solubility, polymeric nanoencapsulation has been shown to protect compounds from the GI environment (Derakhshandek et al. 2010; Gang et al. 2013). The *in vitro* digestion model simulates the gastric and small intestinal phase of digestion hence introducing bile salts and phospholipids following the gastric phase (Garrett et al. 1999). Chitchumroonchokchai et al. (2004) showed that lutein accumulation by Caco-2 cells was greater when the cells were exposed to lutein prepared in synthetic micelles instead of lutein in micelles generated during *in vitro* digestion. Given that we showed that bile salts and phospholipids which are necessary to stimulate synthesis and secretion of chylomicrons appear to facilitate more effective intestinal secretion of PLGA-NP lutein it would be informative to explore the influence of the *in vitro* digestion model on lutein absorption in PLGA-NP to that of the unmodified form.

Aim 2: To investigate the extent to which polymeric nanoencapsulation will increase the absorption of lutein in inverted co-culture models of Caco-2 cells with goblet and M cell like cells.

Despite the widespread use and acceptability of the Caco-2 cell model to investigate intestinal absorption, this model suffers from significant shortcomings that render it less relevant to *in vivo* absorption. This model is composed solely of absorptive cells,

whereas the intestinal epithelium is a conglomerate of absorptive enterocytes and other cells such as the mucus secreting goblet cells and microfold “M cells mainly located in Peyer’s patch. A major obstacle affecting the transport of compounds across the intestinal mucosa that was not examined in this study was the effect of the mucus layer barriers. It is unknown whether the efficacy of absorption of PLGA-NP and synthetic micelles are affected by this mucus layer. In addition, the M cell may be a more efficient cellular route of PLGA-NP compared to the micelle as they lack microvilli but possess broader microfolds to transport antigens via endocytosis (des Rieux et al. 2005). Future investigation could utilize inverted co-culture models of Caco-2 cells with goblet and M cell like cells (Hilgendorf et al. 2000; des Rieux et al. 2005).

Aim 3: To examine the impact of polymeric PLGA nanoencapsulation on lutein bioavailability and pharmacokinetics in ferrets.

No one animal completely mimics human absorption and metabolism of carotenoids. Although the rat is a commonly utilized model, carotenoid uptake observed in our study using an epithelial colorectal adenocarcinoma cell model from humans, did not reflect those anticipated. Future studies could employ alternate animal models (such as the ferret) that may more closely reflect the carotenoid absorbance in humans (Lee et al. 1999; Ribaya-Mercado et al. 1989). Generally, as rats do not efficiently absorb intact carotenoids, high doses, as we did in this study, are fed to rats to achieve an adequate tissue level, which diminishes the relevance to humans. Given that ferrets have been used in many areas of carotenoid research, including absorption and bioavailability, and results generated are similar to those reported in humans (White et al. 1993; Murano et al. 2005) it would informative to examine the bioavailability of PLGA-NP lutein in this

animal model and see if these *in vivo* results are more comparable to the *in vitro* results we observed in Caco-2 cells.

<u>Aim 4:</u> To investigate the impact of polymeric PLGA nanoencapsulation with surface modification on the bioavailability of lutein in rats.

There are a number of different polymers and surface modifications utilized to prepare NP which can affect the nature of the compound encapsulated and the polymer constituting the carrier. It is well documented that polymeric NP present short circulation times because they are rapidly recognized by cells of the mononuclear phagocytic system (Kumari et al. 2010). To address this matter, NP can be coated with molecules that provide a greater hydrophilic layer on the particle surface. The most common moiety for surface modification is the hydrophilic and non-ionic polymer PEG. Surface modification can also be used to target NP toward specific organs and increase selective cellular binding and internalization through receptor-mediated endocytosis. Khalil et al. (2013) showed that compared to the curcumin aqueous suspension, the PLGA and PLGA-PEG NP increased the curcumin bioavailability by 15.6 and 55.4 fold, respectively. Future investigation could explore the impact of PLGA nanoencapsulation with surface modification on the bioavailability of hydrophobic compounds such as lutein.

References

Chitchumroonchokchai C, Schwartz SJ, Failla ML. Assessment of lutein bioavailability from meals and a supplement using simulated digestion and caco-2 human intestinal cells. J Nutr. 2004; 134:2280-2286.

Derakhshandeh K, Hochhaus G, Dadashzadeh S. In vitro cellular uptake and transport study of 9-nitrocamptothecin PLGA nanoparticles across caco-2 cell monolayer model. Iran J Pharm Res. 2010; 10:425-434.

des Rieux A, Ragnarsson EG, Gullberg E, Préat V, Schneider YJ, Artursson P. Transport of nanoparticles across an in vitro model of the human intestinal follicle associated epithelium. Eur J Pharm Sci. 2005; 25:455-465.

Ferruzza S, Rossi C, Scarino ML, Sambuy Y. A protocol for differentiation of human intestinal Caco-2 cells in asymmetric serum-containing medium. Toxicol In Vitro. 2012; 26: 1252-1255.

Gang LI, Dong-Hai LIN, Xin-Xin XIE, Li-Fang QIN, Jun-Teng WANG, Ke LIU. Uptake and transport of furanodiene in Caco-2 cell monolayers: a comparison study between furanodiene and furanodiene loaded PLGA nanoparticles. Chin J Nat Med. 2013; 11:49-55.

Garrett DA, Failla ML, Sarama RJ. Development of an in vitro digestion method to assess carotenoid bioavailability from meals. J Agric Food Chem. 1999; 47:4301-4309.

Hilgendorf C, Spahn-Langguth H, Regårdh CG, Lipka E, Amidon GL, Langguth P. Caco-2 versus Caco-2/HT29-MTX co-cultured cell lines: permeabilities via diffusion, inside- and outside-directed carrier-mediated transport. J Pharm Sci. 2000; 89:63-75.

Khalil NM, do Nascimento TC, Casa DM, Dalmolin LF, de Mattos AC, Hoss I, Romano MA, Mainardes RM. Pharmacokinetics of curcumin-loaded PLGA and PLGA-PEG blend nanoparticles after oral administration in rats. Colloids Surf B Biointerfaces. 2013; 101:353-360.

Kumari A, Yadav SK, Yadav SC. Biodegradable polymeric nanoparticles based drug delivery systems. Colloids Surf B Biointerfaces. 2010; 75:1-18.

Lee CM, Boileau AC, Boileau, TW, Williams, AW, Swanson, KS, Heintz, KA, Erdman JW Jr. Review of animal models in carotenoid research. J Nutr. 1999; 129:2271-2277.

Murano I, Morroni M, Zingaretti MC, Oliver P, Sánchez J, Fuster A, Picó C, Palou A, Cinti S. Morphology of ferret subcutaneous adipose tissue after 6-month daily supplementation with oral beta-carotene. Biochim Biophys Acta. 2005; 1740:305-312.

Reisher SR, Hughes TE, Ordovas JM, Schaefer EJ, Feinstein SI. Increased expression of apolipoprotein genes accompanies differentiation in the intestinal cell line Caco-2. Proc Natl Acad Sci U S A. 1993; 90:5757-5761.

Ribaya-Mercado JD, Holmgren SC, Fox JG, Russell RM. Dietary beta-carotene absorption and metabolism in ferrets and rats. J Nutr. 1989; 119:665-668.

Sambruy Y, De Angelis I, Ranaldi G, Scarino ML, Stammati A, Zucco F. The Caco-2 cell line as a model of the intestinal barrier: influence of cell and culture-related factors on Caco-2 cell functional characteristics. Cell Biol Toxicol. 2005; 21:1-26.

White WS, Peck KM, Ulman EA, Erdman JW Jr. The ferret as a model for evaluation of the bioavailabilities of all-trans-beta-carotene and its isomers. J Nutr. 1993; 123:1129-1139.

Appendix

Cell Maintenance for Caco-2

A. Cell Passage (protocol used for 75 cm^2 cell culture flask) I split when cells reach 70-80% confluence. Everything including your hands that go into the hood should be sterilized by 70% ethanol.

Reagents:

1) Advanced Dulbecco's Modified Eagle Medium (DMEM) [12491-015, Gibco]

(a) In the hood, add the following to 25 mL aliquot of media:

- 10% Fetal Bovine Serum [30-2021, ATCC]
- 1% L-glutamine (200mM) [25030-081, Gibco]

(b) Filter sterilize in a 250 mL disposable PES membrane filter system

(c) Add sterilized mixture back to media bottle

2) Trypsin-EDTA [30-2101, ATCC]

3) Hyclone phosphate buffer saline (PBS) without ca^{2+} or mg^{+} [30256, Thermo]

Procedure:

1. Take out complete media, PBS, and trypsin-EDTA from fridge or freezer to warm up at least 30 min before cell passage.
2. Turn on the hood at least 15 min before using.
3. Spray 70% ethanol on the bench in hood before using.
4. Aspirate out the old media, add 6 mL PBS into the flask, rock the flask carefully and discard the PBS to remove the dead cells or some cell fractions.
5. Add 3 mL trypsin to the flask and rock carefully, make sure it covers the whole bottom. Put the flask into incubator at 37 °C and keep it for 5 min- look under microscope to see if all cells are floating.
6. Take out the flask and add 8 mL fresh media into the flask, pull up and down 10-15 times (washing the bottom of the flask a few times as well) to make sure the cells were distributed evenly in the media.
7. Transfer to 50 ml falcon tube and spin in centrifuge at 2500 rpm for 3-5 min.
8. Aspirate old media (leave a little behind to make sure not to aspirate cells).
9. Add fresh media (multiply number of new flasks that cells will be split into by 5 to get total amount of fresh media to add to falcon tube, i.e., 1 old flask of cells split to 2 new flasks = add 10 mL fresh media to falcon tube) and pull up and down 10-15 times to mix cells well.
10. Add 5 mL of cell suspension to each new flask and add additional 10 mL fresh media to each new flask. Place back into incubator (95% humidity, 5% CO_2, 37 °C) immediately.
11. After protocol is completed, spray down the hood with 70% ethanol and wait at least 15 min before turning the hood off.

B. Media Change in Transwell® System (protocol for 12 well plates) Do media change every 48-72 h. Everything including your hands that go into the hood should be sterilized by 70% ethanol.

Reagents:

1) Advanced Dulbecco's Modified Eagle Medium (DMEM) [12491-015, Gibco]
   (a) In the hood, add the following to 25 mL aliquot of media:
      - 10% Fetal Bovine Serum [30-2021, ATCC]
      - 1% L-glutamine (200mM) [25030-081, Gibco]
      - 1% Penicillin-Streptomycin (10,000 U/mL) [15140122, Gibco]
   (b) Filter sterilize in a 250 mL disposable PES membrane filter system
   (c) Add sterilized mixture back to media bottle
2) Hyclone phosphate buffer saline (PBS) without ca^{2+} or mg^{+} [30256, Thermo]

Procedure:

1. Take out media (Advanced DMEM with 10% FBS and 1% L-glutamine, 1% Penicillin-Streptomycin (10,000 U/mL)) and PBS from fridge to warm up at least 30 min before changing media or until it is room temperature.
2. Turn on the hood at least 15 min before using.
3. Spray 70% ethanol on the bench in hood before using and spray your gloves.
4. Aspirate out the old media below permeable supports and above making sure to be **careful** near the membrane.
5. Add 1.5 mL PBS below and 0.5 mL above cell supports, rock gently with lid on, and aspirate.
6. Add 1.5 mL fresh media below and 0.5 mL above cell supports, rock gently with the lid on. Place back into incubator (95% humidity, 5% CO_2, 37 °C) immediately.
7. After protocol is completed, spray down the hood with 70% ethanol and wait at least 15 min before turning the hood off.

Caco-2 Cell Differentiation Biomarkers
Transwell® System (protocol for 12 well plates)

A. Trans-epithelial Resistance Electrical Resistance (TEER)

Equipment:

1) EVOM2 Epithelial voltohmmeter
2) STX2 chopstick electrode

Procedure:

Protocol based on directions from World Precision Instruments (EVOM2, WPI)

B. Alkaline Phosphatase (ALP) Activity (do this assay last)

Reagents:

1) **1M Diethanolamine Buffer (DEA) [D8885, Sigma] with 0.5 mM MgCl2**
   9.7 ml DEA in 80 ml H20 (add DEA to H20)
   0.01 g $MgCl_2$
   Bring up to 100 ml with H20
   Titrate with 6M HCl to pH 9.8
   (Light protected at room temperature for up to 6 months)

2) **3N NaOH**
6 g NaOH in 40 ml H20 (add NaOH to H20)
Bring up to 50 ml with H20
3) **20 mM Tris Buffer with 137 mM NaCl**
242 mg Tris + 795 mg NaCl in 100 ml H20
Titrate pH to 7.4
4) **1 mg/ml p-Nitrophenyl phosphate [P4744, Sigma] in DEA buffer**
(To be made day of assay)
5) **Digitonin/EDTA solution**
(a) 0.16% digotonin in 2 mM EDTA solution, pH 7.8
2 mM EDTA = 0.6 g/1 L H20; use NaOH to dissolve EDTA and titrate with acid
(b) 0.16g digotonin [D5628, Sigma] + 2 mM EDTA to 100 ml (Store at 2-8 °C)
Right before assay heat to redissolve digitonin in solution
6) **BCA kit for protein determination**

Procedure for ALP determination:

1. Thoroughly vacuum suction medium off wells careful not to touch cells
2. Rinse basolateral well with 1.5 ml tris buffer and apical well with 500 µl DEA buffer
3. Add 1.5 ml tris buffer to basolateral well and 250 µl 1mg/ml pNPP in DEA buffer to apical well
4. Incubate for 10 minutes
5. Add 100 µl of apical solution to fresh 96 well plate and stop reaction by adding 50 µl 3N NaOH/well
6. Measure absorbance on plate reader at 405 nm
7. Thoroughly vacuum suction pNPP/tris buffer off wells careful not to touch cells
8. Rinse basolateral well with 1.5 ml PBS and apical well with 500 ul PBS
9. Lyse cells with Add 210 µl digitonin/EDTA solution to apical well at 37 °C for 10 min
10. Mix on orbital shaker at speed 6 for 5 min
11. Transfer 30 µl aliquots for each well to a new 96 well plate for protein determination by the biocinchoninic acid method.

Procedure for Protein determination:

1. Make working reagent (need 200 µl reagent per 10 µl sample)
   (a) Working reagent ratio = 1mL reagent A + 20 µL reagent B
2. Make calibration standards at concentrations of 2000, 1000, 500, 250, 125, 62.5, 31.25 ug/mL Albumin in PBS and 2 blanks (PBS alone, digitonin alone)
3. In a 96 well plate add 200 µl reagent per 10 µl sample
4. Incubate reaction solutions at 37°C for 30 min (start timer after last sample)
5. While incubating: turn on spectrometer and turn off temperature
6. Determine absorbance at 562 nm

Chylomicron Collection and Apo-B Determination

A. CHYLOMICRON COLLECTION

Reagent:

0.91 and 0.95% saline solution- keep at 4 °C

- 910 and 950 mg NaCl in 100 mL EC-H_2O each

Procedure:

1. Add no less than 0.215 g KBr into 1.5 ml sample
2. Gently rock and let salt dissolve into sample
3. Prepare a 4.9 mL Beckman ultracentrifuge tube
4. Add 1.7 mL 0.95% saline to bottom of Beckman tube
5. Add additional 1.7 mL 0.91% saline to the top of the 0.95% saline layer
6. Gently add 1.5 mL sample with KBr underneath saline by using a 9" glass pipette, avoiding air bubbles when eluting sample and being careful as to not disturb saline environment
7. Put Beckman tubes into NVT-90 rotor and make sure it is balanced
8. Spin the tubes at 40,000 rpm for 90 minutes at 15 °C in Beckman L8-M centrifuge
9. Collect 500 µl twice (total of 1 mL) from the top of the tube after spin. Keep at 4 °C covered in parafilm up to 1 week.

B. APO-B DETERMINATION

Protocol based on directions from AssayPro ELISA kit (ABIN61266, Antibodies-Online.Com)

Briefly, chylomicron cell culture samples should not be diluted as concentrations should already be within the standard curve. The absorbance at 450 nm was determined using a FLUOstar OPTIMA plate reader (BMG LABTECH Inc., Cary, NC). The limit of quantification was 0.008 µg/mL. The intra-day and inter-day coefficient of variation was 5 and 7.5%, respectively. Kit can be stored at 2-8 °C or 20 °C upon arrival up to the expiration date but only 1 month upon opening.

Carotenoid in Synthetic Micelles

Transwell® System (protocol for 12 well plates)

*****WORK UNDER RED OR YELLOW LIGHT*****

Reagents: (Prepare day of assay, if using conventional system cut [conc] by 4)

1) 500 µM 1-oleoyl-rac-glycerol [MO, M7765, Sigma]
   Calculate based on volume of media and dissolve in chloroform
2) 200 µM 2-oleoyl-1-palmitoyl-sn-glycero-3-phosphocholine [PC, 42773, Sigma]
   Calculate based on volume of media and dissolve in chloroform
3) 200 µM 1-palmitoyl-sn-glycero-3-phosphocholine [LC, L5254, Sigma]
   Calculate based on volume of media and dissolve in chloroform
4) 1500 µM of sodium oleate [OA, O7501, Sigma]
   Calculate based on volume of media and dissolve in methanol
5) 800 µM sodium glycodeoxycholate [GDC, G9910, Sigma]
   Calculate based on volume of media and dissolve in 1/3 total volum
6) 450 µM sodium taurodeoxycholate hydrate [TDC, T0557, Sigma]

Calculate based on volume of media and dissolve in 1/3 total volume
7) 750 µM taurocholic acid sodium salt hydrate [TC, T4009, Sigma]
Calculate based on volume of media and dissolve in 1/3 total volume
8) Carotenoid in ethanol (concentration will vary based on experiment)
9) Advanced Dulbecco's Modified Eagle Serum-Free Medium (DMEM) [12491-015, Gibco]

In the hood, add the following to 25 mL aliquot of media: 1% L-glutamine (200mM) [25030-081, Gibco]

Procedure:

1. Combine MO, PC, LC, OA and carotenoid in a 9 mL conical glass tube, vortex, and dry under a stream of nitrogen gas at room temperature.
2. Combine GDC, TDC, and TC in 50 mL falcon tube and filter sterilize (0.22 µM pores).
3. Aliquot media into the conical glass tubes, vortex, and sonicate in a water bath at room temperature for 30 min.

Cell Lysate Collection and Carotenoid Analysis by HPLC-UV

*****WORK UNDER RED OR YELLOW LIGHT*****

A. SAMPLE COLLECTION

Reagents:

1) Hyclone phosphate buffer saline (PBS) without ca^{2+} or mg^{+} [30256, Thermo] with 2 g/L bovine serum albumin
   - To be made day of collection (does not need to be sterile)

2) Trypsin-EDTA [30-2101, ATCC] with 200 U/mL collagenase, Type I [17018-029, Invitrogen]
   - To be made day of collection (does not need to be sterile)

3) Pierce RIPA buffer [89901, Thermo]

Procedure:

For conventional system:

1. Thoroughly vacuum suction medium off wells careful not to touch cells
2. Rinse apical compartment twice with 0.5 mL PBS + albumin solution
3. Add 300 µl RIPA buffer and incubate for 5 min on a on ice and mix on orbital shaker at speed 4 (buffer will also lyse cells).
4. Collect all samples in a 1.7 mL Eppendorf™ tube, flush with nitrogen gas, wrap in parafilm, and store at -80 °C until further analysis

For transwell® system:

1. Thoroughly vacuum suction medium off wells careful not to touch cells
2. Rinse apical and basolateral compartments twice with 0.5 mL PBS + albumin solution
3. Add 350 µl and 600 µl trypsin-EDTA + collagenase solution to apical and basolateral compartments respectively and incubate for 30 min at 37 °C

4. Collect all samples in a 1.7 mL Eppendorf™ tube and centrifuge at 8000 rpm for 5 min.
4. Collect cell pellet and resuspend in 300 µl RIPA buffer to lyse cells. Incubate for 5 min on a on ice and mix on orbital shaker at speed 4 (buffer will also lyse cells).
5. Collect all samples in a 1.7 mL Eppendorf™ tube, flush with nitrogen gas, wrap in parafilm, and store at -80 °C until further analysis

B. SAMPLE EXTRACTION

Reagents:

1) MPA: 0.6 g NH4-Acetate, 40 mL EC-H_2O, 300 mL methyl tert-butyl ether, 1660 mL Methanol
2) MPB: 0.2 g NH4-Acetate, 20 mL EC-H_2O, 900 mL methyl tert-butyl ether, 80 mL Methanol
   filter and degas before using on UV-HPLC
3) 0.85% Saline (850 mg NaCl in 100 mL distilled water)
4) 2 µg/mL β-cryptoxanthin in ethanol (internal standard)
   extinction coefficient 2520 (450 nm) at absorbance .501
5) FOLCH (Chorofom:Methanol 2:1)
6) Hexane

Procedure:

1. Sonicate in room temperature water bath for 30 sec
2. Centrifuge at 14000 rpm for 4 min
3. Collect 25 µl from supernatant for protein determination (see procedure below)
4. Vortex remaining sample and add to 16 x 125 mm glass tube
5. Add 20 uL internal standard and vortex
6. Add 5 mL FOLCH and 1.5 mL 0.85% saline and vortex on high speed for 1.5 minutes
7. Centrifuge at 3000 rpm for 10 minutes at 4 °C
8. Transfer the bottom layer (chloroform) into a new 16 x 125 glass tube
9. Add 5 mL hexane to the first glass tube and vortex at high speed for 1.5 minutes
10. Centrifuge at 3000 rpm for 10 minutes at 4 °C
11. Transfer the upper layer (hexane) into the second glass tube with the previous chloroform extract
12. Dry the combined extract under nitrogen gas (takes around 1.5 hrs)
13. The residue is re-dissolved in 100 µL acetone
14. Sonicate the tube for 30 seconds
15. Transfer the solution to a 1.7 ml microcentrifuge filter tube (0.22uM) and centrifuge at 14000 rpm for 7 minutes
16. Transfer each extracted solution from the microcentrifuge tube into a vial to load on the UV-HPLC

17. A 50 µL aliquot is injected onto a C30 ProntoSIL Carotenoid 3µm 4.6x 150mm column
18. A pre-column is attached before the C30 column

Procedure for protein determination:

1. Make working reagent (need 200 µl reagent per 25 µl sample)
   a) Working reagent ratio = 1mL reagent A + 20 µL reagent B
2. Make calibration standards at concentrations of 1000, 500, 250, 125, 62.5, 31.25 ug/mL albumin in RIPA buffer and 1 blank (RIPA buffer alone)
3. In a 96 well plate add 200 µl reagent per 25 µl sample
4. Incubate reaction solutions at 37°C for 30 min (start timer after last sample)
5. While incubating: turn on spectrometer and turn off temperature
6. Determine absorbance at 562 nm

Carotenoid Analysis in Cell Culture Media Samples by HPLC-UV

*****WORK UNDER RED OR YELLOW LIGHT*****

Reagents:

1) MPA: 0.6 g NH4-Acetate, 40 mL EC-H_2O, 300 mL methyl tert-butyl ether, 1660 mL Methanol
2) MPB: 0.2 g NH4-Acetate, 20 mL EC-H_2O, 900 mL methyl tert-butyl ether, 80 mL Methanol
   filter and degas before using on UV-HPLC
3) 0.85% Saline (850 mg NaCl in 100 mL distilled water)
4) 2 µg/mL β-cryptoxanthin in ethanol (internal standard) extinction coefficient 2520 (450 nm) at absorbance .501
5) FOLCH (Chorofom:Methanol 2:1)
6) Hexane

Extraction Procedure:

1. Add media to 16 x 125 glass tube (if apical add a certain aliquot that is a concentration within the range for detection)
2. Add 20 uL internal standard and vortex
3. Add 5 mL FOLCH (6 mL if analyzing basolateral) and 1.5 mL 0.85% saline and vortex on high speed for 2 minutes
4. Centrifuge at 3000 rpm for 10 minutes at 4 °C
5. Transfer the bottom layer (chloroform) into a new 16 x 125 glass tube
6. Add 5 mL hexane (6 mL if analyzing basolateral) to the first glass tube and vortex at high speed for 2 minutes
7. Centrifuge at 3000 rpm for 15 minutes at 4 °C
8. Transfer the upper layer (hexane) into the second glass tube with the previous chloroform extract
9. Dry the combined extract under nitrogen gas (takes around 1.5 hrs)
10. The residue is re-dissolved in 100 µL acetone
11. Sonicate the tube for 30 seconds
12. Transfer the solution to a 1.7 ml microcentrifuge filter tube (0.22uM) and centrifuge at 14000 rpm for 7 minutes

13. Transfer each extracted solution from the microcentrifuge tube into a vial to load on the UV-HPLC
14. A 50 µL aliquot is injected onto a C30 ProntoSIL Carotenoid 3µm 4.6x 150mm column

Carotenoid Analysis in Plasma by HPLC-UV

*****WORK UNDER RED OR YELLOW LIGHT*****

Reagents:

1) MPA: 0.6 g NH4-Acetate, 40 mL EC-H_2O, 300 mL methyl tert-butyl ether, 1660 mL Methanol
2) MPB: 0.2 g NH4-Acetate, 20 mL EC-H_2O, 900 mL methyl tert-butyl ether, 80 mL Methanol
   filter and degas before using on UV-HPLC
3) 0.85% Saline (850 mg NaCl in 100 mL distilled water)
4) 2 µg/mL β-cryptoxanthin in ethanol (internal standard)
   extinction coefficient 2520 (450 nm) at absorbance .501
5) FOLCH (Chorofom:Methanol 2:1)
6) Hexane

Extraction Procedure:

1. Add 350 µl aliquot to 16 x 125 glass tube
2. Add 20 uL internal standard and vortex
3. Add 5 mL FOLCH and 1.5 mL 0.85% saline and vortex on high speed for 1.5 minutes
4. Centrifuge at 3000 rpm for 10 minutes at 4 °C
5. Transfer the bottom layer (chloroform) into a new 16 x 125 glass tube
6. Add 5 mL hexane to the first glass tube and vortex at high speed for 1.5 minutes
7. Centrifuge at 3000 rpm for 10 minutes at 4 °C
8. Transfer the upper layer (hexane) into the second glass tube with the previous chloroform extract
9. Dry the combined extract under nitrogen gas (takes around 1.5 hrs)
10. The residue is re-dissolved in 100 µL acetone
11. Sonicate the tube for 30 seconds
12. Transfer the solution to a 1.7 ml microcentrifuge filter tube (0.22uM) and centrifuge at 14000 rpm for 7 minutes
13. Transfer each extracted solution from the microcentrifuge tube into a vial to load on the UV-HPLC
14. A 50 µL aliquot is injected onto a C30 ProntoSIL Carotenoid 3µm 4.6x 150mm column

Carotenoid Analysis in Liver by HPLC-UV

*****WORK UNDER RED OR YELLOW LIGHT*****

Reagents:

1) MPA: 0.6 g NH4-Acetate, 40 mL EC-H_2O, 300 mL methyl tert-butyl ether, 1660 mL Methanol
2) MPB: 0.2 g NH4-Acetate, 20 mL EC-H_2O, 900 mL methyl tert-butyl ether, 80 mL Methanol
   filter and degas before using on UV-HPLC
3) 0.85% Saline (850 mg NaCl in 100 mL distilled water)
4) 3.4 µg/mL chlorophyll a in acetone (internal standard)
   extinction coefficient 1712 (660 nm) at absorbance .580
5) FOLCH (Chorofom:Methanol 2:1)
6) Hexane

Extraction Procedure:

1. Pulverize liver in a mortar and pestle over flow of liquid nitrogen and store in -80 °C in a 60 mL amber glass jar
2. Weigh 150 mg liver to a 20 mL glass vial
3. Add 1.5 mL cold 0.9% saline and homogenize with IKA T25 digital ultra-turax homogenizer at speed until liver is dissolved and liquid becomes frothy
4. Aliquot 800 µL to 16 x 125 glass tube
5. Add 9 µl of internal standard and vortex
6. Add 5 mL FOLCH and 1.5 mL 0.85% saline and vortex at high speed for 2 minutes
7. Centrifuge at 3000 rpm for 10 minutes at 4 °C
8. Transfer the bottom layer (chloroform) into a new glass tube
9. Add 5 mL hexane to the first glass tube and vortex at high speed for 1.5 minutes
10. Centrifuge at 3000 rpm for 10 minutes at 4 °C
11. Transfer the upper layer (hexane) into the second tube with the previous chloroform extract
12. Dry the combined extract under nitrogen gas (takes around 1.5 hrs)
13. The residue is re-dissolved in 100 µL acetone
14. Sonicate the tube for 30 seconds
15. Transfer each extracted solution from the microcentrifuge tube into a Transfer the solution to a 1.7 ml microcentrifuge filter tube (0.22uM) and centrifuge at 14000 rpm for 7 minutes
16. Transfer each extracted solution from the microcentrifuge tube into a vial to load on the UV-HPLC
17. A 50 µL aliquot is injected onto a C30 ProntoSIL Carotenoid 3µm 4.6x 150mm column

Carotenoid Analysis in Adipose Tissue by HPLC-UV

*****WORK UNDER RED OR YELLOW LIGHT*****

Reagents:

1) MPA: 0.6 g NH4-Acetate, 40 mL EC-H_2O, 300 mL methyl tert-butyl ether, 1660 mL Methanol
2) MPB: 0.2 g NH4-Acetate, 20 mL EC-H_2O, 900 mL methyl tert-butyl ether, 80 mL Methanol
   filter and degas before using on UV-HPLC
3) 0.85% saline (850 mg NaCl in 100 mL EC-H_2O)
4) 2 µg/mL β-cryptoxanthin in ethanol (internal standard)
   extinction coefficient 2520 (450 nm) at absorbance .501
5) Hexane

Extraction Procedure:

1. Pulverize adipose tissue in a mortar and pestle over flow of liquid nitrogen and store in -80 °C in a 50 mL falcon tube wrapped in foil
2. Weigh 50 mg adipose tissue to a 17 x 60 mm glass vial
3. Add 20 µl internal standard and vortex
4. Add 875 µl methanol and homogenize with IKA T25 digital ultra-turax homogenizer at speed until adipose tissue is broken up and liquid becomes opaque and frothy
5. Rinse homogenizer blade with 875 µl fresh methanol in a new glass vial
6. Transfer homogenized adipose tissue to a new (16 x 125 mm) glass tube and rinse the glass vial with the additional methanol used to rinse the homogenizer blade
7. Add 6 mL hexane and vortex on high speed for 2 minutes
8. Centrifuge at 3000 rpm for 10 minutes at 4 °C
9. Transfer the upper layer (hexane) into a new glass tube. Repeat steps 7-9 one more time
10. Dry the combined extract under nitrogen gas (takes around 1.5 hrs)
11. The residue is re-dissolved in 100 µL acetone
12. Transfer each extracted solution from the microcentrifuge tube into a vial to load on the UV-HPLC
13. A 50 µL aliquot is injected onto a C30 ProntoSIL Carotenoid 3µm 4.6x 150mm column

Carotenoid Analysis in Spleen/Lung by HPLC-UV

*****WORK UNDER RED OR YELLOW LIGHT*****

Reagents:

1) MPA: 0.6 g NH4-Acetate, 40 mL EC-H_2O, 300 mL methyl tert-butyl ether, 1660 mL Methanol
2) MPB: 0.2 g NH4-Acetate, 20 mL EC-H_2O, 900 mL methyl tert-butyl ether, 80 mL Methanol
   filter and degas before using on UV-HPLC
3) 0.9% saline (900 mg NaCl in 100 mL EC-H_2O)

4) 3.4 µg/mL chlorophyll a in acetone (internal standard)
   extinction coefficient 1712 (660 nm) at absorbance .580
5) FOLCH (Chorofom:Methanol 2:1)
6) Hexane

Extraction Procedure:

1. Pulverize tissue in a mortar and pestle over flow of liquid nitrogen and store in -80 °C in 50 mL falcon tube wrapped in foil
2. Weigh 50 mg tissue to a 17 x 60 mm glass vial
3. Add 9 µl of internal standard and vortex
4. Add 2.3 mL cold 0.9% saline and homogenize with IKA T25 digital ultra-turax homogenizer at speed until tissue is dissolved and frothy
5. Rinse homogenizer blade with 500 µl fresh salinel in a new glass vial
6. Transfer homogenized adipose tissue to a new (16 x 125 mm) glass tube and rinse the glass vial with the additional methanol used to rinse the homogenizer blade
7. Add 6 mL FOLCH and vortex on high speed for 2 minutes
8. Centrifuge at 3000 rpm for 10 minutes at 4 °C
9. Transfer the bottom layer (chloroform) into a new glass tube
10. Add 6 mL hexane to the first glass tube and vortex at high speed for 1.5 minutes
11. Centrifuge at 3000 rpm for 10 minutes at 4 °C
12. Transfer the upper layer (hexane) into the second tube with the previous chloroform extract
13. Dry the combined extract under nitrogen gas (takes around 1.5 hrs)
14. The residue is re-dissolved in 100 µL acetone
15. Sonicate the tube for 30 seconds
16. Transfer the solution to a 1.7 ml microcentrifuge filter tube (0.22uM) and centrifuge at 14000 rpm for 7 minutes
17. Transfer each extracted solution from the microcentrifuge tube into a vial to load on the UV-HPLC
18. A 50 µL aliquot is injected onto a C30 ProntoSIL Carotenoid 3µm 4.6x 150mm column